

PRESSURE DROP AND HEAT TRANSFER IN AN INTERNALLY FINNED TUBE

MOHAMMAD ARIF HASAN MAMUN



DEPARTMENT OF MECHANICAL ENGINEERING
BANGLADESH UNIVERSITY OF ENGINEERING &
TECHNOLOGY

DHAKA 1000, BANGLADESH
OCTOBER 1999



#93623#

PRESSURE DROP AND HEAT TRANSFER IN AN INTERNALLY FINNED TUBE

By

MOHAMMAD ARIF HASAN MAMUN

A thesis submitted to the Department of Mechanical Engineering in partial
fulfillment of the requirements for the degree of Master of Science in
Mechanical Engineering

**BANGLADESH UNIVERSITY OF ENGINEERING & TECHNOLOGY
DHAKA 1000, BANGLADESH
OCTOBER 1999**

RECOMMENDATION OF THE BOARD OF EXAMINERS

The board of examiners hereby recommends to the Department of Mechanical Engineering, Bangladesh University of Engineering and Technology (BUET), Dhaka, acceptance of the thesis, **PRESSURE DROP AND HEAT TRANSFER IN AN INTERNALLY FINNED TUBE**, submitted by **Mohammad Arif Hasan Mamun**, in partial fulfillment of the requirements for the degree of Master of Science in Mechanical Engineering.

Chairman (Supervisor) :

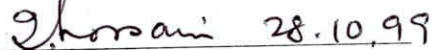


Dr. A. M. Aziz-ul Huq

Professor

Department of Mechanical Engineering
BUET, Dhaka.

Member (Ex-Officio) :



Dr. Md. Imtiaz Hossain

Professor & Head

Department of Mechanical Engineering
BUET, Dhaka.

Member :

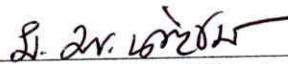


Dr. M. A. Rashid Sarkar

Professor

Department of Mechanical Engineering
BUET, Dhaka.

Member (External) :



Prof. Md. Abdul Quaiyum

Ex-Chairman

Bangladesh Atomic Energy Commission
Ramna, Dhaka.

ABSTRACT

The demand for high-performance heat exchange devices having small spatial dimensions is increasing due to their need in applications such as aerospace and automobile vehicles, cooling of electronic equipment, and so on. This had led to various designs of compact heat exchangers. Offset-fin and plate-fin heat exchangers are among the most widely used designs. Heat exchanger have numerous applications in power plants, industries, automobiles and electrical and electronic equipment.

Present work examines the heat transfer characteristic of steady state turbulent fluid flow through circular smooth tube, circular tube with continuous internal longitudinal fins and circular tube with internal longitudinal fins interrupted in the stream wise direction by arranging them in an in-line manner. Experimental set up was designed and installed to study the heat transfer performance and pressure drop characteristics in the entrance region as well as in the fully developed region of the smooth tube, in-line finned tube and in-line segmented finned tube. The tubes and fin were cast from brass to avoid contact resistance. Air was used as the working fluid. The Reynolds number was based on inlet diameter, Reynolds number varied in the range of 1.86×10^4 to 3.97×10^4 . The test section was heated electrically.

Results indicate that for comparable Reynolds numbers, friction factor of in-line finned tube is 1.93 to 3.5 times higher than that of the smooth tube. For comparable Reynolds number friction factor of in-line segmented finned tube is 1.72 to 2.5 times higher than that of the smooth tube whereas that for the latter is lower than that of the in-line finned tube. Pumping power of a in-line finned tube is 2.44 to 3.41 times higher than that of smooth tube for comparable Reynolds number. Pumping power of a in-line segmented finned tube is 2.21 to 2.34 times higher than that of smooth tube for comparable Reynolds number.

Heat transfer for the in-line finned tube is 1.7 to 1.8 times higher than that of smooth tube for comparable Reynolds number. Heat transfer for the in-line segmented finned tube is 1.77 to 1.9 times higher than that of smooth tube for comparable Reynolds number. It is observed from experiment that for comparable Reynolds number heat transfer and surface heat transfer coefficient for in-line finned tube and in-line segmented finned tube are similar but for in-line segmented finned tube pressure drop is less than that of in-line finned tube.

The results thus show that both inline finned tube and in-line segmented finned tube produces heat transfer enhancement but in-line segmented finned tube results in the same enhancement of heat transfer with less pressure drop.

ACKNOWLEDGEMENT

The author is highly grateful and indebted to his supervisor, Dr. A. M. Aziz-ul Huq, Professor, Department of Mechanical Engineering, Bangladesh University of Engineering & Technology (BUET), Dhaka, for his continuous guidance, supervision, inspiration, encouragement, and untiring support throughout this research work.

The author is also grateful to Dr. Md. Imtiaz Hossain, Professor & Head, Department of Mechanical Engineering, Bangladesh University of Engineering & Technology (BUET), Dhaka, for his continuous assistance to the author at different stages of this work and also for providing the author extensive use of the Laboratory facilities.

The author expresses his thankfulness to Dr. Md. Abdur Rashid Sarkar, Professor, Department of Mechanical Engineering, Bangladesh University of Engineering & Technology (BUET), Dhaka, for his valuable suggestions and sincere co-operation.

The author is also thankful to Mr. Md. Shahidullah, L. D. A. Cum – Typist, Department of Mechanical Engineering, Bangladesh University of Engineering & Technology (BUET), Dhaka, for his help in typing this thesis.

Finally, the author likes to express his sincere thanks to all other Teachers and Staffs of the Mechanical Engineering Department, BUET, Machine Shop and Welding Shop of BUET for their co-operations and helps in the successful completion of the work.

DECLARATION

No portion of the work contained in this thesis has been submitted in support of an application for another degree or qualification of this or any other University or Institution of learning.

A. HASUN

Mohammad Arif Hasan Mamun

October 1999

CONTENTS

	Page No.
ABSTRACT	i
ACKNOWLEDGEMENT	iii
DECLARATION	iv
CONTENTS	v
NOMENCLATURE	vii
LIST OF FIGURES	x
LIST OF GRAPHS	xi
CHAPTER 1 INTRODUCTION	1
1.1 Objective	2
CHAPTER 2 LITERATURE SURVEY	3
CHAPTER 3 HEAT TRANSFER PARAMETERS	7
3.1 Thermal Boundary Conditions	7
3.2 Definition of Parameters	7
CHAPTER 4 EXPERIMENTAL SET UP AND PROCEDURE	12
4.1 Inlet Section	12
4.2 Test Section	13
4.3 Fan Assembly	14
4.4 Flow Measurement by Traversing Pitot	15
4.5 Measurement of Static Pressure	16
4.6 Measurement of Temperature	16
4.7 Procedure of Experiment	20

	Page No.
CHAPTER 5 UNCERTAINTY ANALYSIS	21
CHAPTER 6 RESULTS AND DISCUSSIONS	27
CHAPTER 7 CONCLUSIONS	33
REFERENCES	35
APPENDIX A FIGURES	38
APPENDIX B GRAPHS	49
APPENDIX C SPECIFICATION	98
APPENDIX D SAMPLE CALCULATIONS	104

NOMENCLATURE

All dimensions are in SI Units.

A_x	Cross sectional area of smooth tube (m^2).
A_{xf}	Cross sectional area of finned tube (m^2).
A	Total heat transfer area of a tube (m^2).
A_h	Effective perimeter of Finned Tube (m).
A_s	Effective perimeter of Smooth Tube (m).
D_i	Inside diameter (m).
D_h	Hydraulic diameter (m).
N	Number of fins.
H	Height of the fin (mm).
W	Width of the fin. (mm)
Re	Reynolds number.
Re_i	Reynolds number based on inlet diameter.
h	Surface heat transfer co-efficient ($W/m^2\text{ }^\circ C$).
T	Temperature. ($^\circ C$)
T_i	Inlet temperature. ($^\circ C$)
T_o	Outlet temperature. ($^\circ C$)
M	Mass flow rate. (kg/s)

Q	Total heat input to the air (W).
Q'	Heat input to the air per unit area (W/m^2).
x	Axial distance (m).
L	Length of the tube (m)
C_p	Specific heat of air ($\text{J}/\text{kg}^\circ\text{C}$).
P	Pressure (N/m^2).
P^*	Dimensionless pressure drop.
P_i	Inlet static pressure (N/m^2).
V_i	Mean velocity in inlet section (m/s).
V	Mean velocity in finned tube (m/s).
ρ	Density of air (kg/m^3).
μ	co-efficient of viscosity of air (micro kg/sec-m).
ν	Kinematic viscosity (m^2/s)
k	Thermal conductivity of air ($\text{W}/\text{m}^\circ\text{C}$).
f	Friction factor.
t	Room temperature ($^\circ\text{C}$)
b	Atm. Pressure (mm of Hg)
w	Uncertainty
ω	Specific gravity

Subscripts

- h Based on hydraulic diameter.
- s Smooth tube i.e. unfinned tube.
- f Finned tube.
- w Wall temperature.
- b Bulk temperature.
- x Axial distance.

LIST OF FIGURES

	Page No.
FIG. A1. Schematic diagram of experimental set up	38
FIG. A2. Schematic diagram of experimental set up with dimensions	39
FIG. A3A. Half of the circular tube with fins	40
FIG. A3B. Shaped inlet	41
FIG. A4. Schematic diagram of in-line segmented finned tube	42
FIG. A5. Location of the thermocouples	43
FIG. A6. Location of the thermocouples	44
FIG. A7. Traversing pitot holding device	45
FIG. A8. Electric circuit diagram for heating system	46
FIG. A9. Location of thermocouple for measurement of outlet temperature	47
FIG. A10. Location of pitot tube for measurement of velocity head	48

LIST OF GRAPHS

	Page No.
Fig.B1 Pressure Drop Along the Axial Length of the Smooth Tube	49
Fig.B2 Distribution of Friction Factor Along Axial Distance of Smooth Tube	50
Fig. B3 Wall and Bulk Temperature Distribution Along Axial Distance of Smooth Tube	51
Fig. B4 Wall and Bulk Temperature Distribution Along Axial Distance of Smooth Tube	52
Fig. B5 Local Heat Transfer Coefficient Along Axial Distance of Smooth Tube at Different Reynolds Number	53
Fig. B6 Difference of Wall and Bulk Temperature Along the Length of the Smooth Tube	54
Fig.B7 Pressure Drop Along the Length of Smooth Tube	55
Fig.B8 Distribution of Friction Factor Along the Length of the Smooth Tube	56
Fig. B9 Wall and Bulk Temperature Distribution Along the Length of Smooth Tube	57
Fig. B10 Wall and Bulk Temperature Distribution Along the Length of Smooth Tube	58
Fig. B11 Local Heat Transfer Coefficient Along the Length of Smooth Tube at Different Reynolds Number	59
Fig. B12 Difference of Wall and Bulk Temperature Along the Length of the Smooth Tube	60
Fig. B13 Heat Transfer Results of Smooth Tube	61
Fig.B14 Pressure Drop Along the Axial Length of In-Line Finned Tube	62

	Page No.
Fig.B15 Distribution of Friction Factor Along Axial Distance of In-Line Finned Tube	63
Fig. B16 Wall and Bulk Temperature Distribution Along Axial Distance of In-Line Finned Tube	64
Fig. B17 Wall and Bulk Temperature Distribution Along Axial Distance of In-Line Finned Tube	65
Fig. B18 Local Heat Transfer Coefficient Along Axial Distance of In-Line Finned Tube at Different Reynolds Number	66
Fig. B19 Difference of Wall and Bulk Temperature Along the Length of the In-Line Finned Tube	67
Fig. B20 Wall, Fin-Tip and Bulk Temperature Distribution Along Axial Distance of In-Line Finned Tube ($Re_i = 37675$)	68
Fig.B21 Pressure Drop Along the Length of In-Line Finned Tube	69
Fig.B22 Distribution of Friction Factor Along the Length of the In-Line Finned Tube	70
Fig. B23 Wall and Bulk Temperature Distribution Along the Length of In-Line Finned Tube	71
Fig. B24 Wall and Bulk Temperature Distribution Along the Length of In-Line Finned Tube	72
Fig. B25 Local Heat Transfer Coefficient Along the Length of In-Line Finned Tube at Different Reynolds Number	73
Fig. B26 Difference of Wall and Bulk Temperature Along the Length of In-Line Finned Tube	74
Fig. B27 Wall, Fin-Tip and Bulk Temperature Distribution Along Axial Distance Of In-Line Finned Tube ($Re_i = 37675$)	75
Fig.B28 Pressure Drop Along the Axial Length of In-Line Segmented Finned Tube	76

	Page No.
Fig.B29 Distribution of Friction Factor Along Axial Distance of In-Line Segmented Finned Tube	77
Fig. B30 Wall and Bulk Temperature Distribution Along Axial Distance of In-Line Segmented Finned Tube	78
Fig. B31 Wall and Bulk Temperature Distribution Along Axial Distance of In-Line Segmented Finned Tube	79
Fig. B32 Local Heat Transfer Coefficient Along Axial Distance of In-Line Segmented Finned Tube at Different Reynolds Number	80
Fig. B33 Difference of Wall and Bulk Temperature Along the Length of the In-Line Segmented Finned Tube	81
Fig. B34 Wall, Fin-Tip and Bulk Temperature Distribution Along Axial Distance of In-Line Segmented Finned Tube ($Re_i = 37543$)	82
Fig.B35 Pressure Drop Along the Length of In-Line Segmented Finned Tube	83
Fig.B36 Distribution of Friction Factor Along the Length of the In-Line Segmented Finned Tube	84
Fig. B37 Wall and Bulk Temperature Distribution Along the Length of In Line Segmented Finned Tube	85
Fig. B38 Wall and Bulk Temperature Distribution Along the Length of In Line Segmented Finned Tube	86
Fig. B39 Local Heat Transfer Coefficient Along the Length of In Line Segmented Finned Tube at Different Reynolds Number	87
Fig. B40 Difference of Wall and Bulk Temperature Along the Length of In Line Segmented Finned Tube	88
Fig. B41 Wall, Fin-Tip and Bulk Temperature Distribution Along Axial Distance Of In Line Segmented Finned Tube ($Re_i = 37543$)	89

	Page No.
Fig. B42 Friction Factor at Different Reynolds Number of Smooth, In-Line Finned and In-Line Segmented Finned Tube	90
Fig. B43 Variation of Average Heat Transfer Coefficient with Reynolds number of Different Tubes	91
Fig. B44 Variation of pumping Power with Reynolds Number of Smooth Tube, In-Line Finned Tube and In-Line Segmented Finned Tube	92
Fig. B45 Velocity Distribution Along the Diameter of Smooth Tube	93
Fig. B46 Velocity Distribution Along the Diameter of In-Line Finned Tube	94
Fig. B47 Velocity Distribution Along the Diameter of In-Line Segmented Finned Tube	95
Fig. B48 Calibration Curve of Thermocouple	96
Fig. B49 Calibration Curve of Pressure Transducer	97

CHAPTER - I

INTRODUCTION



The subject of enhanced heat transfer has developed to the stage that it is of serious interest for heat exchanger application. The refrigeration and automotive industries routinely use enhanced surfaces in their heat exchangers. The process industry is aggressively working to incorporate enhanced heat transfer surfaces in their heat exchangers. Virtually every heat exchanger is a potential candidate for enhanced heat transfer. However, each potential application must be tested to see if enhanced heat transfer “makes sense”.

Fins have extensive applications in power plants, chemical process industries, and electrical and electronic equipment for augmentation of heat transfer. Enhancement techniques that improve the overall heat transfer characteristics of turbulent flow in tubes are important to heat exchanger designers. Efficient design of heat exchanger equipment with fins can improve system performance considerably. Among several available techniques for augmentation of heat transfer in heat exchanger tubes, the use of internal fin appear to be very promising method as evident from the result of the past investigations.

The demand for high-performance heat exchange devices having small spatial dimensions is increasing due to their need in applications such as aerospace and automobile vehicles, cooling of electronic equipment, and so on. This had led to various designs of compact heat exchangers. Offset-fin and plate-fin heat exchangers are among the most widely used designs. In an offset-fin heat exchanger, the interruptions of the fin surface prevent the flow from becoming fully developed; the restarting of the boundary layer at each new leading edge gives a higher heat transfer. Also, when longitudinal external fins are used on circular tubes, they are sometimes interrupted in the stream wise direction to improve their performance. It is, therefore, of interest to investigate the performance of an internal longitudinally finned circular tube with fin surface interrupted in the axial direction.

Number of studies have been made both experimentally and analytically with tubes having internal fins in laminar and turbulent flow. In case of analytical investigations, the analysis for laminar and turbulent flow is based on the differential equations for momentum and energy conservation in the flowing fluid. From the experimental study, it is evident that for both laminar and turbulent flow regimes, the finned tube and segmented finned tube exhibited substantially higher heat transfer coefficient when compared with smooth (unfinned) tubes.

1.1 OBJECTIVES

Since finned surfaces have extensive application in power plants, chemical process industries etc., a research work has been undertaken to study the heat transfer performance in turbulent flow regime of air in a circular tube having internal in-line and in-line segmented fins.

The study has the following objectives:

- i. To study the friction factor, pressure drop and temperature variations for turbulent fluid flow through circular smooth tube, circular tube with continuous internal longitudinal fins, circular tube with internal longitudinal fins interrupted in the stream wise direction by arranging them in an in-line manner for steady state temperature condition.
- ii. To study the heat transfer characteristics for turbulent fluid flow through circular smooth tube, circular tube with continuous internal longitudinal fins, circular tube with internal longitudinal fins interrupted in the stream wise direction by arranging them in an in-line manner for steady state temperature condition.

CHAPTER - II

LITERATURE SURVEY

Enhancement techniques that improve the overall heat transfer characteristics of laminar and turbulent flow in tubes are important to heat exchanger designers. It is evident that for both laminar and turbulent flow regimes, the finned tubes exhibited substantially higher heat transfer coefficients when compared with corresponding smooth (unfinned) tubes, and thus significant savings can be made from employing finned tubes.

Kelkar and Patankar [1990] [25] numerically has analyzed internally finned tubes, whose fins are segmented along their length. The fin segment is of length H in the flow direction, separated by an equal distance H before the next fin. The analysis present that the inline segmented fins give only 6% higher Nusselt number than that of continuous fins and staggered arrangement give only 6% below Nusselt number than that of continuous fins. However, the inline arrangement gives 22% lower friction than continuous fins. It can be noted that staggered arrangement uses the same fin surface area as continuous fins. However, the inline arrangement has half the fin surface area, because of the axial spaces between fins.

Numerical predictions of developing fluid flow and heat transfer in a circular tube with internal longitudinal continuous fins have been reported by Choudhury and Patankar (1985) and Prakash and Liu (1981). A numerical investigation of fluid flow and heat transfer in two-dimensional staggered fin arrays has been presented by Sparrow et al. (1977), while performance comparisons for two-dimensional in-line and staggered fin arrays have been made by Sparrow and Liu (1979). Experimental investigations of offset-fin arrays have been presented by London and Shah (1968) and Joshi and Webb (1982). The effect of plate thickness on heat transfer for two-dimensional staggered fin arrays has been studied numerically by Patankar and Prakash (1981). Three-dimensional flow and heat transfer in offset-fin arrays has been analyzed numerically by Kelkar and Patankar

(1985). For all values of fin height, number of fins, and Rayleigh number, the Nusselt number and friction factor were found to increase significantly with Rayleigh number.

Heat transfer and pressure drop measurements were made by A. P. Watkinson, D. L. Miletti, G.R. Kubanek [24] on integral inner-fin tubes of several designs in laminar oil flow. Data are presented for eighteen 12.7 to 32 mm diameter tubes containing from six to fifty straight or spiral fins over the Prandtl number range of 180 to 250, and the Reynolds number range of 50 to 3000, based on inside tube diameter and nominal area. At a Reynolds number of 500, heat transfer was enhanced over smooth tube values by 8 to 224% depending on tube geometry. At constant pumping power and the same Reynolds number, the increase in heat transfer ranged from 1 to 187%.

Empirically determined correlating equations has been presented by T. C. Carnavos [23] who predict turbulent flow heat transfer and pressure loss performance within acceptable limits in the overall ranges of $0 < \alpha < 30^\circ$, $10,000 < Re < 100,000$, and $0.7 < Pr < 30$. There is no strong indication that these types of tubes are Prandtl number sensitive. However, there is an indication that the spiral fin tubes deviate the most from the slope of 0.8, which becomes more pronounced at the higher helix angles and lower Reynolds numbers. The best performers were in the group of tubes with the higher helix angles and internal heat transfer surface relative to a smooth tube.

Hu and Chang [10] analyzed fully developed laminar flow in internally finned tubes by assuming constant and uniform heat flux in tube and surfaces. By using 22 fins extended to about 80% of the tube radius, they showed an enhancement as high as 20 times that of unfinned tube could be realized. Soliman et al. [18] also analyzed fully developed laminar flow, but accounting for conduction in the tube wall and fins, and keeping the outer surface of the tube at a constant temperature. In a later study, Prakash and Patankar [17] investigated the influence of buoyancy on heat transfer in vertical internally-finned tube under fully developed laminar flow condition. Analyses of thermally-developed laminar flow in internally finned tubes were carried out by Prakash and Liu [16] and Rustum and Soliman [18] by numerically solving the governing equations. They concluded that

accordingly, and thus delays the development of the local Nusselt number in the entrance region of the duct. Mafiz et al. [12-13] studied experimentally steady state turbulent flow heat transfer performance of circular tubes having six integral internal longitudinal fins and there in his work Mafiz found an abrupt pressure fluctuation near the entrance region of the tube. This study indicates that significant enhancement of heat transfer is possible by using internal fins without sacrificing additional pumping power. Experimental data for pressure drop and heat transfer coefficient in internally finned tubes has been reported, among others, by Hiding and Coogan [8], Bergles et al. [1] Watkinson [21], and Rustum and Soliman (19). Bulk of these data are characterized the laminar flow regimes using air, water and oil as working fluids.

CHAPTER - III

HEAT TRANSFER PARAMETERS

In this chapter the basic definition of heat transfer parameters and thermal boundary conditions in connection with the present work have been discussed.

3.1 THERMAL BOUNDARY CONDITIONS

In the present experiment, uniform wall temperature is considered.

3.2 DEFINITION OF PARAMETERS

Hydraulic Diameter:

For internal flows the hydraulic diameter D_h is often used as characteristic length. It is defined as

$$D_h = \frac{4x(\text{Cross sectional area of the flow})}{\text{Wetted perimeter}}$$

$$= \frac{4x\pi D_i^2 \frac{1}{4}}{\pi D_i + 2NH} \text{ m} \quad (3.1)$$

(Assuming thin fin)

In the present study, fins can not be assumed as thin and hydraulic diameter D_h was obtained as follows:

$$D_h = \frac{4 A_{xf}}{\pi D_i + 2NH} \text{ m} \quad (3.2)$$

where $A_{xf} = \left(\frac{\pi D_i}{4} - NWH \right) \text{ sq. m}$

Reynolds Number:

Reynolds number based on inside diameter is defined as

$$\text{Re}_i = \frac{\rho V D_i}{\mu} \quad (3.3)$$

Reynolds number based on hydraulic diameter is defined as

$$\text{Re}_h = \frac{\rho V D_h}{\mu} \quad (3.4)$$

Pressure Drop and Fanning Friction Factor:

The dimensionless pressure drop at any axial location x, is given by the following equation,

$$P^*(x) = - \Delta P(x) / 1/2 \rho V^2 \quad (3.5)$$

Where $\Delta P = P_i - P(x)$

$P_i = \text{Pressure at inlet (N/m}^2\text{)}$

$P(x) = \text{Pressure at any axial location, x (N/m}^2\text{)}$

The local friction factor based on hydraulic diameter is given by

$$F_h = \frac{(-\Delta P / x) D_h}{2 \rho V^2} \quad (3.6)$$

The local friction factor based on inside diameter is given by

$$F_i = \frac{(-\Delta P / x) D_h}{2\rho V^2} \quad (3.7)$$

Heat Transfer: Uniform Heat input per unit axial length:

Total Heat input to the air

$$Q = MC_p (T_i - T_o) \quad W \quad (3.8)$$

For Smooth Tube

Heat input to the air per unit area

$$Q' = MC_p (T_i - T_o) / A_s L \quad W/m^2 \quad (3.9)$$

The local bulk temperature of the fluid $T_b(x)$ can be defined as by the following heat balance equation

$$T_b(x) = T_i + \frac{Q' A_s x}{MC_p} \quad ^\circ C \quad (3.10)$$

The local heat transfer coefficient at any axial location (for both tube and fin) can be defined as

$$h_x = \frac{Q'}{(T_w - T_b)_x} \quad W/m^2 ^\circ C \quad (3.11)$$

The Average heat transfer Coefficient can be defined as

$$\bar{h} = \frac{Q}{A(T_{wav} - T_{hav})} \quad W/m^2 ^\circ C \quad (3.12)$$

For In line Finned Tube

Heat input to the air per unit area

$$Q' = MC_p (T_i - T_o) / A_h L \quad \text{W/m}^2 \quad (3.13)$$

The local bulk temperature of the fluid $T_b(x)$ can be defined as by the following heat balance equation

$$T_b(x) = T_i + \frac{Q' A_h x}{MC_p} \quad ^\circ\text{C} \quad (3.14)$$

The local heat transfer coefficient at any axial location (for both tube and fin) can be defined as

$$h_x = \frac{Q'}{(T_w - T_b)_x} \quad \text{W/m}^2\text{ }^\circ\text{C} \quad (3.15)$$

The Average heat transfer Coefficient can be defined as

$$\bar{h} = \frac{Q}{A(T_{wav} - T_{hav})} \quad \text{W/m}^2\text{ }^\circ\text{C} \quad (3.16)$$

For In line Segmented Finned Tube

Heat input to the air per unit area

$$Q' = \frac{MC_p (T_o - T_i)}{(A_h + A_s + A_f) L} \quad \text{W/m}^2 \quad (3.17)$$

The local bulk temperature of the fluid $T_b(x)$ can be defined as by the following heat balance equation

$$T_b(x) = T_i + \frac{Q' A_h x}{MC_p} \quad ^\circ\text{C} \quad \text{When } x < L_1 \quad (3.18)$$

$$T_b(x)_l = (T_i)_{l-1} + \frac{Q' A_h (0.2)}{MC_p} \quad ^\circ\text{C} \quad \text{When } L_1 < x < 2L_1 \quad (3.19)$$

$$T_b(x)_l = (T_i)_{l-1} + \frac{Q' A_h (0.2)}{MC_p} \quad ^\circ\text{C} \quad \text{When } 2L_1 < x < 3L_1 \quad (3.20)$$

The local heat transfer coefficient at any axial location (for both tube and fin) can be defined as

$$h_x = \frac{Q'}{(T_w - T_b)_x} \quad \text{W/m}^2\text{ }^\circ\text{C} \quad (3.21)$$

The Average heat transfer Coefficient can be defined as

$$\bar{h} = \frac{Q}{A(T_{wav} - T_{hav})} \quad \text{W/m}^2\text{ }^\circ\text{C} \quad (3.22)$$

Pumping power can be defined as

$$\begin{aligned} P_m &= (-\Delta P/\rho) M \\ &= \frac{4 F L}{D_i} \frac{V^2}{2} A_x V \rho \quad \text{W} \end{aligned} \quad (3.23)$$

CHAPTER - IV

EXPERIMENTAL SET UP AND PROCEDURE

Experimental set up was designed, fabricated and installed to study the friction factor and heat transfer performance of circular smooth tube, circular tube with continuous internal longitudinal fins, circular tube with internal longitudinal fins interrupted in the stream wise direction by arranging them in an in-line manner. The schematic diagram is shown in the figure (A1 and A2). Air was used as the working fluid. Air in the test section was supplied by a centrifugal fan fitted at the end of the set up. It was driven by a motor [3 phase, 3hp, 420V, 4.1A]. The maximum flow rate under the free operation was approximately 30 m³/min. A butterfly type valve was used to control the flow rate of air during the experiment in the test section and it was installed after the test section. The set up consisted of three sections:

- I. inlet and flow measuring section
- II. heat transfer test section and
- III. fan assembly.

4.1 INLET SECTION

The unheated inlet section (shaped inlet) cast from aluminum and heat transfer test section cast from brass are of same diameter. The open end of the pipe would probably act to some extent as a sharp edged orifice, and the air flow would contract and not fill the pipe completely for a short distance from the end. This effect was avoided here in the experiment by fitting a shaped inlet. The pipe shaped inlet, 530 mm long, (Fig. A3B) were made integral to avoid any flow disturbances at upstream

of the test section of flow measurement. The coordinates of the curvature of the shaped inlet was suggested by Owner and Pankhurst (7) which is represented in table (C2), Appendix-C.

4.2 TEST SECTION

Circular Smooth tube

The test section contains circular smooth tube(1520 mm long and 70 mm inside diameter) to avoid contact resistance. The fin and tube assembly was cast from brass, because of its high thermal conductivity and easy machinability.

Circular in line Finned Tube

The test section contains eight internal integral longitudinal fins (3mm width and 15mm height, Aspect ratio 5) with circular tube(1520 mm long and 70 mm inside diameter) to avoid contact resistance. The fin and tube assembly was cast from brass, because of its high thermal conductivity and easy machinability. Two halves of circular tube with integral fins were cast separately and joined together to give the shape of a circular tube. Fig. (A3A) depicts the tube configuration and dimension. As two halves were joined at the line of symmetry, it did not effect thermal and hydrodynamic results of the experiment.

Circular in line Segmented Finned Tube

The test section contains circular tube (1520 mm long and 70 mm inside diameter) with eight internal integral in line segmented longitudinal fins (3mm width and 15mm height, Aspect ratio 5).Fins are present in the first 0.5066 m of length and last 0.5066 m of length and in the middle 0.5066 m of length is smooth tube. The fin and tube assembly was cast from brass, because of its high thermal conductivity and easy machinability. Two halves of circular tube with integral fins were cast separately and joined together to give the shape of a circular tube. Fig. (A4) depicts the tube configuration and dimension. As two halves were joined at the line of symmetry, it did not effect thermal and hydrodynamic results of the experiment.

All of the test sections were wrapped with mica sheet, glass fiber tape and insulation tape. Over mica sheet nichrome wire (of resistance 0.610 ohm/m) was spirally wound uniformly with spacing of 8 mm between the fins. The nichrome wire was covered with mica sheet, glass fiber tape and insulation tape to make it electrically insulated by covering with asbestos. The test section was placed in the test rig with the help of the bolted flanges, between which asbestos sheets were installed which act as heat guards in the longitudinal direction.

The test section electric heater was supplied power by 5 KVA variable voltage transformer connected to 220 VAC power through a magnetic contactor and temperature controller. The temperature controller was fitted to sense the air outlet temperature and give signal to heater for switching it off or on automatically. It protects the experimental set up from being excessively heated which may happen at the time of experiment when the heating system is in operation continuously for hours to bring the system in steady state condition. It also controls the air outlet temperature.

Electric heat input by nichrome wire was kept constant for all the experiments. In all the experiments 110V and 11.5 Amp were maintained.

The electrical power to the test section was determined by measuring the current and voltage supplied to the heating element. The voltage was measured with a voltmeter and current was measured by an a.c. ammeter. Fig. (A8) shows the electrical circuit diagram of the heating system of the test section. The particulars of the electric heater, temperature controller and fan are given in table (C1) in Appendix-C.

4.3 FAN ASSEMBLY

A diffuser of cone angle 12° was made of M.S plate and fitted to the suction side of the fan. The diffuser was used for minimizing head loss at the suction side. To arrest vibration of the fan a flexible duct was installed between the inlet section of the fan and 7.62 cm diameter pipe of the set up as shown in the Fig. (A2). A butterfly type

valve was used to control air flow rate during experiment at the suction side before the flexible duct.

4.4 FLOW MEASUREMENT BY TRAVERSING PITOT

Flow of air through the experimental set up was measured at inlet section with the help of a traversing pitot. A shaped inlet made of aluminum was installed at the inlet to the test section to have an easy entry and symmetrical flow. At 4 pipe diameters, according to Owner and Pankhurst (7), from the inlet a traversing pitot was installed. A drawing of the Micrometer traversing pitot is shown in Fig. (A7).

To find out the location of pitot tube for measurement of velocity head, the tube diameter was divided into five equal concentric areas and then their center were found out by using the following calculation. And the locations for the traversing pitot is shown in the Fig. (A10). Arithmetic mean method is given bellow:

$$\frac{1}{5}\pi R^2 = \pi r_1^2$$

$$r_1 = 0.447R$$

$$\frac{1}{5}\pi R^2 = \pi r_2^2 - \pi r_1^2$$

$$\Rightarrow \frac{1}{5}R^2 + (0.447R)^2 = r_2^2$$

$$\therefore r_2 = 0.632R$$

Similarly,

$$r_3 = 0.774R$$

$$r_4 = 0.894R$$

$$r_5 = 1R$$

Now

$$\pi r_{5-4}^2 = \frac{\pi R^2 + \pi(0.894R)^2}{2}$$

$$\therefore r'_{5-4} = 0.948R$$

$$\text{Again } \pi r'^2 = \frac{\pi(0.894R)^2 + \pi(0.774R)^2}{2}$$

$$\therefore r'_{4-3} = 0.836R$$

Similarly

$$r'_{3-2} = 0.7065R$$

$$r'_{2-1} = 0.547R$$

$$r'_{1-0} = 0.316R$$

Mean velocity was measured by traversing pitot tube along the diameter of the pipe at ten measuring points.

4.5 MEASUREMENT OF STATIC PRESSURE

The static pressure tapings were made at the inlet of the test section as well as equally spaced 8 axial location of all the test section as shown in Fig. (A.5). Pipe wall pressure tapings for measurement of static pressure were made of brass and installed carefully such that just flush inside the surface of test section. The outside parts of these were made tapered to ensure an air tight fitting into the plastic tubes which were connected to the manometer and pressure transducer. Epoxy glue (Araldite) was used for proper fixing of the static pressure tapings. U-tube manometers at an inclination 30° were attached with the pressure tapping. The manometric fluid used in the U-tube manometer was water.

4.6 MEASUREMENT OF TEMPERATURE

The temperatures at the different axial locations of all the test section were measured with the help of K-type thermocouples along with data acquisition system and computer at five minutes interval. The temperature measuring locations are-

- i. Fluid bulk temperature at the outlet of the test section.

- ii. Wall temperature at 8 axial locations of the test section.
- iii. Fin-tip temperature at 8 axial location of the test section.

The bulk temperature of the air at the outlet of the test section was measured using a thermocouple at the outlet of the test section.

To find out the location of thermocouple for measurement of outlet temperature, the tube diameter was divided into three equal concentric areas and then their center were found out by using the following calculation. And the locations for the thermocouple is shown in the Fig. (A9). Arithmetic mean method is given below:

$$D=0.07 \text{ m}$$

$$r_1=.035 \text{ m}$$

$$A = \pi r_1^2 = .0038485$$

$$\frac{A}{3} = A_1 = A_2 = A_3 = .0012828$$

$$A_1 = \pi r_1^2 - \pi r_2^2$$

$$A_2 = \pi r_2^2 - \pi r_3^2$$

$$A_3 = \pi r_3^2$$

$$Q_1 = A_1 V \rho C_p (T_{b1} - T_i)$$

$$Q_2 = A_2 V \rho C_p (T_{b2} - T_i)$$

$$Q_3 = A_3 V \rho C_p (T_{b3} - T_i)$$

$$Q = AV\rho C_p (T_{hav} - T_i) = Q_1 + Q_2 + Q_3 = A_1 V \rho C_p (T_{b1} + T_{b2} + T_{b3} - 3T_i)$$

$$\frac{A}{A_1} (T_{hav} - T_i) = (T_{b1} + T_{b2} + T_{b3} - 3T_i)$$

$$T_{hav} = \frac{T_{b1} + T_{b2} + T_{b3}}{3}$$

$$A_1 = \pi r_1^2 - \pi r_2^2$$

$$.0012828 = \pi (.035)^2 - \pi r_2^2$$

$$r_2 = 0.0286m$$

$$A_2 = \pi r_2^2 - \pi r_3^2$$

$$0.012828 = \pi (0.0286)^2 - \pi r_3^2$$

$$r_3 = 0.02024m$$

Now

$$\pi R_1^2 = \frac{\pi r_1^2 + \pi r_2^2}{2}$$

$$R_1 = 0.03196$$

$$\pi R_2^2 = \frac{\pi r_2^2 + \pi r_3^2}{2}$$

$$R_2 = 0.02475$$

$$R_3 = 0.0143$$

$$R_1' = 0.035 - R_1 = 0.00304$$

$$R_2' = 0.035 - R_2 = 0.01025$$

$$R_3' = 0.035 - R_3 = 0.02068$$

Mean outlet temperature was measured by traversing the thermocouple along the diameter of the pipe at three measuring points.

For Smooth Tube

8 thermocouples were installed in 8 cross section (Fig. A6) with one in each cross section to measure the wall temperature of the test section. All the thermocouples and the data acquisition systems were calibrated before their use. Thermal contact between the brass tube and the thermocouple junction was assured by peening thermocouples junction into grooves in the wall. Thermocouples were inserted into the holes and peened into the grooves of the tube wall.

For In Line Finned Tube

16 thermocouples were installed in 8 cross section (Fig. A6) with two in each cross section to measure the wall as well as the fin-tip temperatures of the test section. All the thermocouples and the data acquisition systems were calibrated before their use. Thermal contact between the brass tube and the thermocouple junction was assured by peening thermocouples junction into grooves in the wall. Holes were drilled across the height of the fin in 8 cross section to measure the temperature of the fin-tip. Thermocouples were inserted into the holes and peened into the grooves of the fin-tip.

For In Line Finned Tube

14 thermocouples were installed in 8 cross section (Fig. A6) with two in each cross section to measure the wall as well as the fin-tip temperatures of the test section in 6 cross section. All the thermocouples and the data acquisition systems were calibrated before their use. Thermal contact between the brass tube and the thermocouple junction was assured by peening thermocouples junction into grooves in the wall. Holes were drilled across the height of the fin in 8 cross section to measure the temperature of the fin-tip. Thermocouples were inserted into the holes and peened into the grooves of the fin-tip.

4.7 PROCEDURE OF EXPERIMENT

The fan was first switched on and allowed to run for five minutes so that the transient characteristic died out. The flow of air through the test section was varied and kept constant with the help of a flow control valve. Then electrical heating circuit was switched on.

The pressure tapping for measuring static pressure were connected with inclined (30°) U-tube manometers (The manometric fluid was water) and pressure transducers. The readings for the velocity head were taken by traversing the pitot along the diameter of the pipe. Inclined tube manometer was used for measuring velocity head and the fluid in the manometer was high speed diesel with sp. gr. 0.855.

The electrical current was adjusted with the help of a Regulating Transformer (or Variac) to attain steady state condition for a particular Reynolds number. Steady state condition for temperature at the different locations of the test section was defined according to D.L. Gee and R.L. Webb (5) by two measurements. First the variation in wall thermocouples was observed until constant values were attained; then the outlet air temperature was monitored. Steady state condition was attained when the outlet air temperature did not deviate over 10-15 minutes time. All the thermocouples readings were taken at steady state condition.

After one run of the experiment at a particular Reynolds number, the Reynolds number was changed with the help of the flow control valve keeping electrical power input constant. All the thermocouples readings and static pressure readings were taken at every tapping along the axial direction for each run of the experiment.

CHAPTER - V

UNCERTAINTY ANALYSIS

A more precise method of estimating uncertainty in experimental results has been presented by Kline and McClintock [26]. The method is based on a careful specification of the uncertainties in the various primary experimental measurements.

Determination of Mean Velocity:

$$V = 20.56 \left(\frac{273+t}{b} \right)^{1/2} (h)^{1/2}$$

Room Temperature

$$t = 30.8 \pm 0.02\% ^\circ C$$

atm..pressure

$$b = 743.5 \pm 0.1 \text{mm of Hg}$$

$$h = 0.58 \pm 0.001 \text{cm of fluid}$$

The uncertainty in this value is calculated as follows. The various terms are:

$$w_t = 30.8 \times 0.0002 = 0.0062 ^\circ C$$

$$w_b = 0.1 \text{mm of Hg}$$

$$w_h = 0.001 \text{cm of fluid}$$

Change of velocity with respect to temperature

$$\begin{aligned} \frac{\partial V}{\partial t} &= 20.56 \times \frac{1}{2} \left(\frac{273+t}{b} \right)^{-1/2} \frac{1}{b} (h)^{1/2} \\ &= 20.56 \times \frac{1}{2} \left(\frac{273+30.8}{743.5} \right)^{-1/2} \frac{1}{743.5} (0.58)^{1/2} \\ &= 0.0165 \end{aligned}$$

Change of velocity with respect to Atm. Pressure

$$\begin{aligned}\frac{\partial V}{\partial b} &= 20.56 \frac{1}{2} \left(\frac{273+t}{b} \right)^{-1/2} (273+t) b^{-3/2} (h)^{1/2} \\ &= 20.56 \frac{1}{2} \left(\frac{273+30.8}{743.5} \right)^{-1/2} (273+30.8) (743.5)^{-3/2} (0.58)^{1/2} \\ &= 0.183\end{aligned}$$

Change of velocity with respect to manometric head

$$\begin{aligned}\frac{\partial V}{\partial h} &= 20.56 \left(\frac{273+t}{b} \right)^{1/2} \frac{1}{2} (h)^{-1/2} \\ &= 20.56 \left(\frac{273+30.8}{743.5} \right)^{1/2} \frac{1}{2} (0.58)^{-1/2} \\ &= 8.64\end{aligned}$$

Thus, the uncertainty in the velocity is

$$\begin{aligned}w_v &= \left[\left(\frac{\partial V}{\partial t} w_t \right)^2 + \left(\frac{\partial V}{\partial b} w_b \right)^2 + \left(\frac{\partial V}{\partial h} w_h \right)^2 \right]^{1/2} \\ &= \left[(0.0165 \times 0.0062)^2 + (0.183 \times 0.1)^2 + (8.64 \times 0.001)^2 \right]^{1/2} \\ &= 0.02024 \text{ m/s}\end{aligned}$$

Total Heat input to the air

$$Q = MC_p (T_o - T_i)$$

$$Q = \rho A_x V C_p (T_o - T_i)$$

$$A_x = 0.00385 \pm 0.001$$

$$V = 10.16 \pm 0.02024$$

$$T_o = 41.13 \pm 0.02\%$$

$$T_i = 30.8 \pm 0.02\%$$

The uncertainty in this value is calculated as follows. The various terms are:

$$w_A = 0.001$$

$$w_V = 0.02024$$

$$w_{T_o} = 41.13 \times 0.0002 = 0.00823$$

$$w_{T_i} = 30.8 \times 0.0002 = 0.0062$$

Change of total heat input with respect to area

$$\begin{aligned} \frac{\partial Q}{\partial A} &= \rho V C_p (T_o - T_i) \\ &= 1.14 \times 10.45 \times 1006 \times (41.13 - 30.8) \\ &= 0.124 \times 10^6 \end{aligned}$$

Change of total heat input with respect to velocity

$$\begin{aligned} \frac{\partial Q}{\partial V} &= \rho A C_p (T_o - T_i) \\ &= 1.14 \times 0.00385 \times 1006 \times (41.13 - 30.8) \\ &= 45.61 \end{aligned}$$

Change of total heat input with respect to outlet temperature

$$\begin{aligned}\frac{\partial Q}{\partial T_o} &= \rho A V C_p \\ &= 1.14 \times .00385 \times 10.45 \times 1006 \\ &= 46.14\end{aligned}$$

Change of total heat input with respect to inlet temperature

$$\begin{aligned}\frac{\partial Q}{\partial T_i} &= -\rho A V C_p \\ &= -1.14 \times .00385 \times 10.45 \times 1006 \\ &= -46.14\end{aligned}$$

Thus, the uncertainty in the Total Heat Input to the air

$$\begin{aligned}w_Q &= \left[\left(\frac{\partial Q}{\partial A} w_A \right)^2 + \left(\frac{\partial Q}{\partial V} w_V \right)^2 + \left(\frac{\partial Q}{\partial T_o} w_{T_o} \right)^2 + \left(\frac{\partial Q}{\partial T_i} w_{T_i} \right)^2 \right]^{1/2} \\ &= \left[(0.124 \times 10^6 \times 0.00001)^2 + (45.61 \times 0.02024)^2 + (46.14 \times 0.00823)^2 + (-46.14 \times 0.0062)^2 \right]^{1/2} \\ &= 1.62W\end{aligned}$$

Friction Factor:

Local friction factor based on inside diameter is given by

$$F_i = \frac{(\Delta P / x) D_i}{2\rho V^2}$$

$$\Delta P = 0.99456 \pm 0.25\%$$

$$x = 0.06 \pm 0.00001$$

$$D_i = 0.07 \pm 0.00001$$

$$V = 11.92987 \pm 0.02024$$

$$w_{\Delta P} = 0.99456 \times 0.0025 = 0.00249$$

$$w_x = 0.00001$$

$$w_{D_i} = 0.00001$$

$$w_V = 0.02024$$

Change of friction factor with respect to pressure drop

$$\begin{aligned} \frac{\partial F_i}{\partial \Delta P} &= \frac{D_i}{2\rho V^2 x} \\ &= \frac{0.07}{2 \times 0.9947 \times (11.92987)^2 \times 0.06} \\ &= 0.00412 \end{aligned}$$

Change of friction factor with respect to axial distance

$$\begin{aligned} \frac{\partial F_i}{\partial x} &= -\frac{\Delta P D_i}{2\rho V^2 x^2} \\ &= \frac{0.99456 \times 0.07}{2 \times 0.9947 \times (11.92987)^2 \times (0.06)^2} \\ &= 0.068 \end{aligned}$$

Change of friction factor with respect to inside diameter

$$\begin{aligned}\frac{\partial F_i}{\partial D_i} &= -\frac{\Delta P}{2\rho V^2 x} \\ &= \frac{0.99456}{2 \times 0.9947 \times (11.92987)^2 \times (0.06)} \\ &= 0.059\end{aligned}$$

Change of friction factor with respect to velocity

$$\begin{aligned}\frac{\partial F_i}{\partial V} &= -2 \frac{\Delta P D_i}{2\rho V^3 x} \\ &= \frac{0.99456 \times 0.07}{0.9947 \times (11.92987)^3 \times (0.06)} \\ &= 0.00069\end{aligned}$$

Thus, the uncertainty in the Friction factor

$$\begin{aligned}w_{F_i} &= \left[\left(\frac{\partial F_i}{\partial \Delta P} w_{\Delta P} \right)^2 + \left(\frac{\partial F_i}{\partial x} w_x \right)^2 + \left(\frac{\partial F_i}{\partial D_i} w_{D_i} \right)^2 + \left(\frac{\partial F_i}{\partial V} w_V \right)^2 \right]^{1/2} \\ &= \left[(0.00412 \times 0.00249)^2 + (-0.068 \times 0.00001)^2 + (0.059 \times 0.00001)^2 + (-0.00069 \times 0.02024)^2 \right]^{1/2} \\ &= 0.00373\end{aligned}$$

CHAPTER - VI

RESULTS AND DISCUSSION

In this experimental work fluid flow and heat transfer performance were studied. Pressure drop characteristics and heat transfer performance were calculated for circular smooth tube, a circular tube with continuous internal longitudinal fins, a circular tube with internal longitudinal fins interrupted in the stream wise direction by arranging them in an in-line manner.

Analysis For Smooth Tube:

The graph of dimensionless pressure drop P^* VS. X/L and X/D is shown in the figure B1 and B7 respectively. The pressure gradient is high in the entrance region, then pressure recovers and finally approaches the fully developed values away from the entrance section. Figures B2 and B8 show the friction factor F_i VS. X/L and X/D respectively. It can be noticed that the friction factor is high near the entrance region due to large pressure drop then falls gradually to fully developed value. It can be noted that as the Reynolds number increases Friction factor decreases.

Figure B3,B4 and B9,B10 shows the wall and bulk temperature distribution VS. X/L and X/D respectively for six different Reynolds number. The wall temperature was found by direct measurement as described earlier and the bulk temperature was determined by energy balance equation (equation 3.10). At higher Reynolds number the wall temperature is low because more heat is taken away by the air. The figure shows that there is a portion of the test section where the wall and the bulk temperature distribution are parallel, yielding a uniform value of $(T_w - T_b)$.

Figure B5 and B11 shows the variation of Local Heat Transfer Coefficient VS. X/L and X/D respectively. Heat Transfer Coefficient is large in the entrance

region due to the development of thermal boundary layer with the entrance section at the leading edge. At this portion the cold air start to mix up with the hot tube. It decreases with increasing the axial distance approaching the fully developed values. The figure shows that at higher Reynolds number, the curve of the local Heat Transfer Coefficient along the length of the finned tube is higher. This is expected because a higher flow rate results in increment of heat transfer coefficient at tube surface.

Figure B6 and B12 shows $(T_w - T_b)_x$ VS. X/L and X/D respectively for different Reynolds number. The $(T_w - T_b)_x$ value is low in the entrance region, then it rises gradually and reaches to the fully developed value.

Figure B13 shows the heat transfer results of smooth tube as a function of Reynolds number and compares with that of the theoretical value. It can be noticed that the slope of the heat transfer curve for experimental value and that of the theoretical value are almost same.

Analysis For In-Line Finned Tube:

The graph of dimensionless pressure drop P^* VS. X/L and X/D is shown in the figure B14 and B21 respectively. The pressure gradient is high in the entrance region, then pressure recovers and finally approaches the fully developed values away from the entrance section. The dimensionless pressure drop of In Line Finned Tube is higher than that of Smooth Tube. Friction factor was calculated from the pressure measured from 60 mm down stream of the inlet section. Figure B15 and B22 shows the friction factor F_i VS. X/L and X/D respectively. It can be noticed that the friction factor is high near the entrance region due to large pressure drop then falls gradually to fully developed value. It can be noted that as the Reynolds number increases Friction factor decreases. It also can be noted that friction factor for a In Line Finned Tube is much higher than that of a Smooth Tube, but the slope of the friction factor curve of the finned tube is nearly equal to the Smooth Tube.

Figure B16, B17 and B23, B24 shows the wall and bulk temperature distribution VS. X/L and X/D respectively for six different Reynolds number. The wall temperature was found by direct measurement as described earlier and the bulk temperature was determined by energy balance equation (equation 3.14). At higher Reynolds number the wall temperature is low because more heat is taken away by the air. The figure shows that there is a portion of the test section where the wall and the bulk temperature distribution are almost parallel, yielding a uniform value of $(T_w - T_b)$ as expected from constant heat rate. Just up-stream of the exit, the slope of the wall temperature gradually falls due to end effect.

Figure B18 and B25 shows the variation of Local Heat Transfer Coefficient VS. X/L and X/D respectively. Heat Transfer Coefficient is large in the entrance region due to the development of thermal boundary layer with the entrance section as the leading edge. At this portion the cold air start to mix up with the hot tube. It decreases with increasing the axial distance approaching the fully developed values. Just up-stream of the exit, the slope of the Heat Transfer Coefficient gradually rises due to end effect. The figure shows that at higher Reynolds number, the curve of the local Heat Transfer Coefficient along the length of the finned tube is higher. This is expected because a higher flow rate results in increment of heat transfer coefficient at both tube surface and the surface of the fins. The average Heat Transfer Coefficient of In Line Finned Tube is higher than that of Smooth Tube.

Figure B19 and B26 shows $(T_w - T_b)_x$ VS. X/L and X/D respectively for different Reynolds number based on inside diameter. The $(T_w - T_b)_x$ value is low in the entrance region, then it rises gradually and reaches to the fully developed value. Just up-stream of the exit, the slope of $(T_w - T_b)_x$ gradually falls due to end effect.

Figure B20 and B27 shows the wall, bulk and fin tip temperature distribution VS. X/L and X/D respectively for one Reynolds number.

Analysis for In-Line Segmented Finned Tube:

The graph of dimensionless pressure drop P^* VS. X/L and X/D is shown in the figure B28 and B35 respectively. The pressure gradient is high in the entrance region, then pressure recovers. In the middle unfinned portion of the tube pressure gradient is very low and finally approaches the fully developed values away from the entrance section. The dimensionless pressure drop of In Line Segmented Finned Tube is higher than that of Smooth Tube and lower than that of In Line Finned Tube. Friction factor was calculated from the pressure measured from 60 mm down stream of the inlet section. Figure B29 and B36 show the friction factor f_i VS. X/L and X/D respectively. It can be noticed that the friction factor is high near the entrance region due to large pressure drop then falls gradually to fully developed value. It can be noted that as the Reynolds number increases Friction factor decreases. It can be noted that friction factor for a In Line Segmented Finned Tube is much higher than that of a Smooth Tube and lower than that of In Line Finned Tube.

Figure B30, B31 and B37, B38 shows the wall and bulk temperature distribution VS. X/L and X/D respectively for six different Reynolds number. The wall temperature was found by direct measurement as described earlier and the bulk temperature was determined by energy balance equation (equation 3.18, 3.19, 3.20). At higher Reynolds number the wall temperature is low because more heat is taken away by the air. The figure shows that in the middle smooth portion of the test section the wall temperature distribution are higher. Just up-stream of the exit, the slope of the wall temperature gradually falls due to end effect.

Figure B32 and B39 shows the variation of Local Heat Transfer Coefficient VS. X/L and X/D respectively. Heat Transfer Coefficient is large in the entrance region due to the development of thermal boundary layer with the entrance section as the leading edge. At this portion the cold air start to mix up with the hot tube. It decreases with increasing the axial distance. In the middle smooth portion of the tube Heat Transfer Coefficient decreases as the fin is absent in that portion. After

that portion Heat Transfer Coefficient increases and just up-stream of the exit, the slope of the Heat Transfer Coefficient gradually rises due to end effect. The figure shows that at higher Reynolds number, the curve of the local Heat Transfer Coefficient along the length of the finned tube is higher. This is expected because a higher flow rate results in increment of heat transfer coefficient at both tube surface and the surface of the fins. The average Heat Transfer Coefficient of in-line segmented finned tube is higher than that of In Line Finned Tube and Smooth Tube.

Figure B35 and B40 shows $(T_w - T_b)_x$ VS. X/L and X/D respectively for different Reynolds number based on inside diameter. The $(T_w - T_b)_x$ value is low in the entrance region. In the middle smooth portion of the tube $(T_w - T_b)_x$ value increases as the fin is absent in that portion. After that portion it decreases gradually. Just up-stream of the exit, the slope of $(T_w - T_b)_x$ gradually falls due to end effect.

Figure B34 and B41 show the wall, bulk and fin tip temperature distribution VS. X/L and X/D respectively for one Reynolds number.

Comperative Analysis for Smooth Tube, In-Line Finned Tube and In-Line Segmented Finned Tube:

Figure B42 shows the variation of friction factor F_i with Reynolds number for the three tubes. For all the tubes Friction factor decreases as the Reynolds number increases. It can be noted that friction factor for a in-line finned tube is much higher than that of a Smooth Tube. Friction factor of a in-line finned tube is 1.93 to 3.5 times higher than that of smooth tube for comparable Reynolds number. It can be noted that friction factor for in-line segmented finned tube is higher than that of a Smooth Tube and lower than that of In Line Finned Tube. Friction factor

of a in-line segmented finned tube is 1.72 to 2.5 times higher than that of smooth tube for comparable Reynolds number.

Figure B43 shows the variation of Average Heat Transfer Coefficient h with Reynolds number for different tubes. For all the tubes Average Heat Transfer Coefficient increases as the Reynolds number increases. It can be noted that Average Heat Transfer Coefficient for a in-line finned tube is much higher than that of a smooth tube, in-line finned tube [Jalal(27)] and nearly similar that of in-line finned tube [Mafiz(12-13)] for comparable Reynolds number. It can be noted that Average Heat Transfer Coefficient for in-line segmented finned tube is higher than that of a Smooth Tube and nearly similar that of in-line finned tube for comparable Reynolds number.

Figure B44 shows the variation of Pumping power, P_m with Reynolds number for the three tubes. For all the tubes Pumping power increases as the Reynolds number increases. It can be noted that Pumping power for a in-line finned tube is much higher than that of a Smooth Tube. Pumping power of a in-line finned tube is 2.44 to 3.41 times higher than that of smooth tube for comparable Reynolds number. It can be noted that Pumping power for in-line segmented finned tube is higher than that of a Smooth Tube and lower than that of In Line Finned Tube. Pumping power of a in-line segmented finned tube is 2.21 to 2.34 times higher than that of smooth tube for comparable Reynolds number.

Figure B45, B46, B47 shows the velocity distribution along the tube diameter of Smooth Tube, In-Line Finned Tube and In-Line Segmented Finned Tube.

Figure B48 and B49 shows the Calibration curve of the thermocouples and Calibration curve of the pressure transducers respectively.

CHAPTER-VII

CONCLUSIONS

Steady state fluid flow and heat transfer performance of a circular smooth tube, a circular tube with continuous internal longitudinal fins, a circular tube with internal longitudinal fins interrupted in the stream wise direction by arranging them in an in-line were studied experimentally. Results indicate that the heat transfer performances for a in-line finned tube is higher than that for a smooth tube. Results also indicate that for the in-line segmented fin arrangement gives almost as much heat transfer augmentation as the in-line finned tube but with a much lower pressure drop penalty.

The findings of the present study are summarized below:

1. Friction factor of in-line finned tube Tube is 1.93 to 3.5 times higher than that of smooth tube. Friction factor of in-line segmented finned tube is 1.72 to 2.5 times higher than that of smooth tube.
2. For all the Tubes the local friction factor is high near the inlet, and drops gradually to the fully developed value.
3. Pumping power for a in-line finned tube is much higher than that of a Smooth Tube. Pumping power of a in-line finned tube is 2.44 to 3.41 times higher than that of smooth tube for comparable Reynolds number. Pumping power for in-line segmented finned tube is higher than that of a Smooth Tube and lower than that of In Line Finned Tube. Pumping power of a in-line segmented finned tube is 2.21 to 2.34 times higher than that of smooth tube for comparable Reynolds number.
4. For smooth tube Local Heat Transfer Coefficient is high in the entrance region as at this portion the cold air start to mix up with the hot tube and it decreases with increasing the axial distance approaching the fully developed value. For in line finned tube Local Heat Transfer Coefficient is high in the entrance region and it

decreases with increasing the axial distance approaching the fully developed values. Just up-stream of the exit, the slope of the Heat Transfer Coefficient gradually rises due to end effect. For In Line Segmented Finned Tube Local Heat Transfer Coefficient is high in the entrance region and it decreases with increasing the axial distance. In the middle unfinned portion of the tube Local Heat Transfer Coefficient increases. After that portion Local Heat Transfer Coefficient decreases and Just up-stream of the exit, the slope of the Local Heat Transfer Coefficient gradually rises.

5. For all the tubes at higher Reynolds number, the curve of the Local Heat Transfer Coefficient along the length of the finned tube is higher.
6. Heat transfer for the in-line finned tube is 1.7 to 1.8 times higher than that of smooth tube for comparable Reynolds number. Heat transfer for the in-line segmented finned tube is 1.77 to 1.9 times higher than that of smooth tube for comparable Reynolds number. It is observed from experiment that for comparable Reynolds number heat transfer and surface heat transfer coefficient for in-line finned tube and in-line segmented finned tube are similar but for in-line segmented finned tube pressure drop and pumping power is less than that of in-line finned tube.

The results thus show that both inline finned tube and in-line segmented finned tube results in heat transfer enhancement but in-line segmented finned tube results in the same heat transfer enhancement with less pressure drop and with less pumping power.

REFERENCES

1. Bergles, A.E. Brown, J.S. and Snider, W.D., 1971, "Heat Transfer Performance of Internally Tubes", ASME Paper No. 71, HT-31, American Society of Mechanical Engineers, New York.
2. Carnavos, T. C., Aug, 1977 " Cooling Air in Turbulent Flow with Internally Finned Tubes," AI Ch E paper no. 4, 17th National Heat Transfer Conference.
3. Carnavos, T. C., Apr - June, 1980 " Heat Transfer Performance of Internally Finned Tubes in Turbulent Flow," Heat Transfer Engineering Journal Vol. 1 No. 4, pp. 32-37.
4. Chowdhury, D. and Patankar, S.V., 1985, "Analysis of Developing Laminar Flow and Heat Transfer in Tubes with Radial Internal Fins", Proc. ASME National Heat Transfer Conference, pp. 57-63.
5. D. L. Gee and R. L. Webb, " Forced Convection Heat Transfer in Helically Rib - Roughed Tubes", International Journal of Heat and Mass Transfer Vol. 23 pp. 1127-1136,1980.
6. Edwards, D.P. and Jensen, M.K., 1994, "Pressure Drop and Heat Transfer Predictions of Turbulent Flow in Longitudinal Finned Tubes", Advances in Enhanced Heat Transfer, ASME HTD-Vol. 287, pp. 17-23.
7. E Ower & R. C. Pankhurst, " The Measurement of Air Flow."
8. Hiding, W.E. and Coogan, C.H., 1964, "Heat Transfer and Pressure Loss Measurements in Internal Finned Tubes", Symposium on Air Cooled Heat Exchangers, ASME, National Heat Transfer Conference, Clevelant, Ohio, pp. 57-85.

9. Holman, J.P., 1994, "Experimental Methods for Engineers", Sixth Edition, McGraw Hill, New York.
10. ✓ Hu, M.H. and Chang, Y.P., 1973, "Optimization of Finned Tubes for Heat Transfer in Laminar Flow", Journal of Heat Transfer, Vol. 95, pp. 332-338.
11. Kays, W.M. and Crawford, M.F., 1993, "Convective Heat and Mass Transfer", Third Edition, McGraw Hill, New York.
12. Mafiz, Huq and Rahman, " An Experimental Study of Heat Transfer in an Internally Finned Tube." Proceedings ASME Heat Transfer Division, Volume 2, pp. 211-217, 1996.
13. Mafiz, Huq and Rahman, " Experimental Measurements of Heat Transfer in an Internally Finned Tube." Accepted for publication in the journal of International Communication in Heat and Mass Transfer, CJ97/1890, 1998.
14. ✓ Nandakumar, K. and Masliyah, J.H., 1975, "Fully Developed Viscous Flow in Internally Finned Tubes", Chemical Engineering Journal, Vol. 10, pp. 113-120.
15. ✓ Patankar, S.V., Ivanovic, M. and Sparrow, E.M., 1979, "Analysis of Turbulent Fluid Flow and Heat Transfer in Internally Finned Tubes and Annuli", Journal of Heat Transfer, Vol. 101, pp. 29-37.
16. ✓ Prakash, C. and Liu, Y.D., 1985, "Analysis of Laminar Flow and Heat Transfer in the Entrance Region of an Internally Finned Circular Duct", Journal of Heat Transfer, Vol. 107, pp. 84-91.
17. ✓ Prakash, C. and Patankar, S.V., 1981, "Combined Free and forced Convection in Vertical Tubes with Radial Internal Fins", Journal of Heat Transfer, Vol. 103, pp. 566-572.

18. ✓ Rustum, I.M. and Soliman, H.M., 1988, "Numerical Analysis of Laminar forced Convection in the Entrance Region of Tubes with Longitudinal Internal Fins", Journal of Heat Transfer, Vol. 110, pp. 310-313.
19. Rustum, I.M. and Soliman, H.M., 1988, "Experimental Investigation of Laminar Mixed Convection in Tubes with Longitudinal Internal Fins", Journal of Heat Transfer, Vol. 110, pp. 366-372.
20. Soliman, H.M., Chau, T.S. and Trupp, A.C., 1980, "Analysis of Laminar Heat Transfer in Internally Finned Tubes with Uniform Outside Wall Temperature", Journal of Heat Transfer, Vol. 102, pp. 598-604.
21. Watkinson, A.P., 1973, "Turbulent Heat Transfer and Pressure Drop in Internally Finned Tubes", AIChE Symposium Series, Vol. 69, No. 131, pp. 94-103.
22. Zhang, H. Y. and Ebdian, M. A., 1992, "Heat Transfer in the Entrance Region of Semicircular Ducts with Internal Fins", Journal of Thermophysics and Heat Transfer, Vol. 6, No. 2, pp. 296-301.
23. Carnavos T. C, June, 1980, ".Heat Transfer Performance Of Internally Finned Tubes In Turbulent Flow", Heat Transfer Engineering Vol. 1, No.4.
24. Watkinson A. P., Miletti D. L., Kubanek G.R., 1975, "Heat Transfer And Pressure Drop Of Internally Finned Tubes In Laminar Oil Flow" ASME , American Society of Mechanical Engineers, New York.
25. Kelkar K. M. and Patankar S. V., August 1987, "Numerical Prediction of Fluid Flow and Heat Transfer in a circular Tube with Longitudinal Fins Interrupted in The Streamwise Direction." Presented at the National Heat Transfer Conference, Pittsbrugh, Pennsylvania.
26. Kline S.J and McClintock F.A, "Describing Uncertainties in Single Experiments" Mech. Engg. Jan 1953.
27. Jalal Uddin, Md. " Study of Pressure Drop Characteristics and Heat Transfer Performance in an Internally Finned Tube." Thesis submitted to the Dept of Mechanical Engg. BUET. 1998.

APPENDIX A
FIGURES

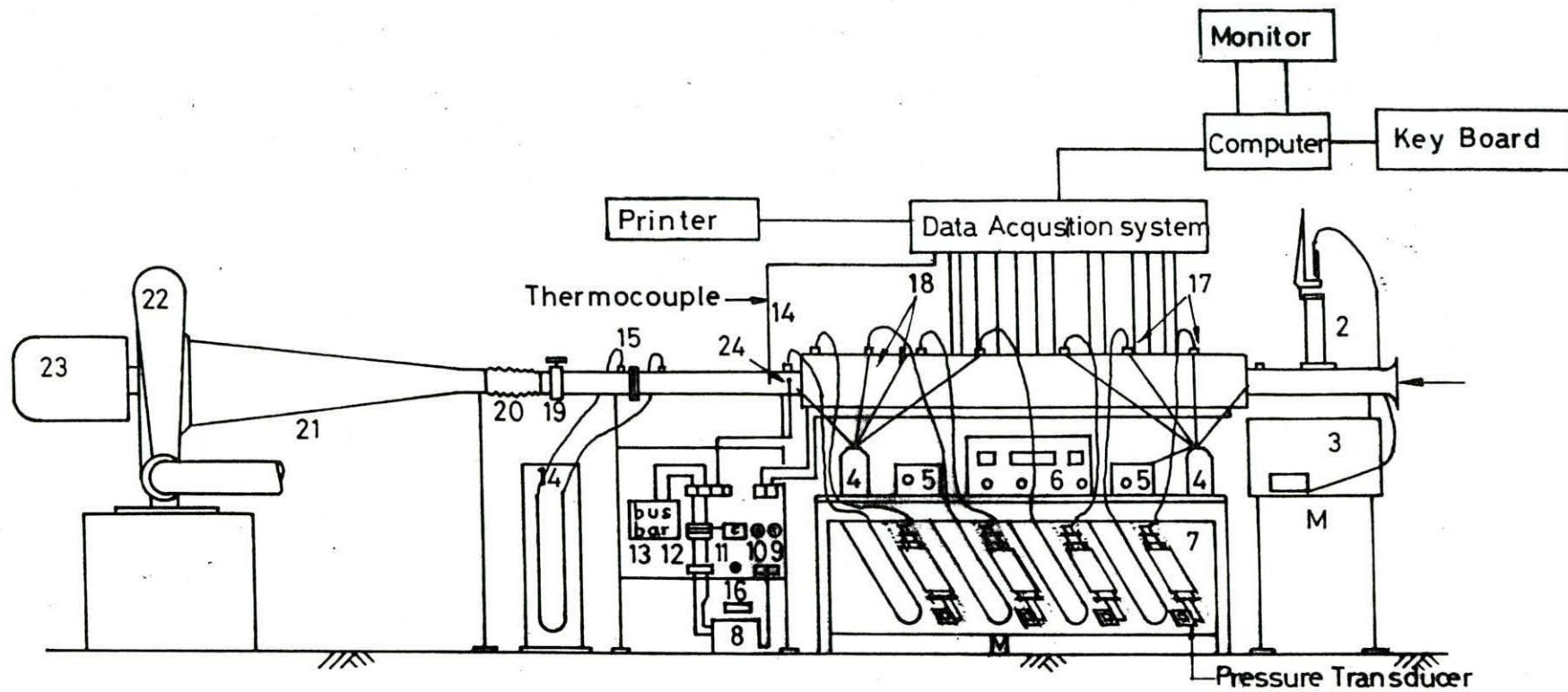


FIG. SCHEMATIC DIAGRAM OF EXPERIMENTAL SET UP

1520 MM
70 MM

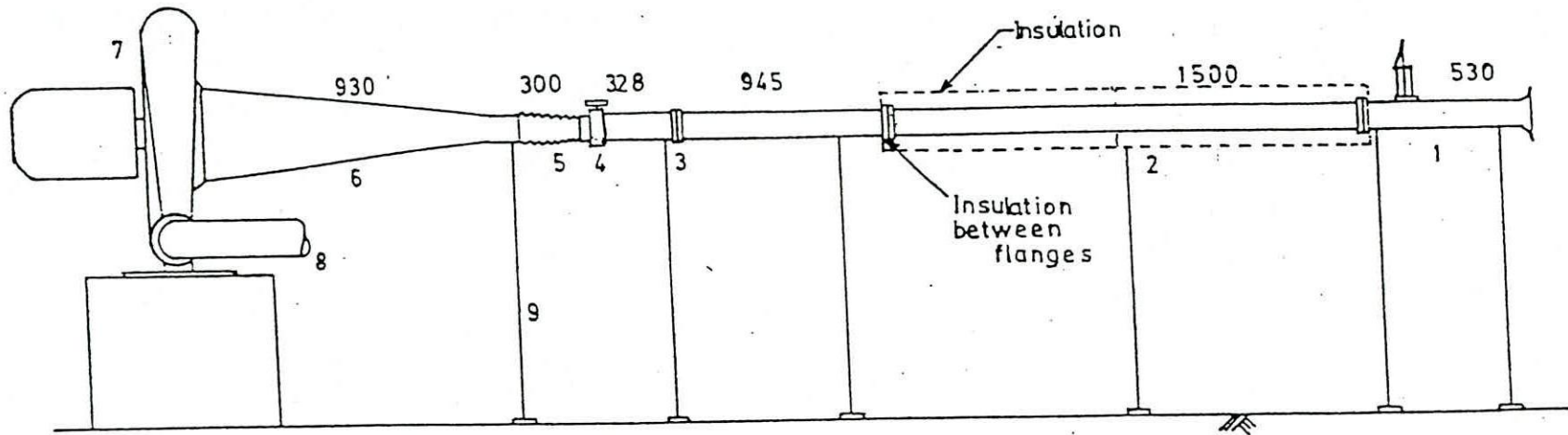
5KVA variable
voltage transformer

- 1. Shaped inlet
- 2. Traversing pitot
- 3. Inclined tube manometer
- 4. Ice bath
- 5. Selector switch
- 6. Microvoltmeter (DVM)
- 7. U-tube manometers
- 8. Variable voltage transformer

- 9. Ammeter
- 10. Voltmeter
- 11. Temperature controller
- 12. Magnetic contactor
- 13. Bus bar
- 14. U-tube manometer
- 15. Orifice meter
- 16. Heater on off lamp

- 17. Pressure tapping
- 18. Thermocouples
- 19. Flow control valve
- 20. Flexible pipe
- 21. Diffuser
- 22. Fan
- 23. Motor

30 m³/min



1	Shaped inlet
2	Test section
3	Orifice meter
4	Gate valve
5	Flexible duct
6	Diffuser
7	Pan
8	Outlet
9	Supports

All dimensions in mm.

FIG. A2 SCHEMATIC DIAGRAM OF EXPERIMENTAL SET UP WITH DIMENSIONS

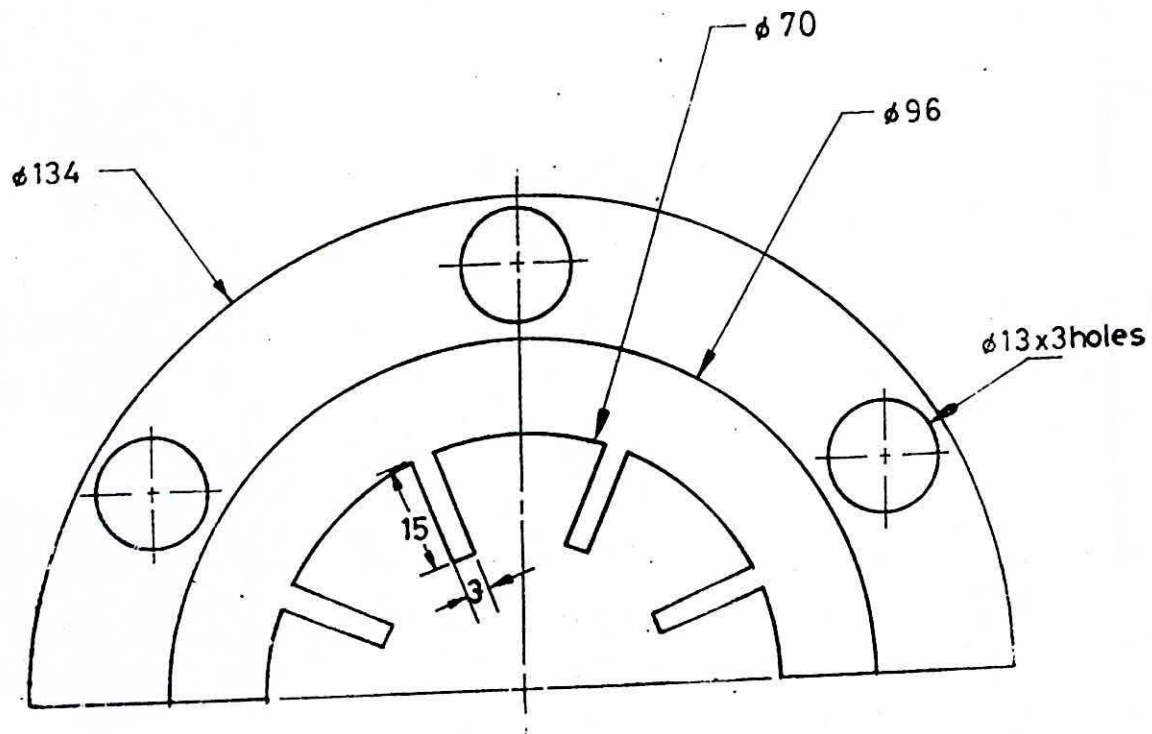


FIG. 3A HALF OF THE CIRCULAR TUBE WITH FINS

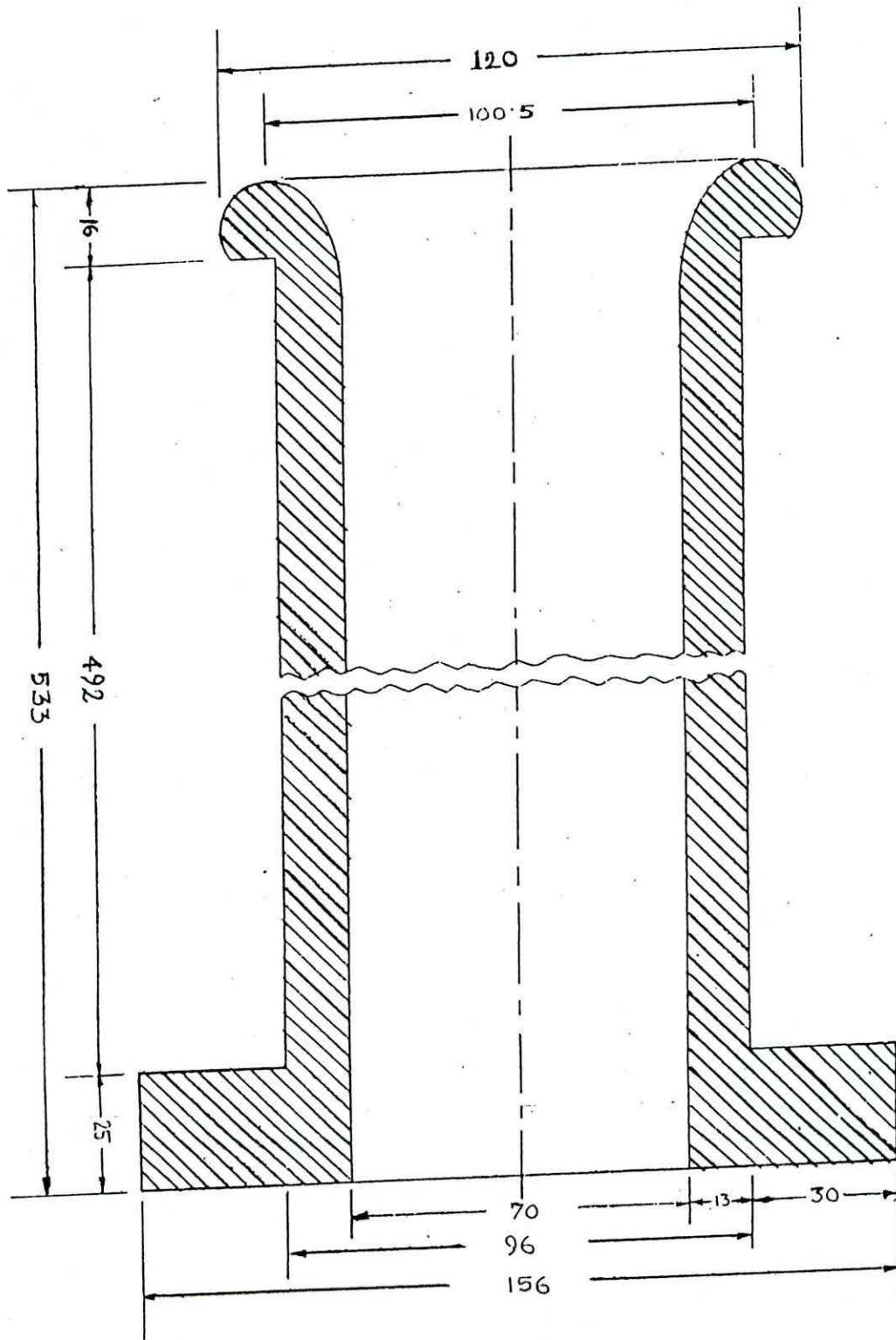


FIG. A. 3B SHAPED INLET

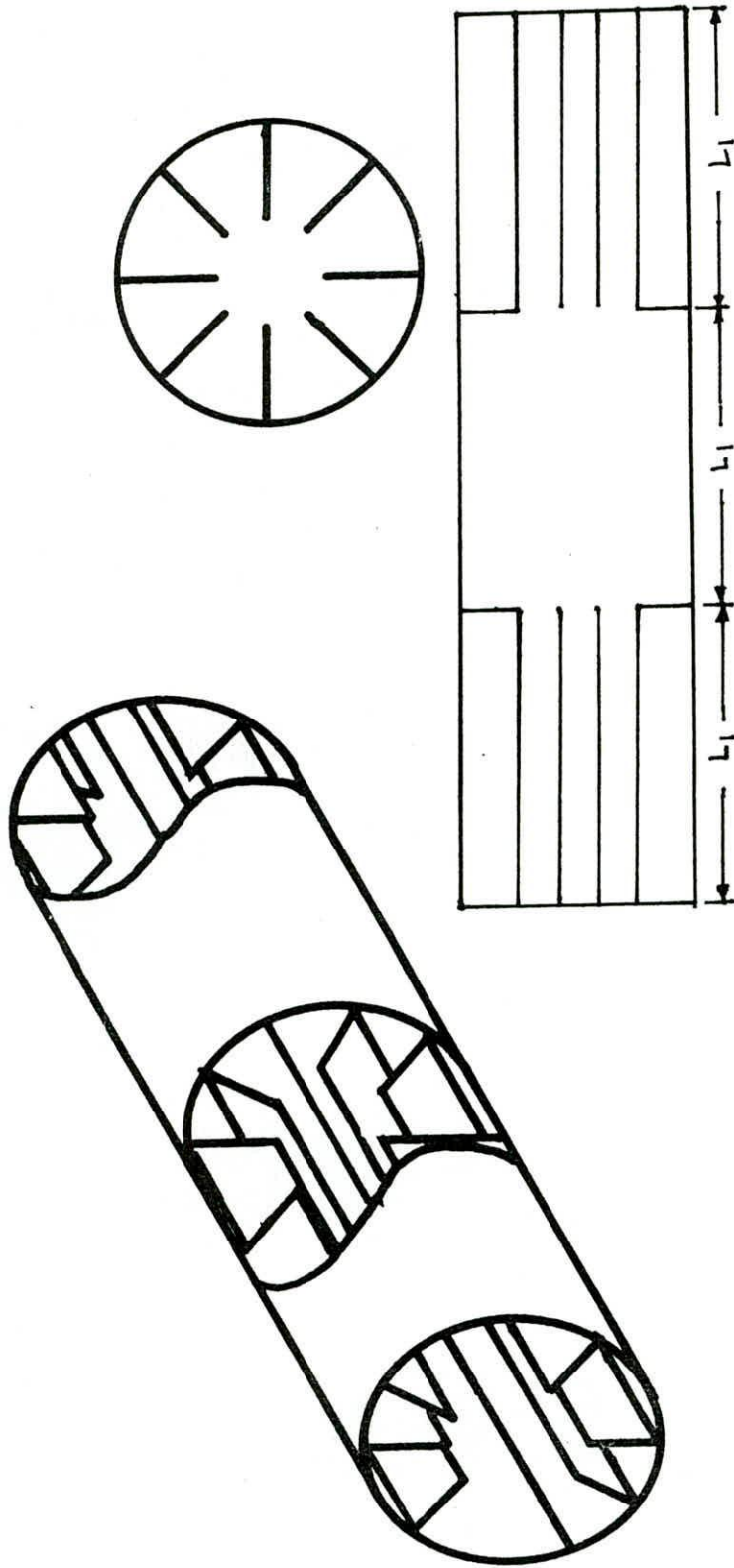


Fig. A4 Schematic Diagram of Inline Segmented Fin Tube

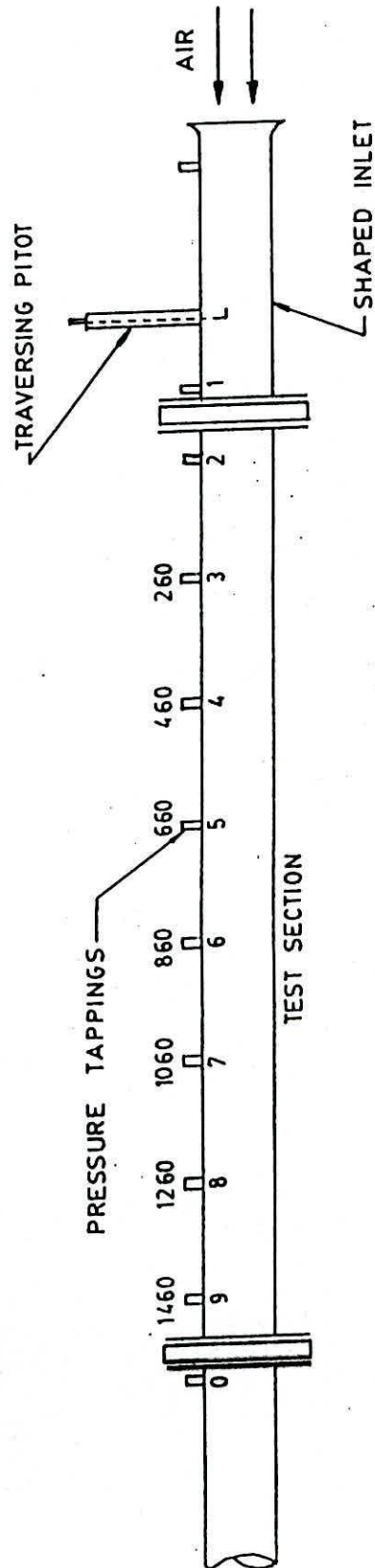
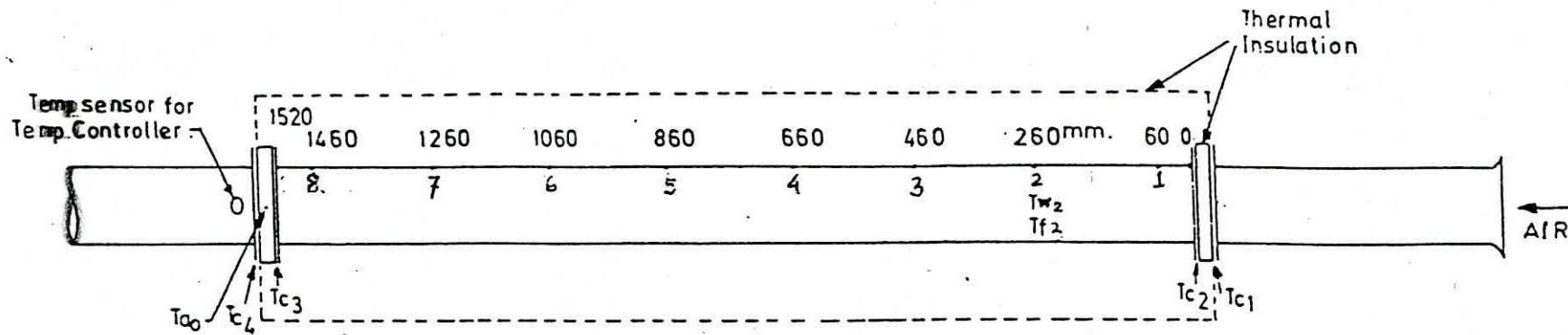


FIG. A5. LOCATION OF PRESSURE TAPPING



- W ~ Wall
- f ~ Fin
- i ~ Inlet
- o ~ Outlet
- a ~ Air
- c ~ Coupling/Flange

- Ta0 ~ Air outlet temp
- Tc ~ Temp at the flange
- Tw2 ~ Wall temp at 2
- Tf2 ~ Fin-tip temp at 2

FIG. A6 LOCATION OF THERMOCOUPLES

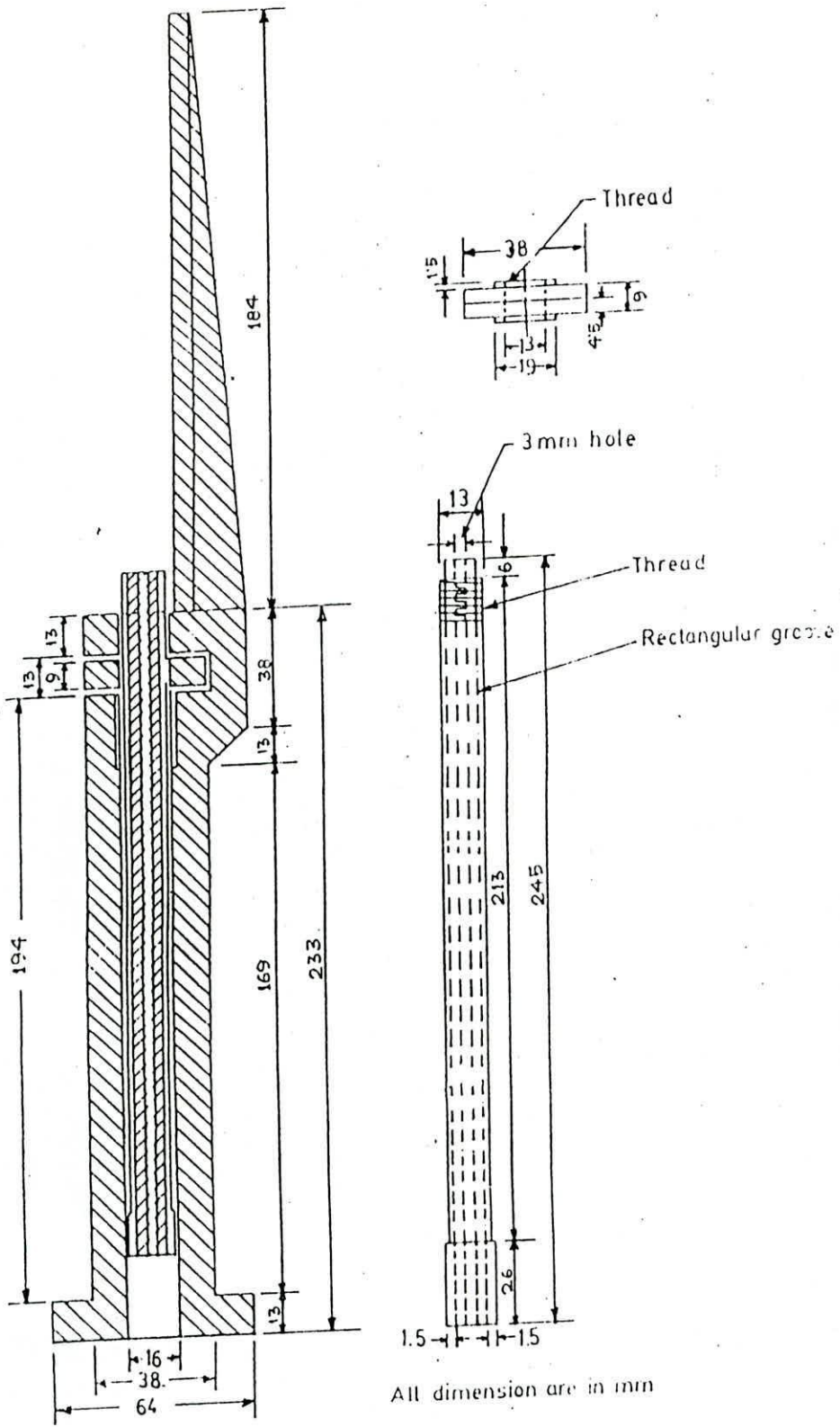


FIG. A7 TRAVERSING PITOT. HOLDING DEVICE

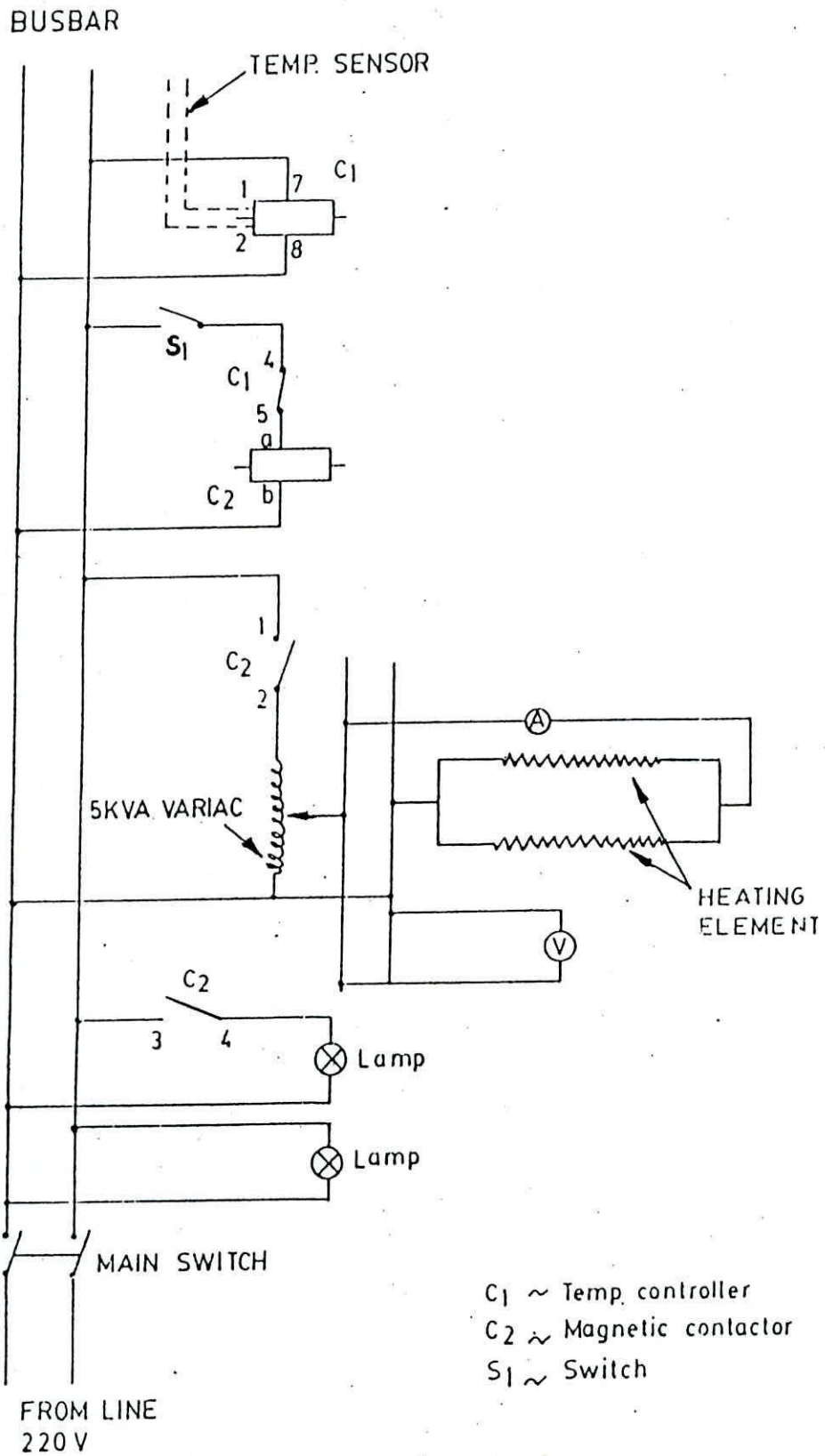


FIG. A8 ELECTRIC CIRCUIT DIAGRAM FOR HEATING SYSTEM

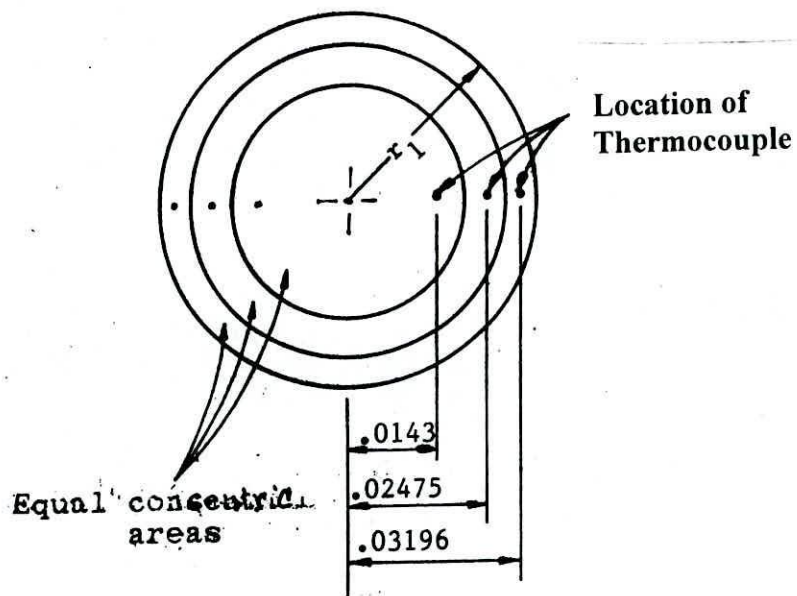


Fig. A9 . Location of Thermocouple for Measurement of Outlet Temperature

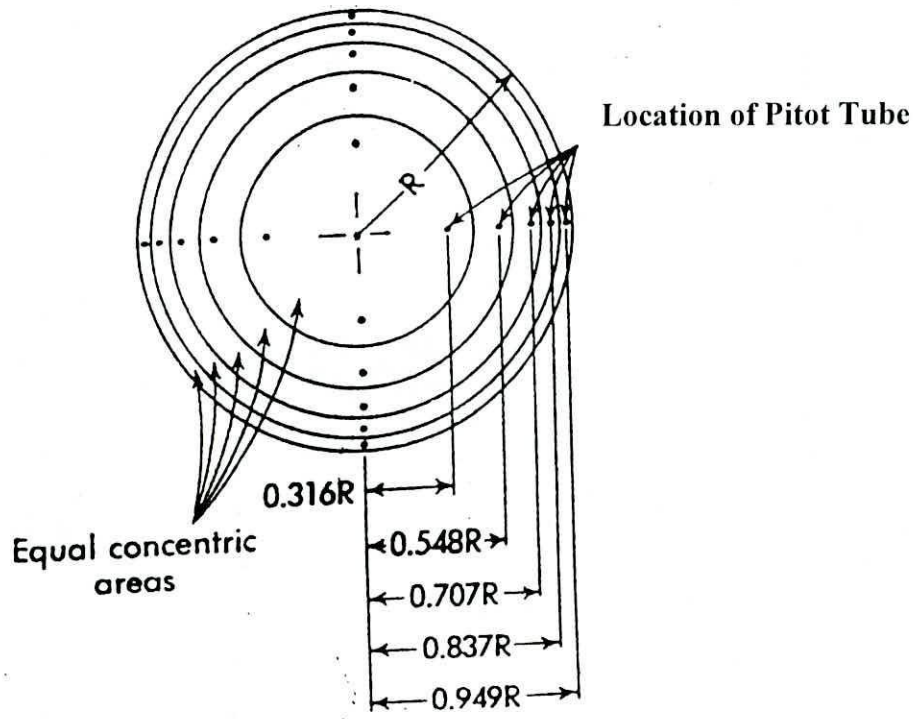


Fig. A10 Location of Pitot Tube for Measurement of Velocity

APPENDIX B
GRAPHS

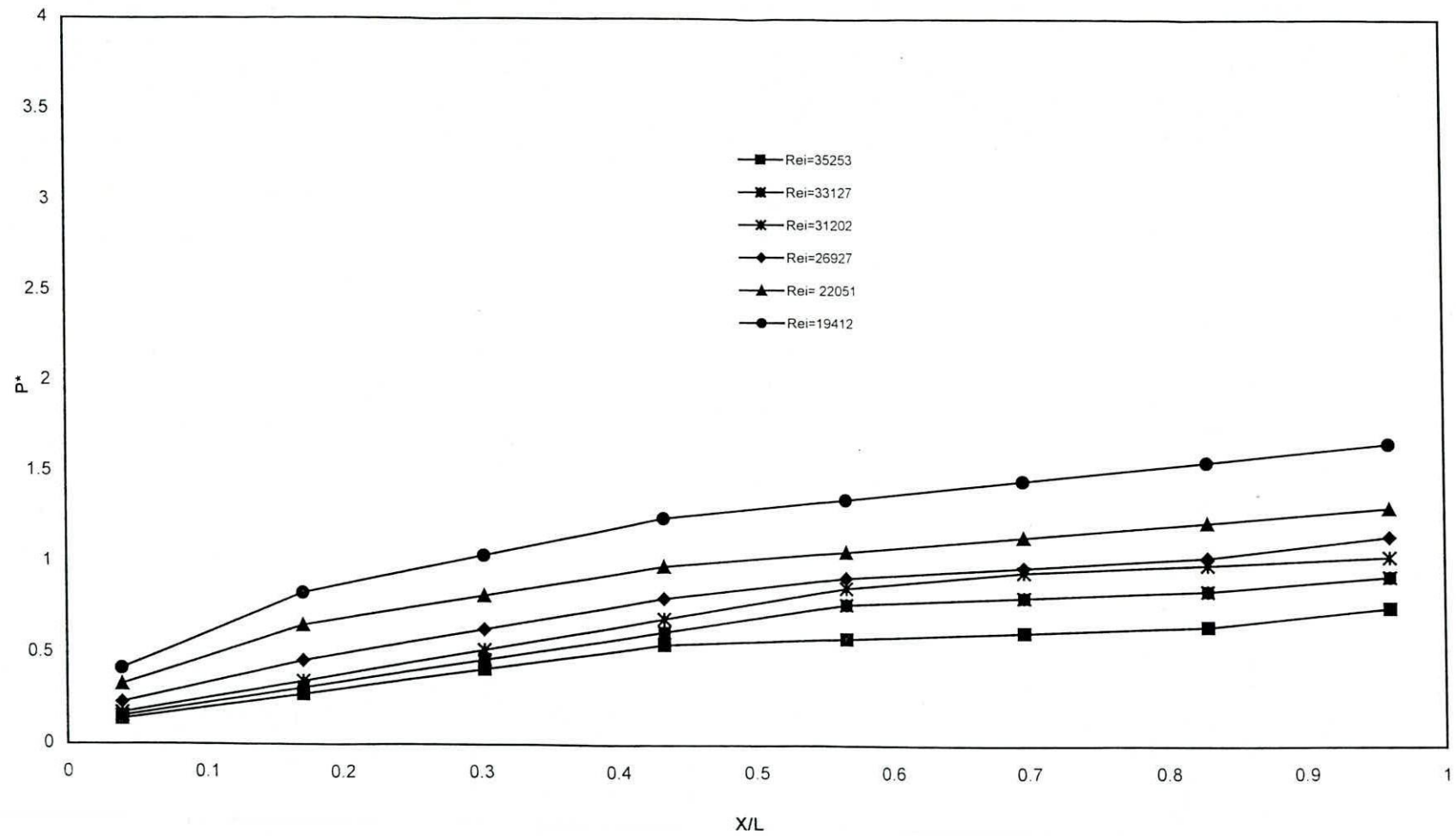


Fig. B1 Pressure Drop Along Axial Distance of Smooth Tube.

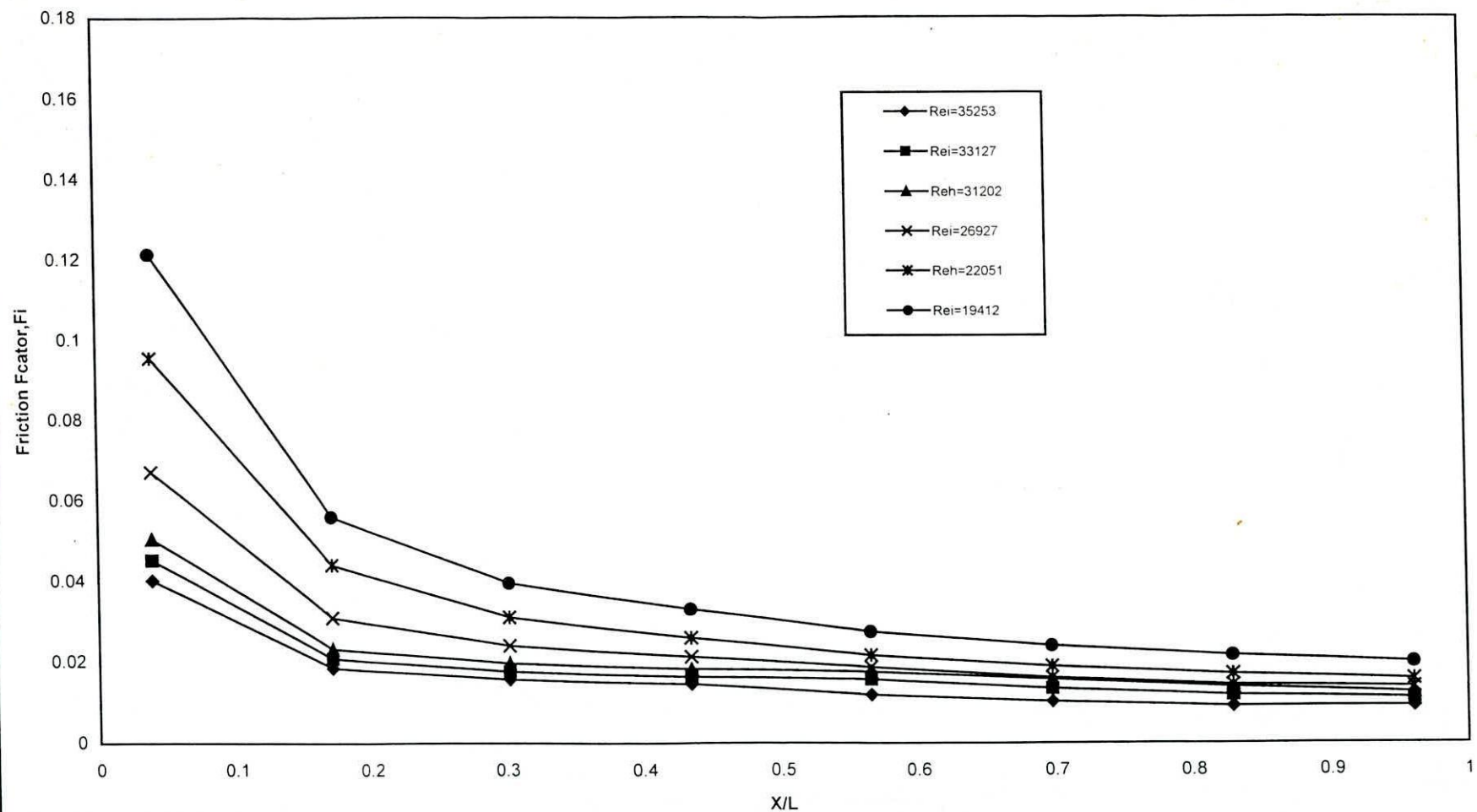


Fig.B2 Distribution of Friction Factor Along Axial Distance of Smooth Tube

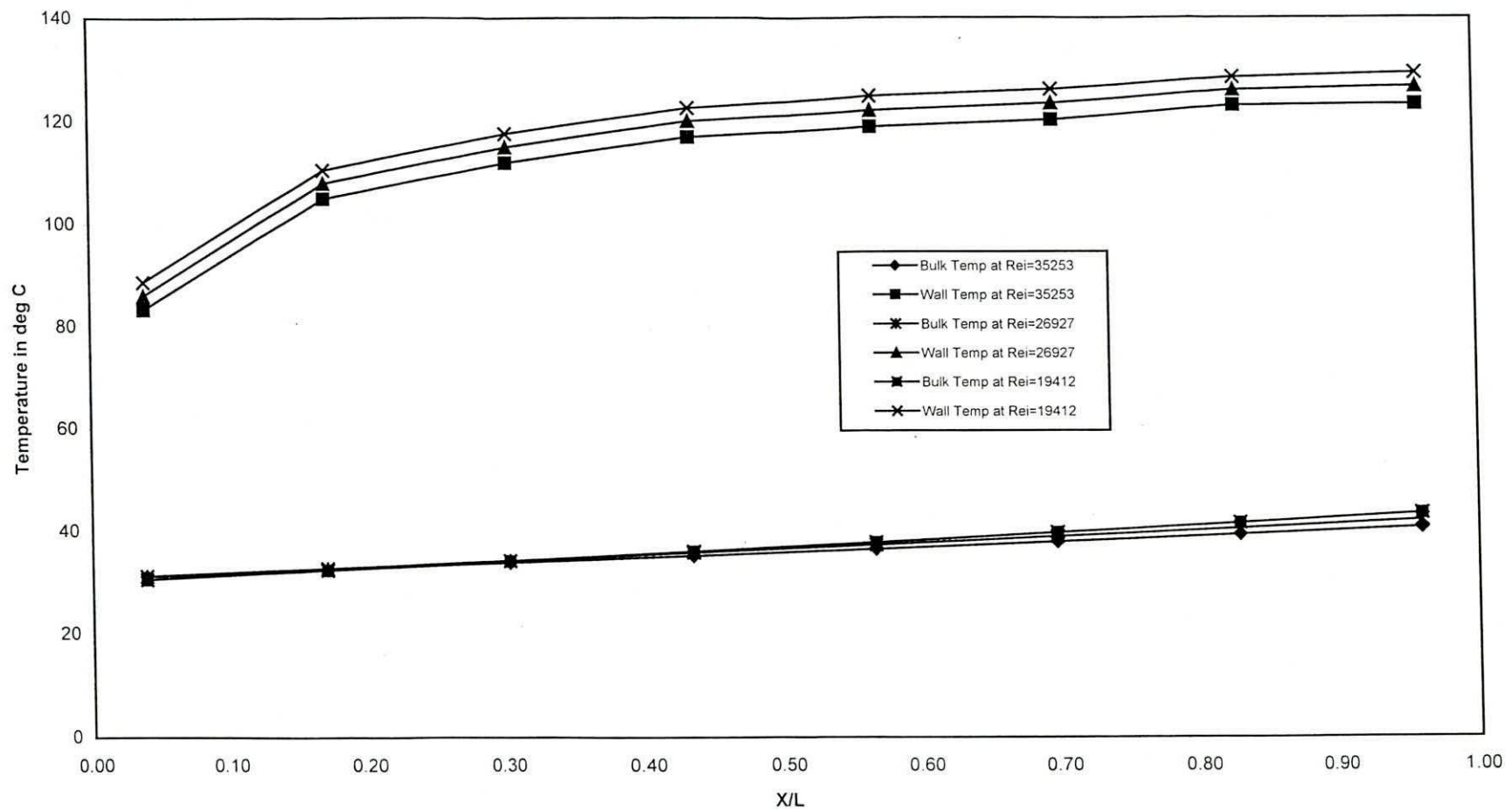


Fig. B3 Wall and Bulk Temperature Distribution Along the Axial Distance of Smooth Tube

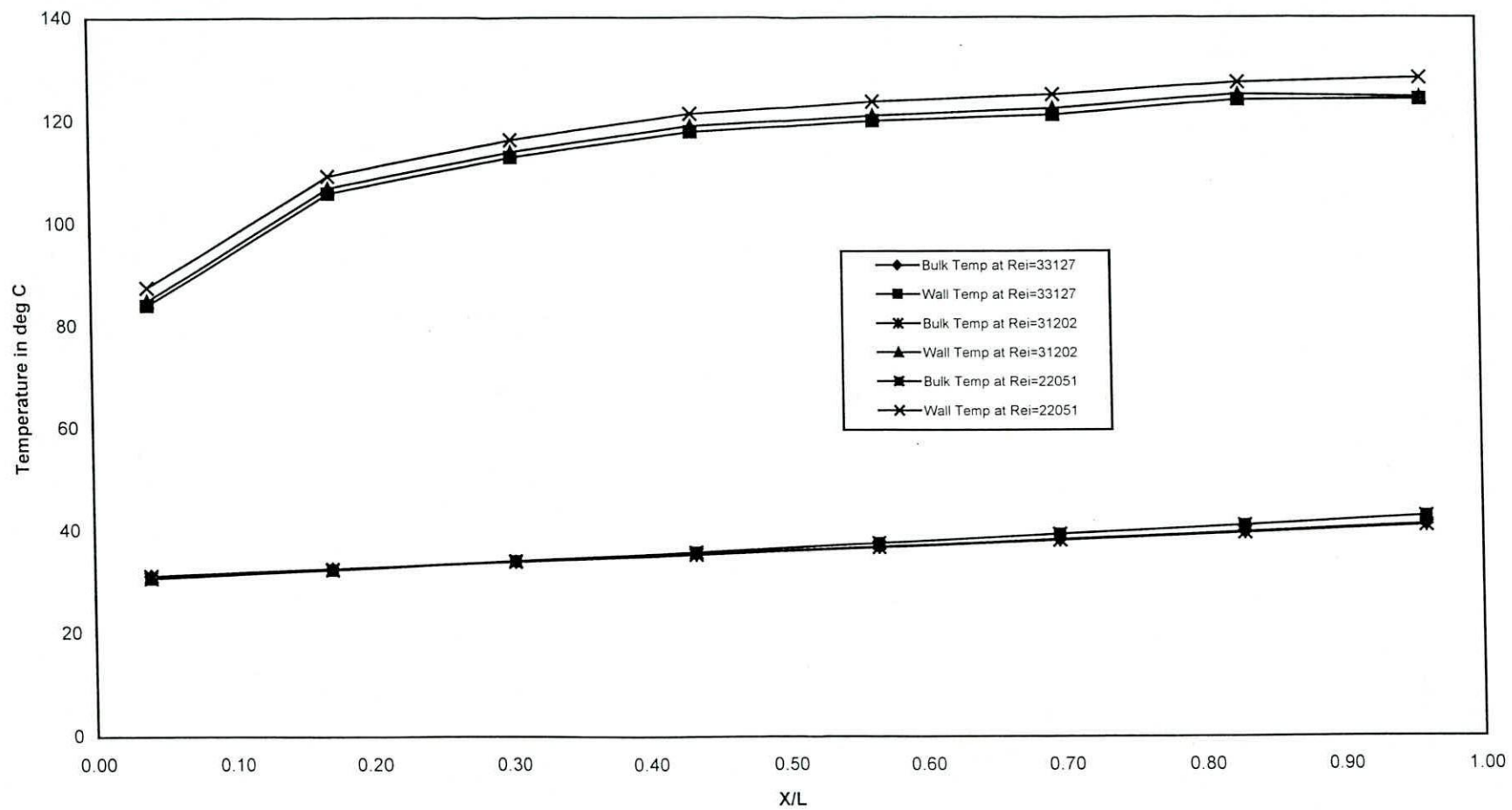


Fig. B4 Wall and Bulk Temperature Distribution Along axial Distance of Smooth Tube

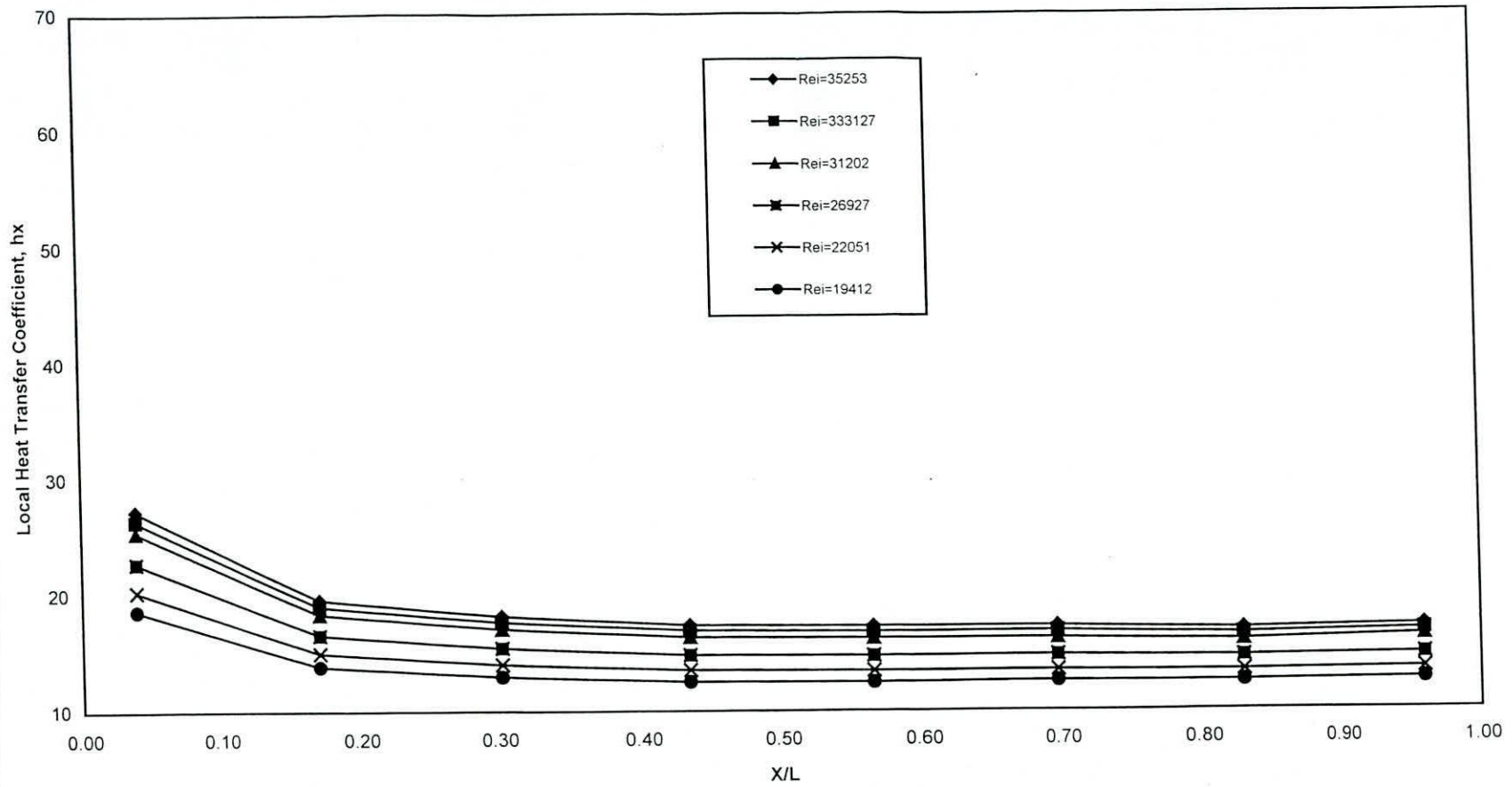


Fig. B5 Local Heat Transfer Coefficient Along Axial Distance of Smooth Tube at Different Reynolds Number

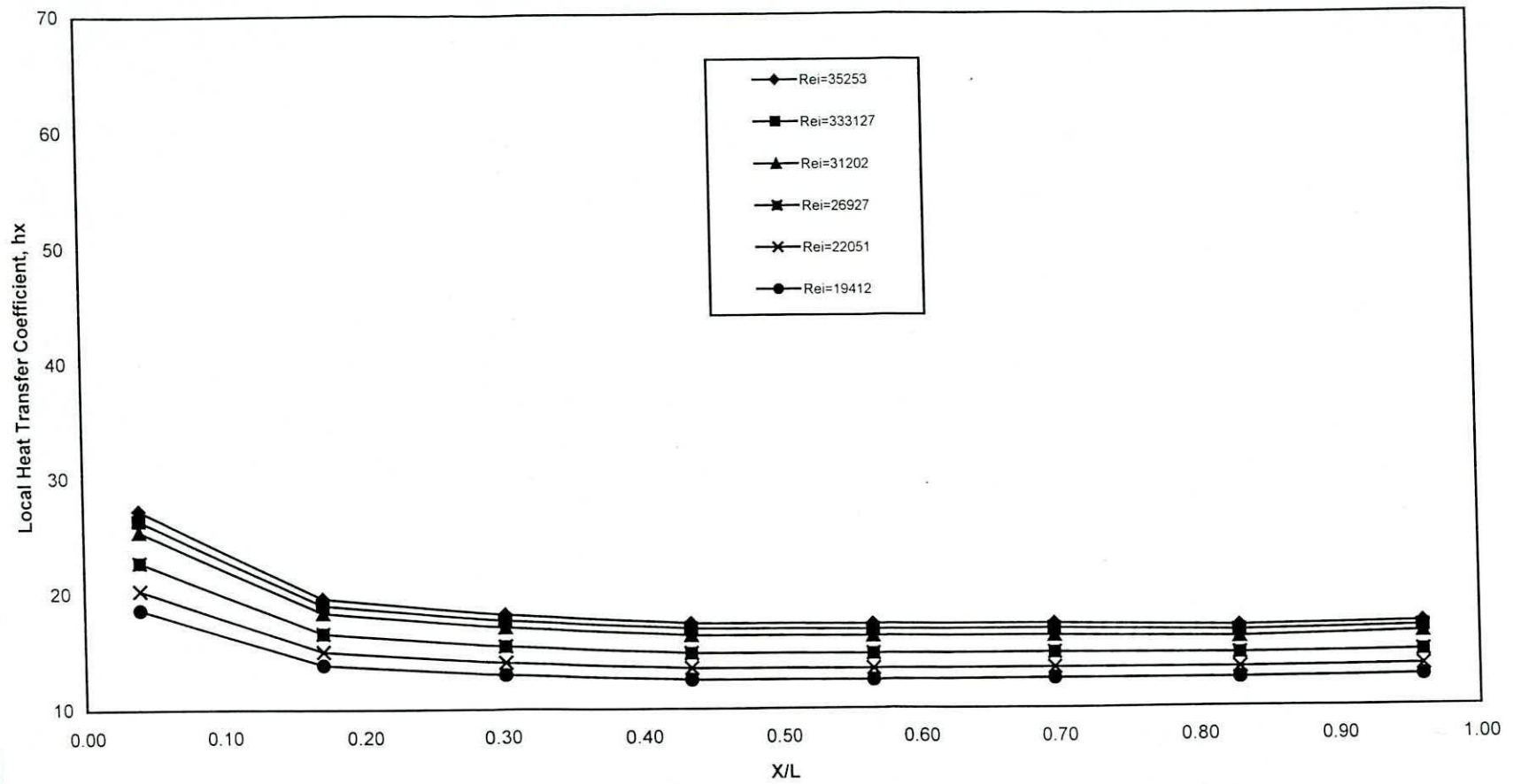


Fig. B5 Local Heat Transfer Coefficient Along Axial Distance of Smooth Tube at Different Reynolds Number

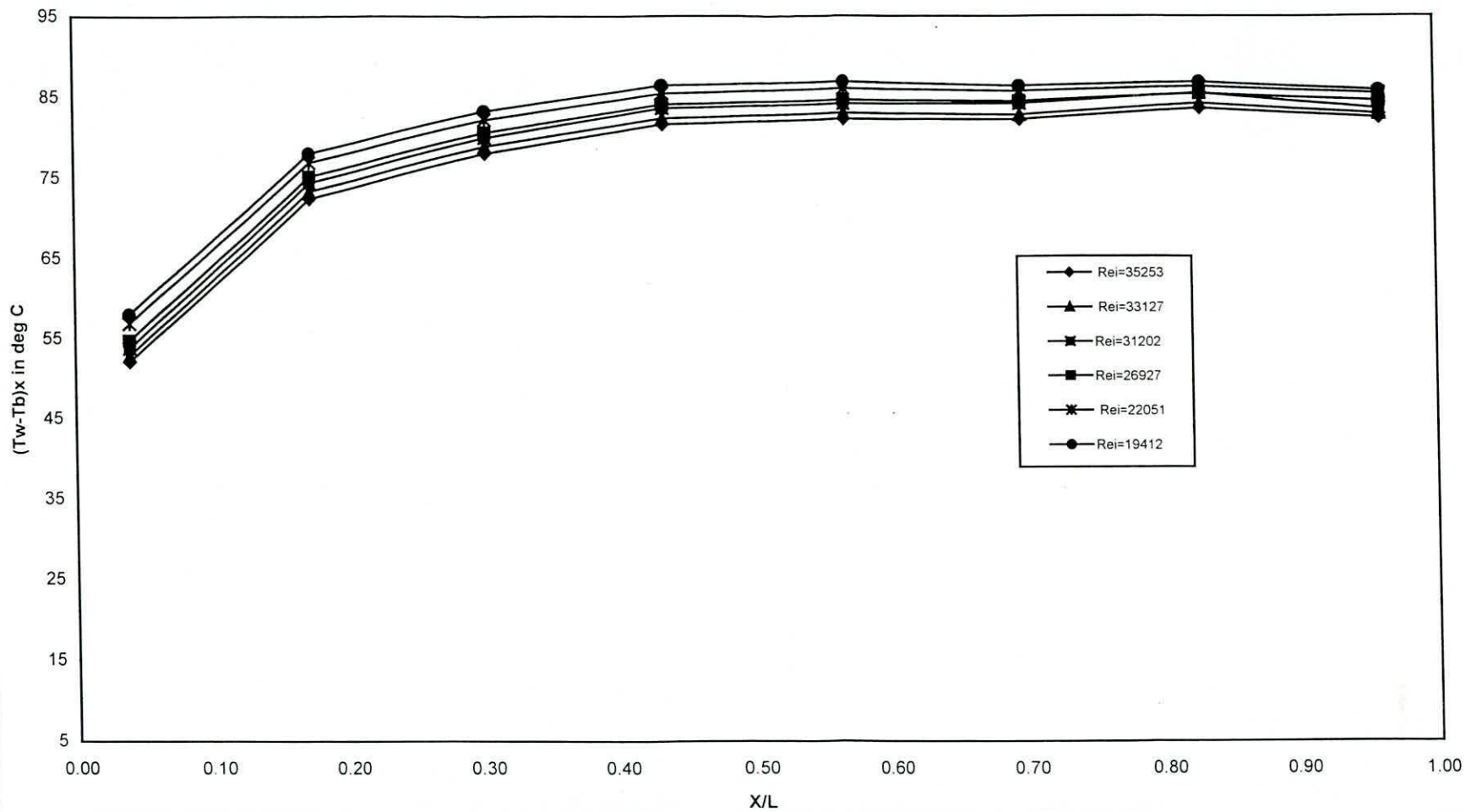


Fig. B6 Difference Between Wall and Bulk Temperature Along Axial Distance of the Smooth Tube

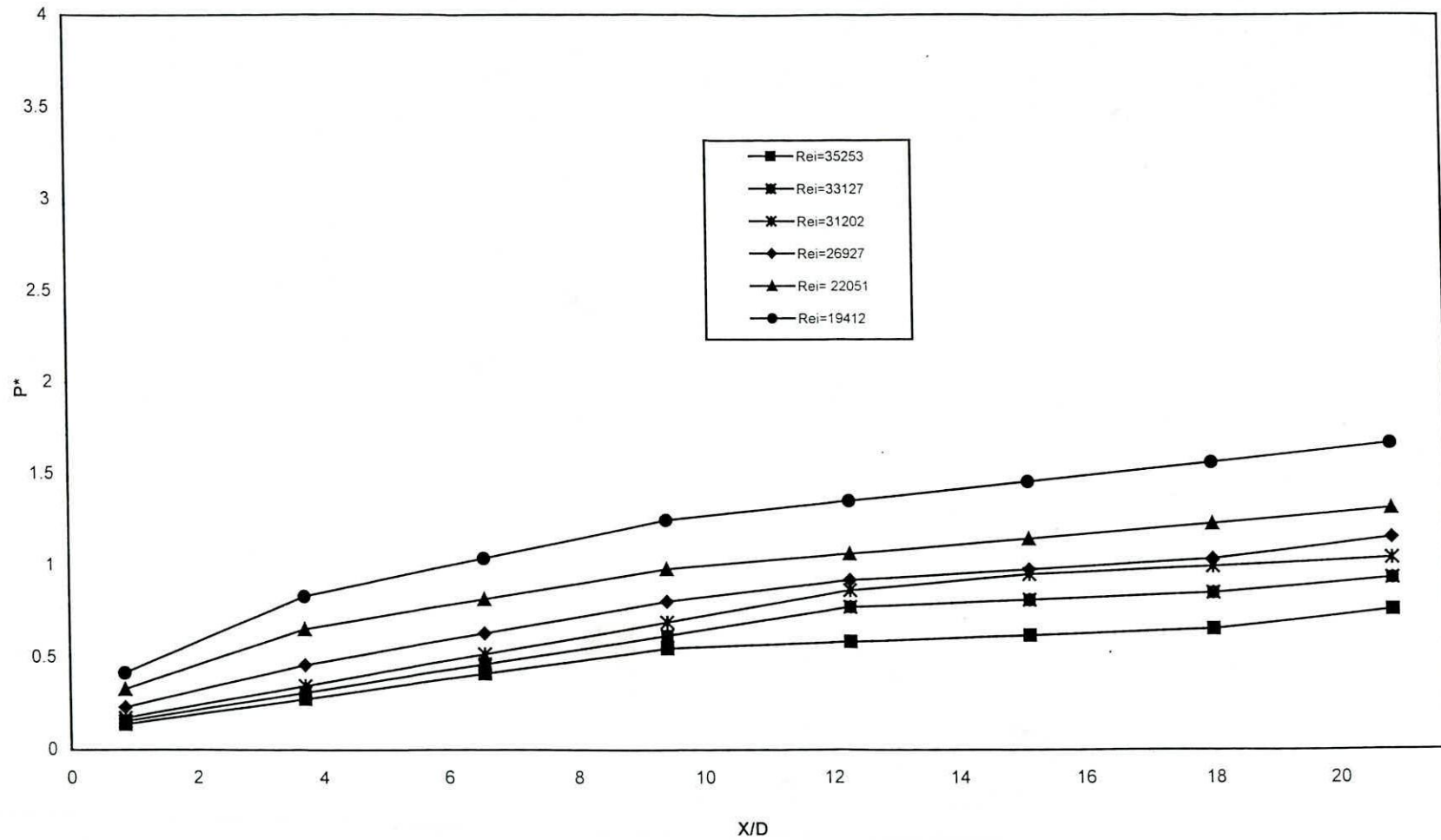


Fig.B7 Pressure Drop Along the Length of the Smooth Tube.

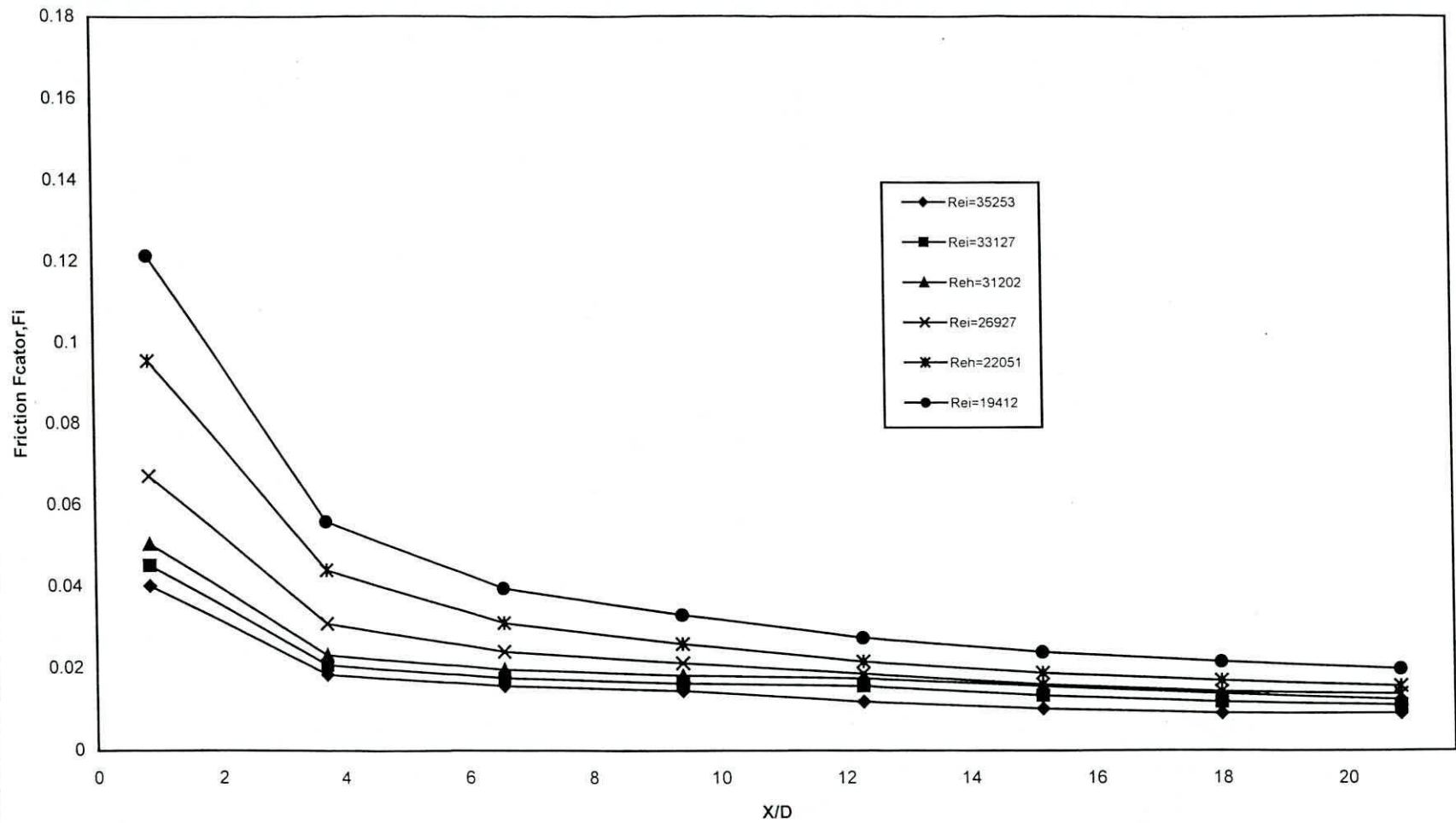


Fig. B8 Distribution of Friction Factor Along The Length of Smooth Tube

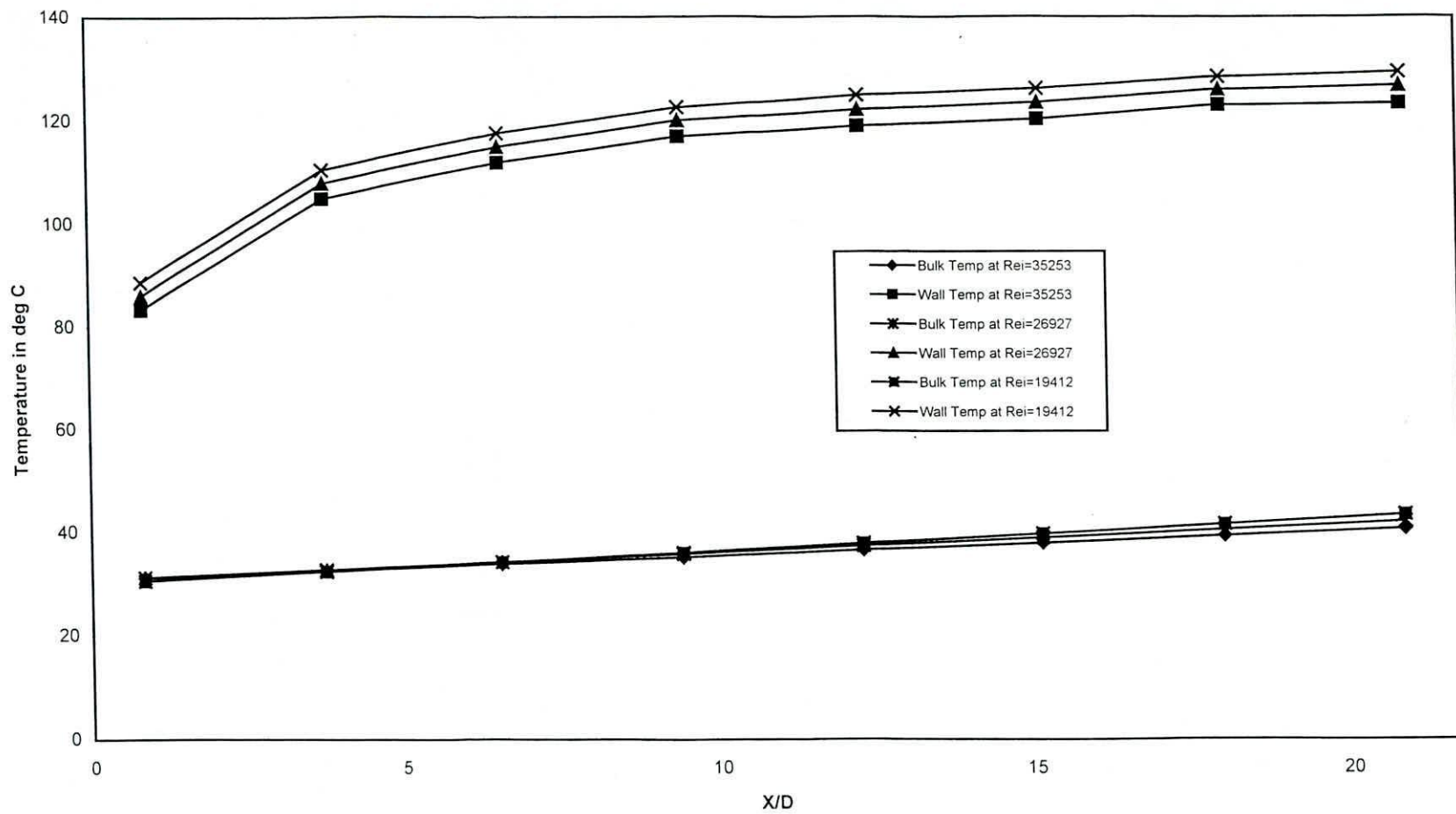


Fig. B9 Wall and Bulk Temperature Distribution Along the Length of Smooth Tube

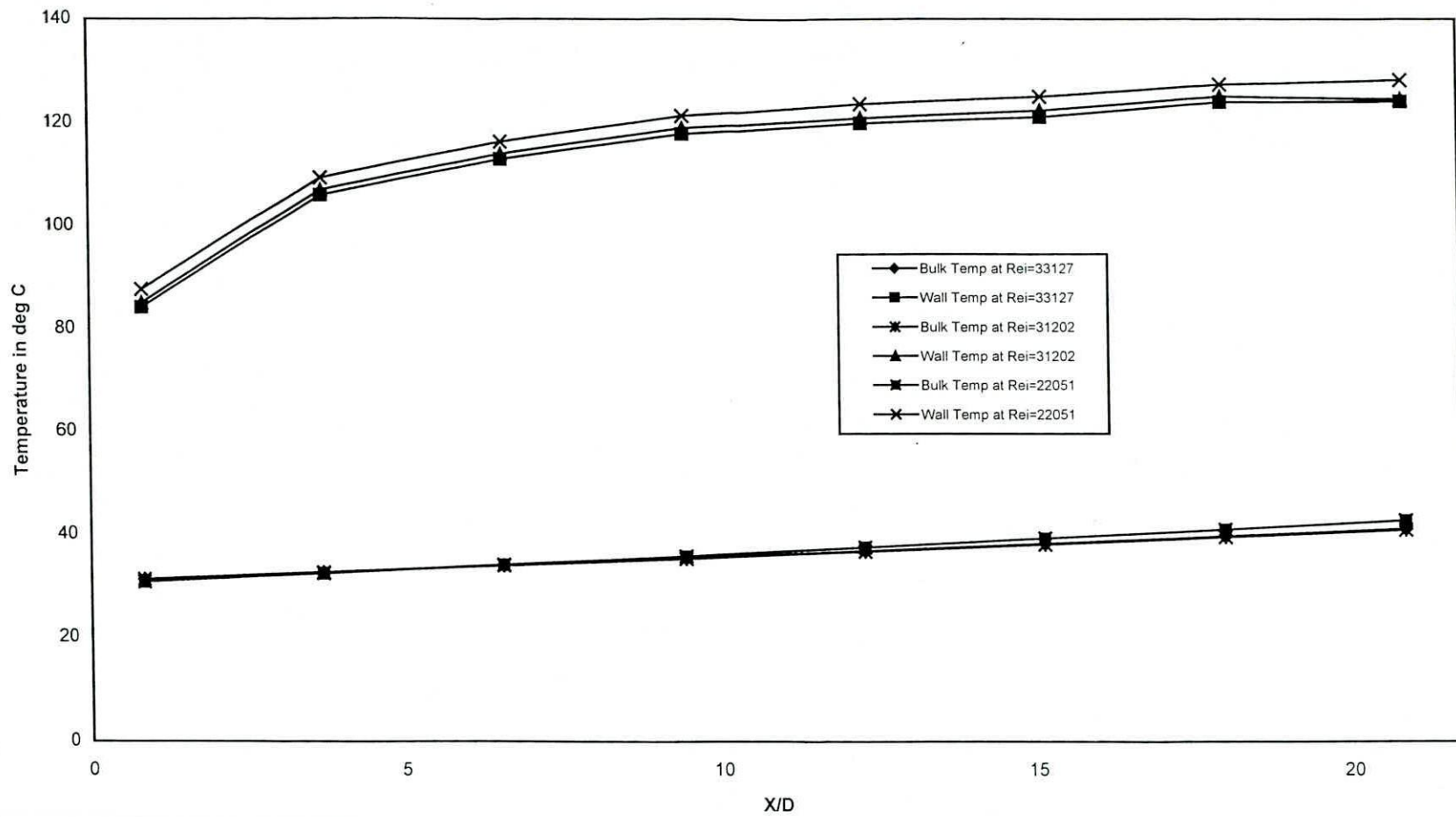


Fig. B10 Wall and Bulk Temperature Distribution Along the Length of Smooth Tube

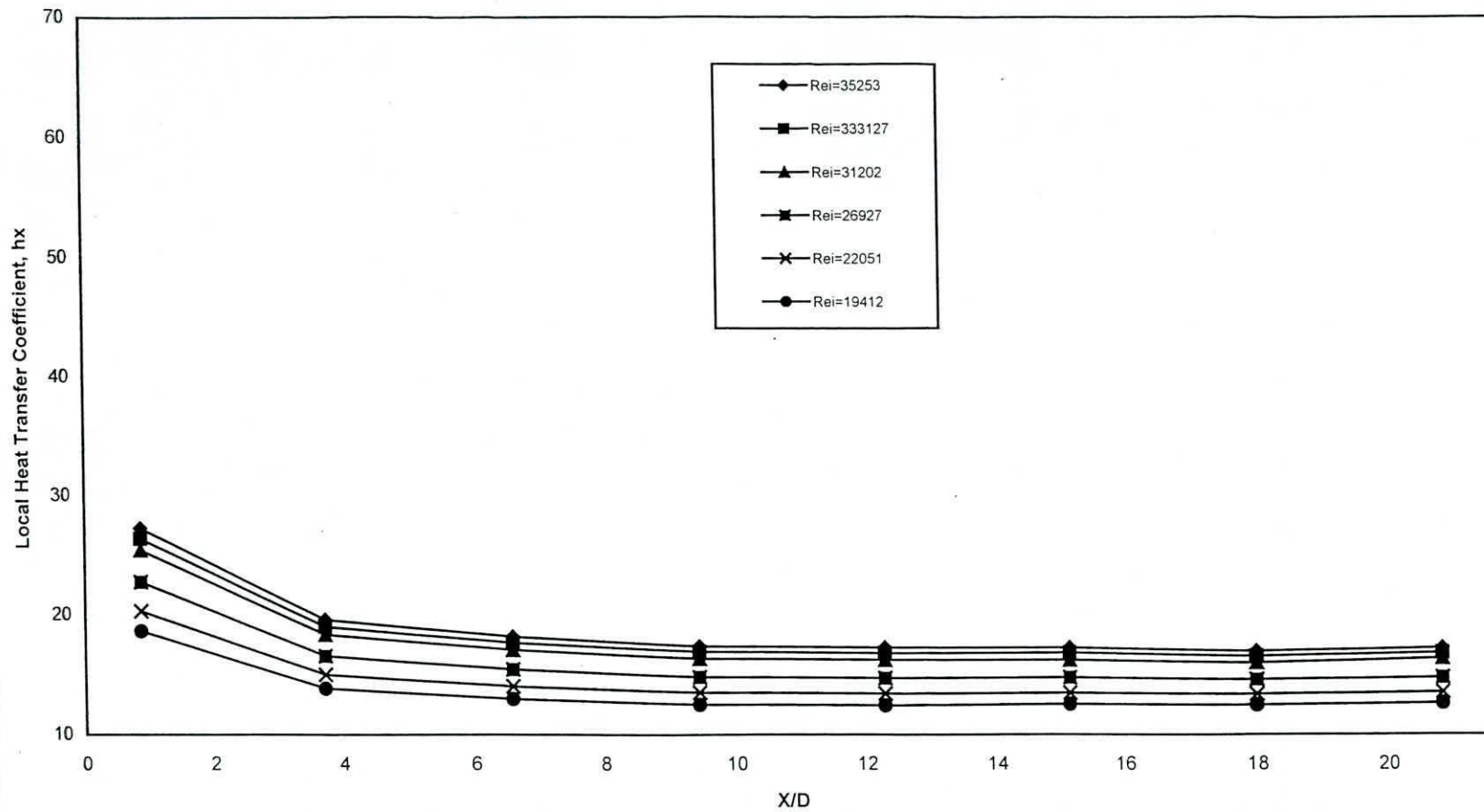


Fig. B11 Local Heat Transfer Coefficient Along The Length of Smooth Tube at Different Reynolds Number

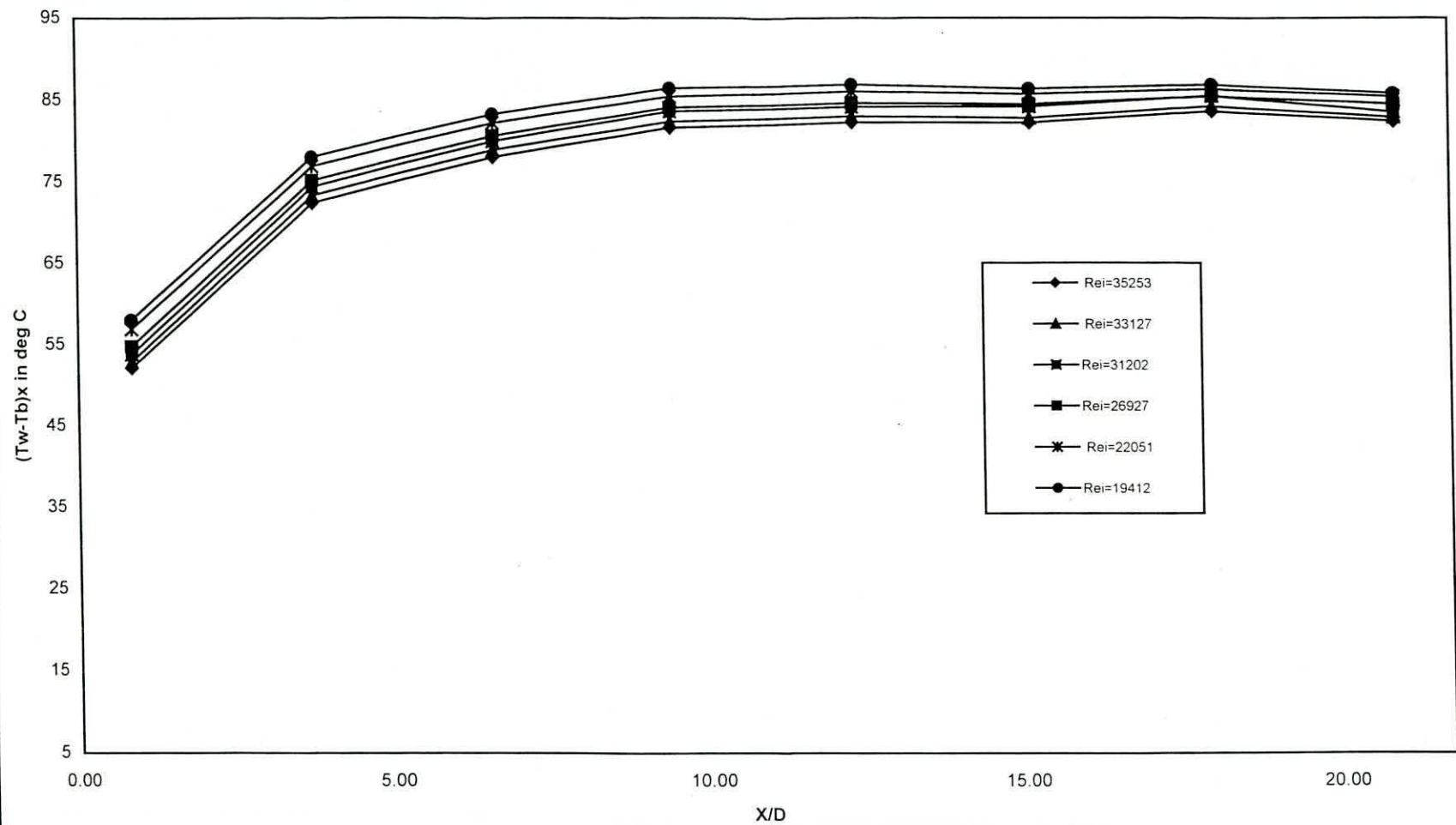
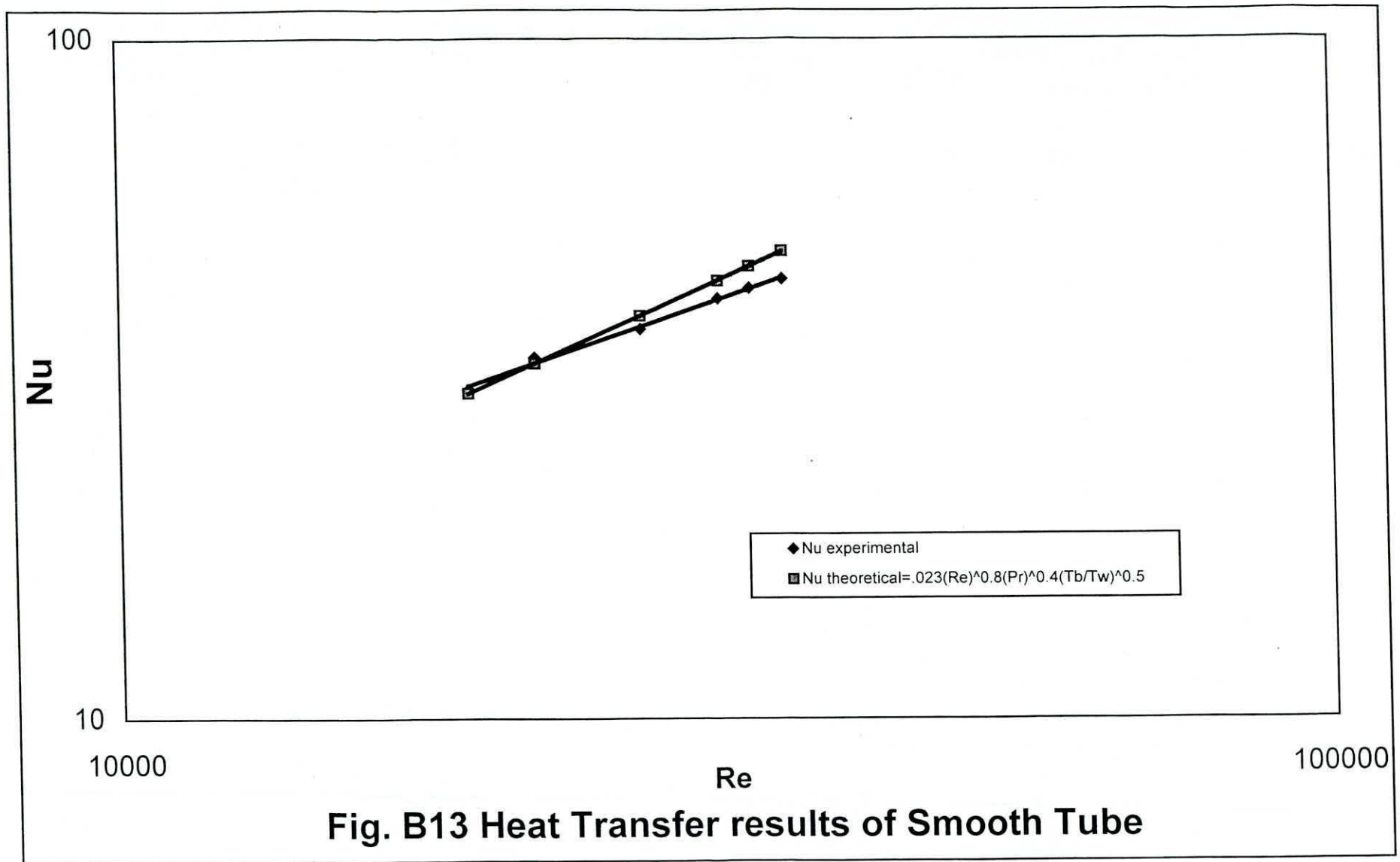


Fig. B12 Difference Between Wall and Bulk Temperature Along the Length of Smooth Tube



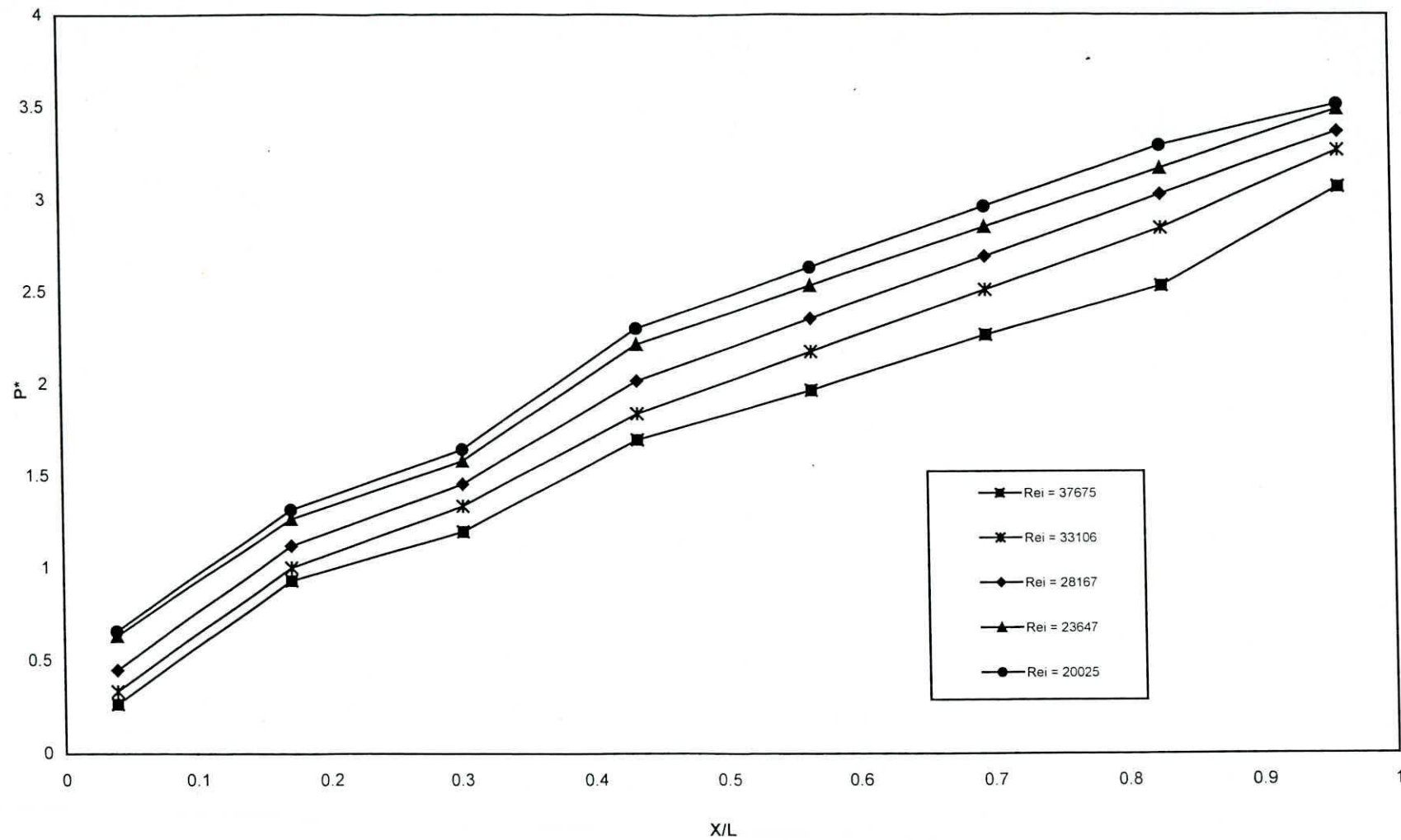


Fig.B14 Pressure Drop Along Axial Distance of In Line Finned Tube.

93623

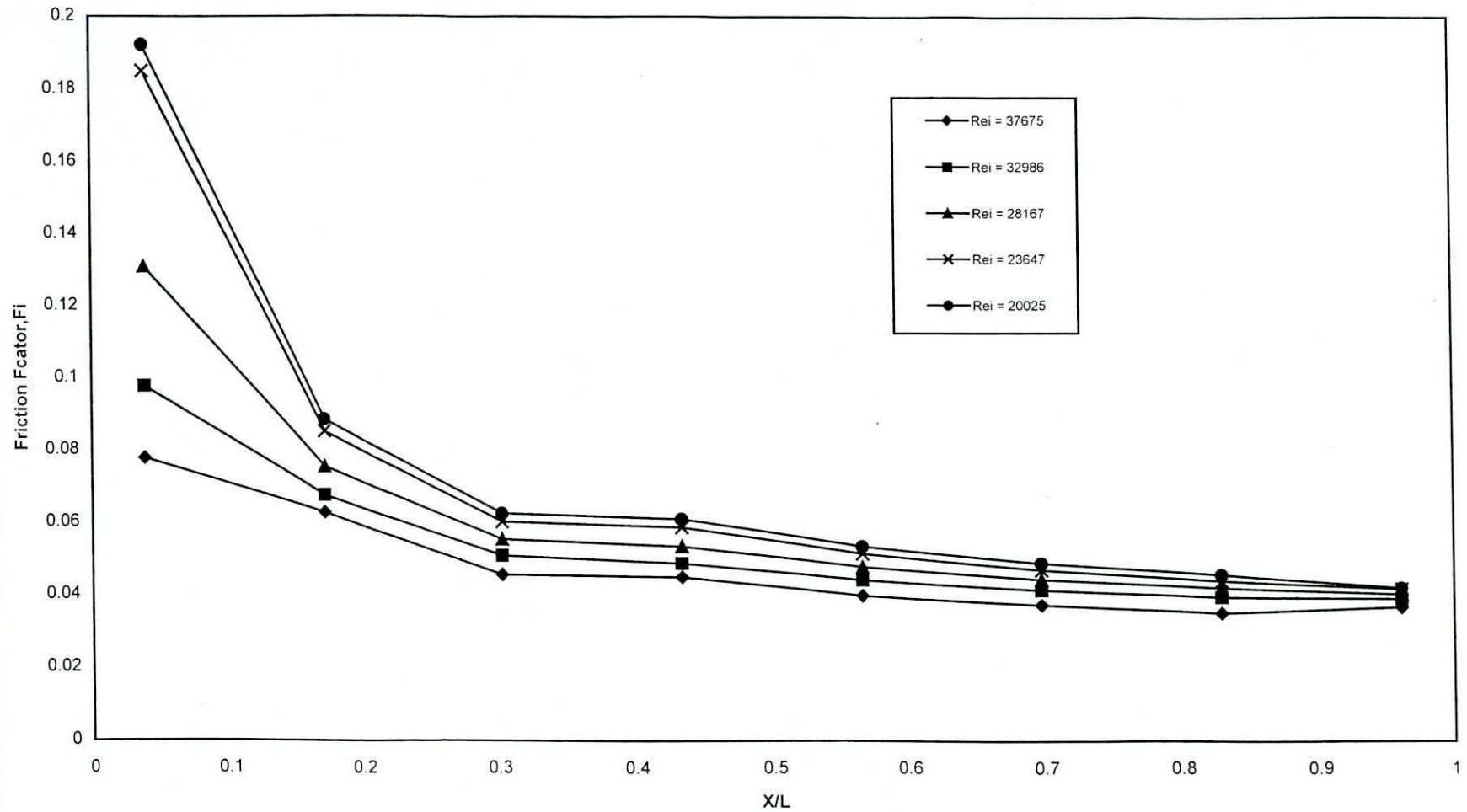


Fig.B15 Distribution of Friction Factor Along Axial Distance of In Line Finned Tube

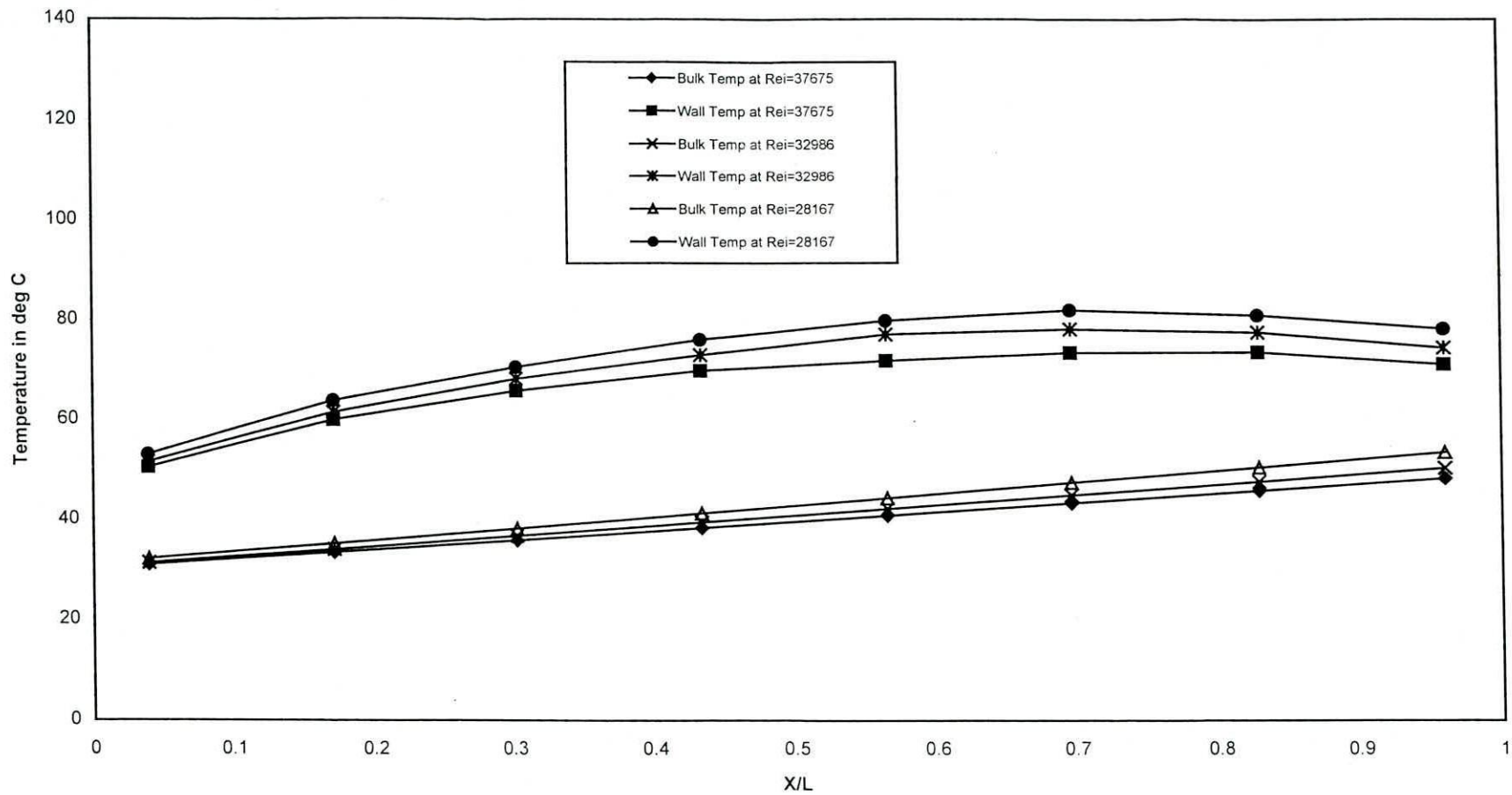


Fig. B16 Wall and Bulk Temperature Distribution Along Axial Distance of In Line Finned Tube

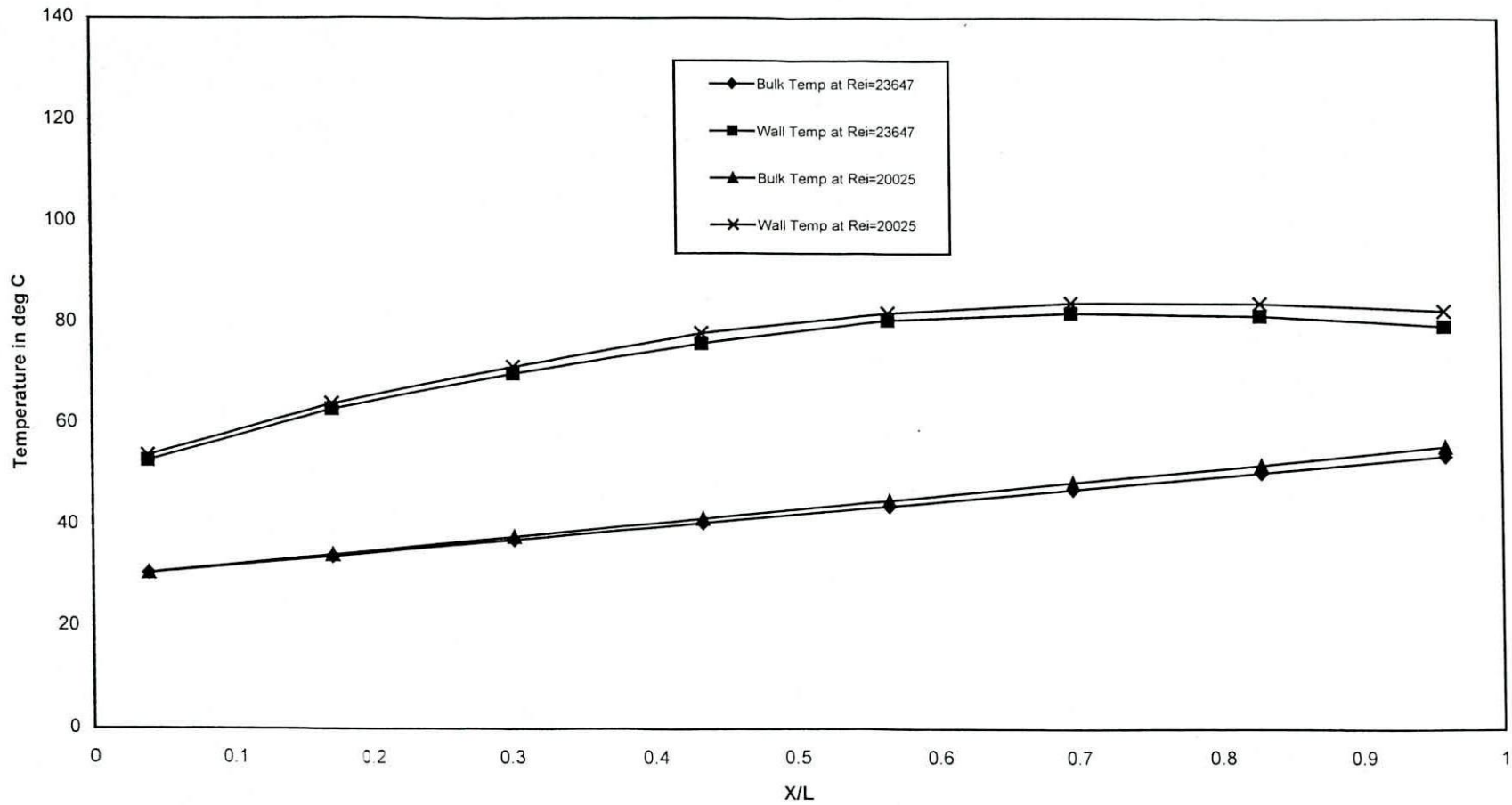


Fig. B17 Wall and Bulk Temperature Distribution Along Axial Distance of In Line Fined Tube

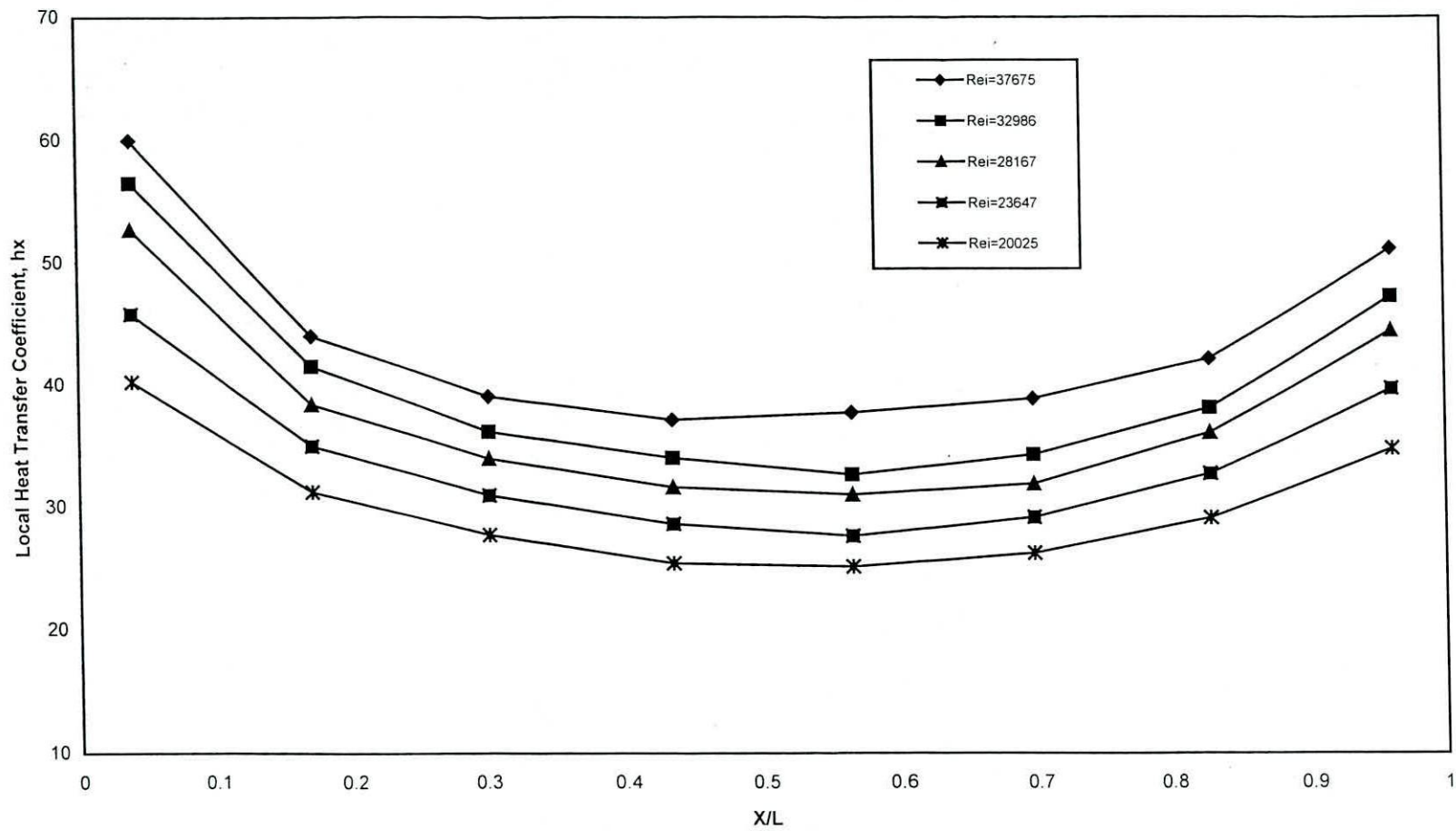


Fig. B18 Local Heat Transfer Coefficient Along Axial Distance of In Line Fined Tube at Different Reynolds number

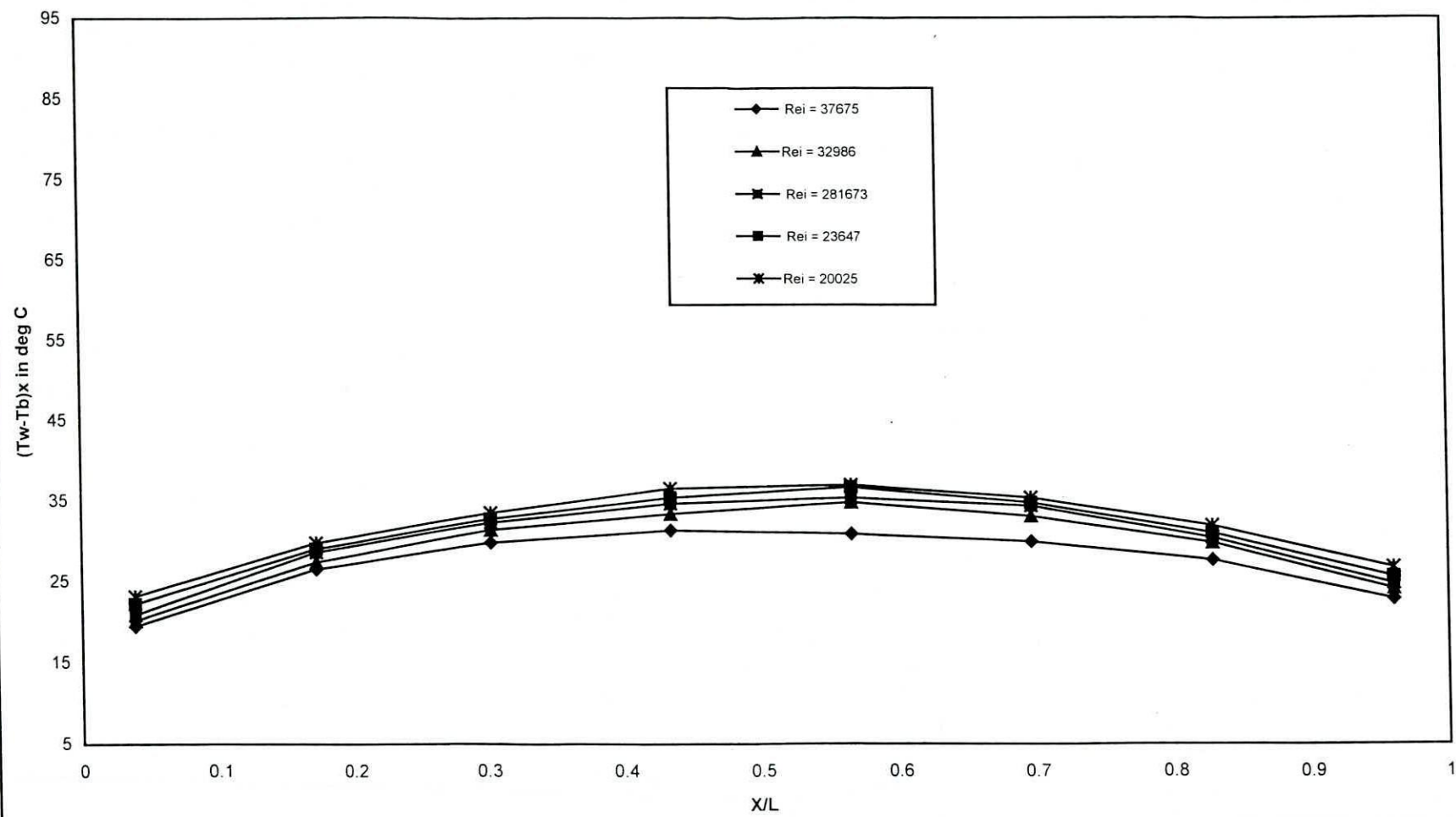


Fig. B19 Difference Between Wall and Bulk Temperature Along Axial Distance of In Line Finned Tube

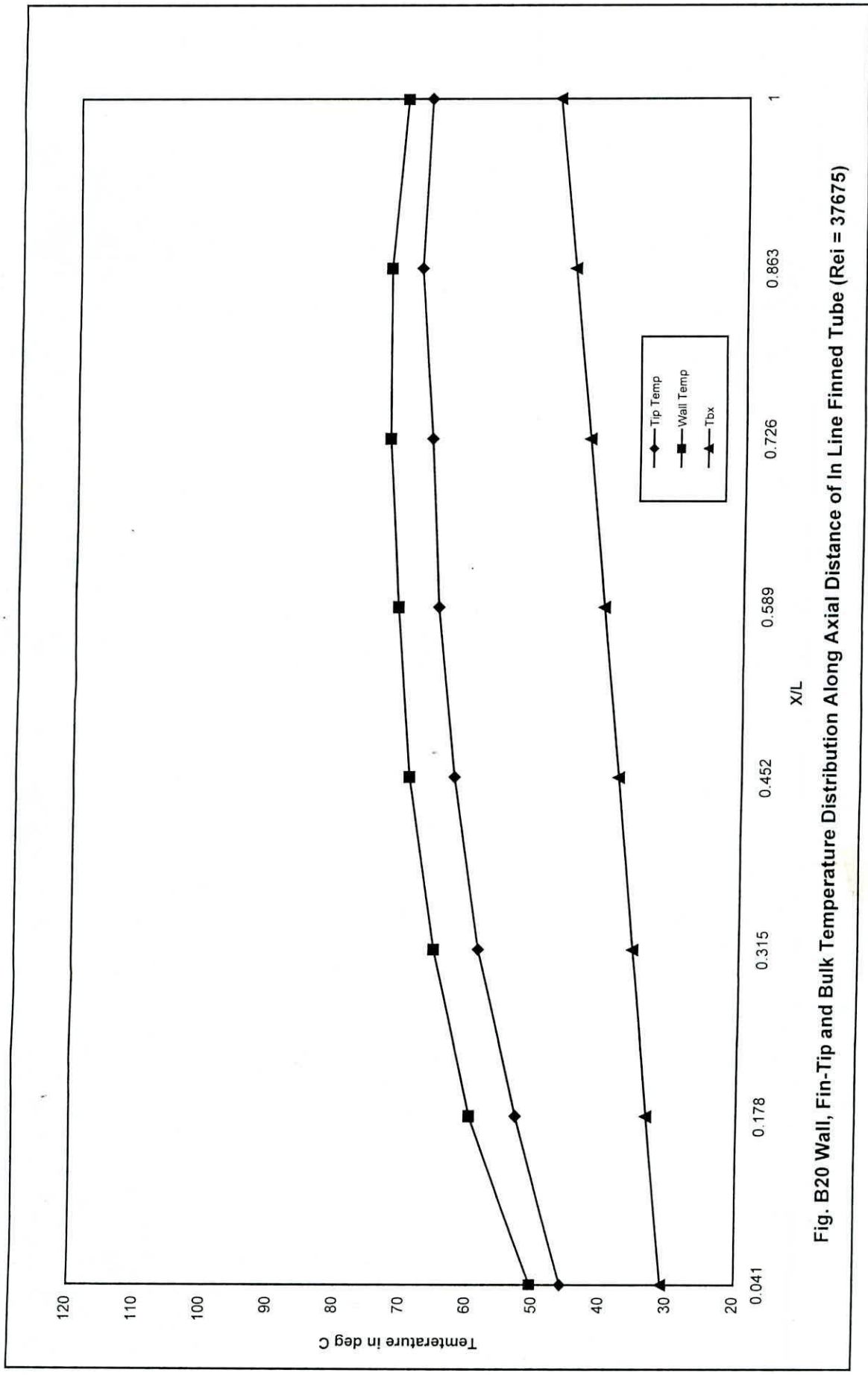


Fig. B20 Wall, Fin-Tip and Bulk Temperature Distribution Along Axial Distance of In Line Finned Tube (Rei = 37675)

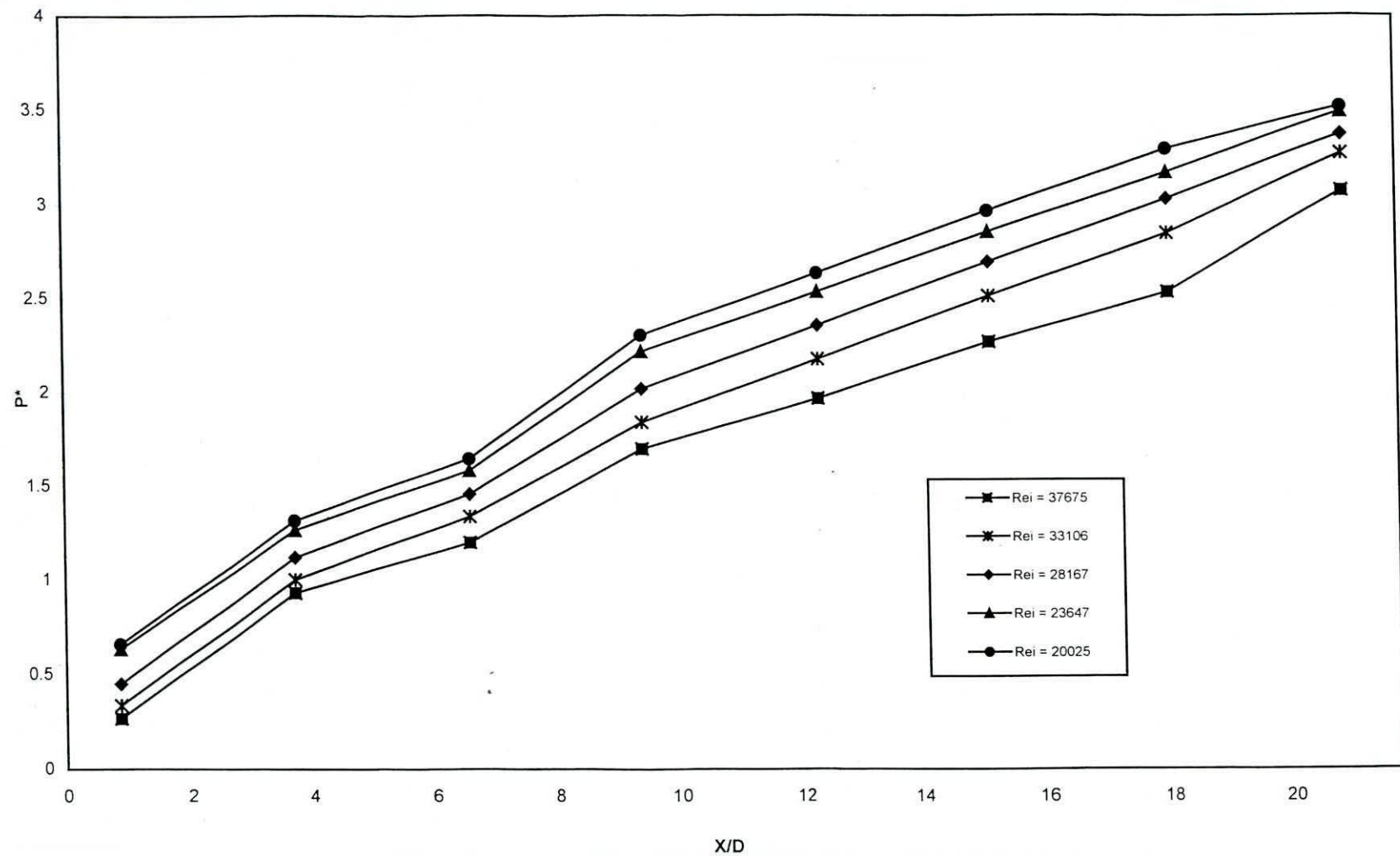


Fig.B21 Pressure Drop Along the Length of In Line Finned Tube.

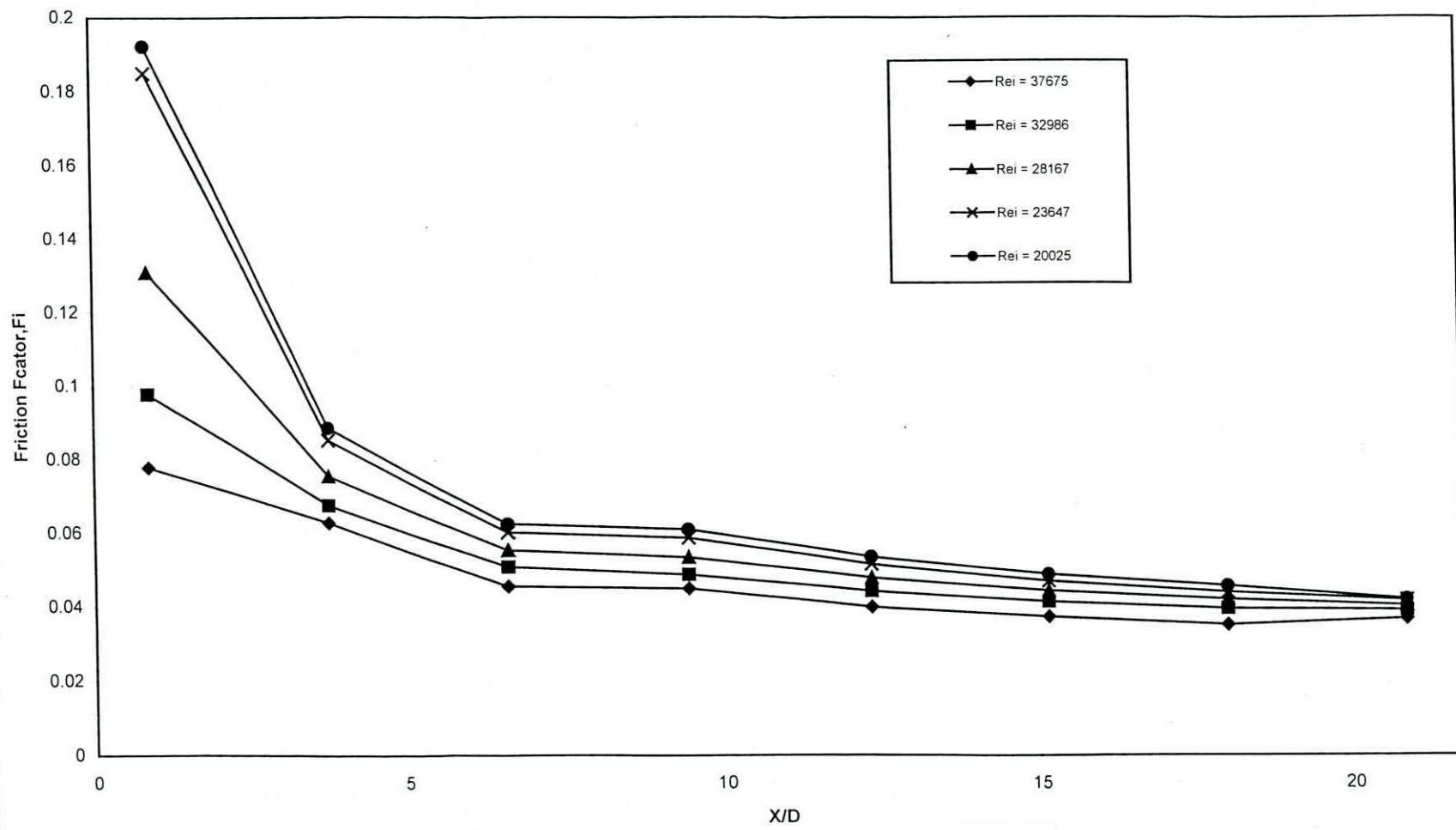


Fig.B22 Distribution of Friction Factor Along the Length of In Line Finned Tube

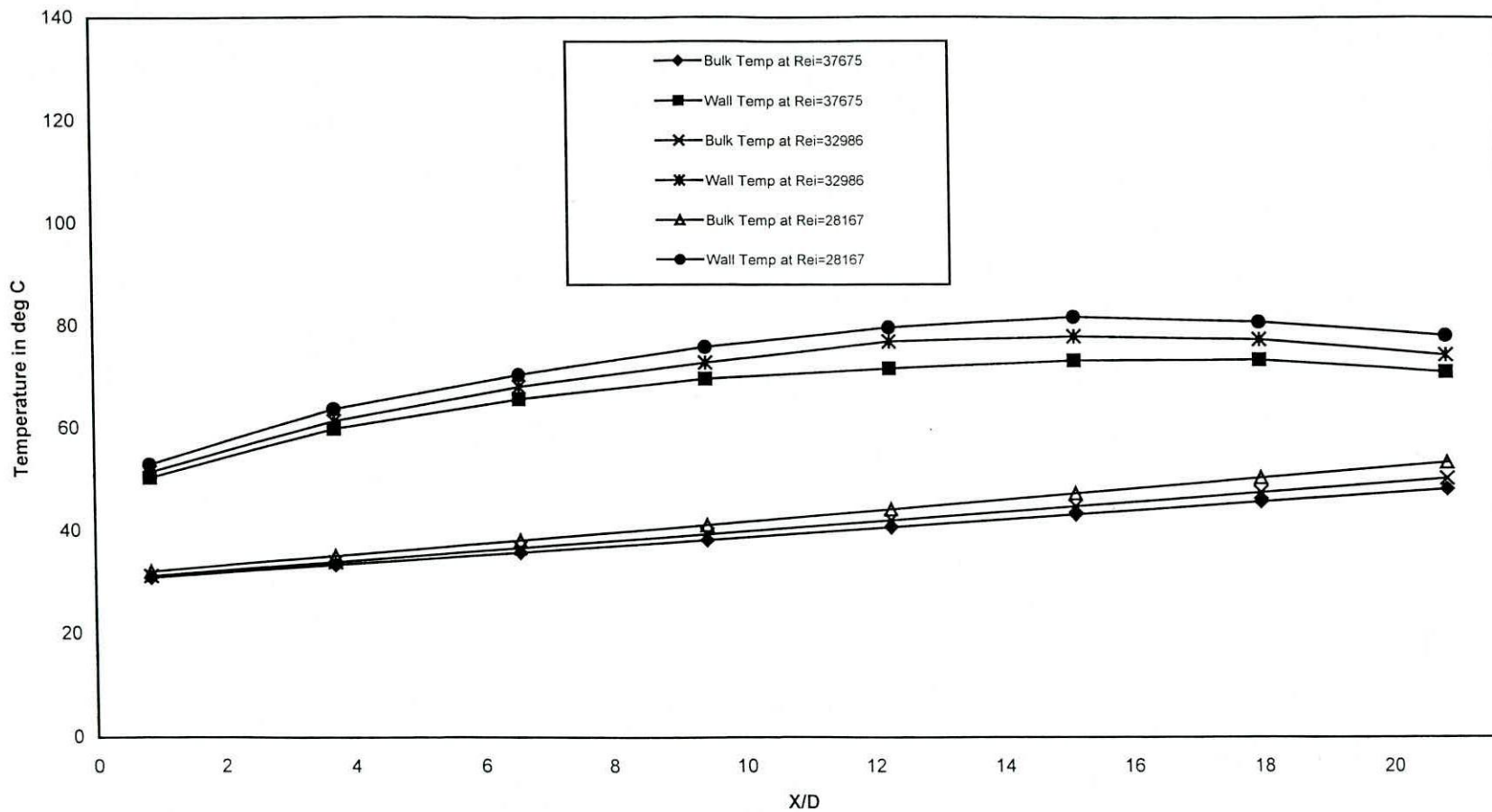


Fig. B23 Wall and Bulk Temperature Distribution Along The Length of In Line Finned Tube

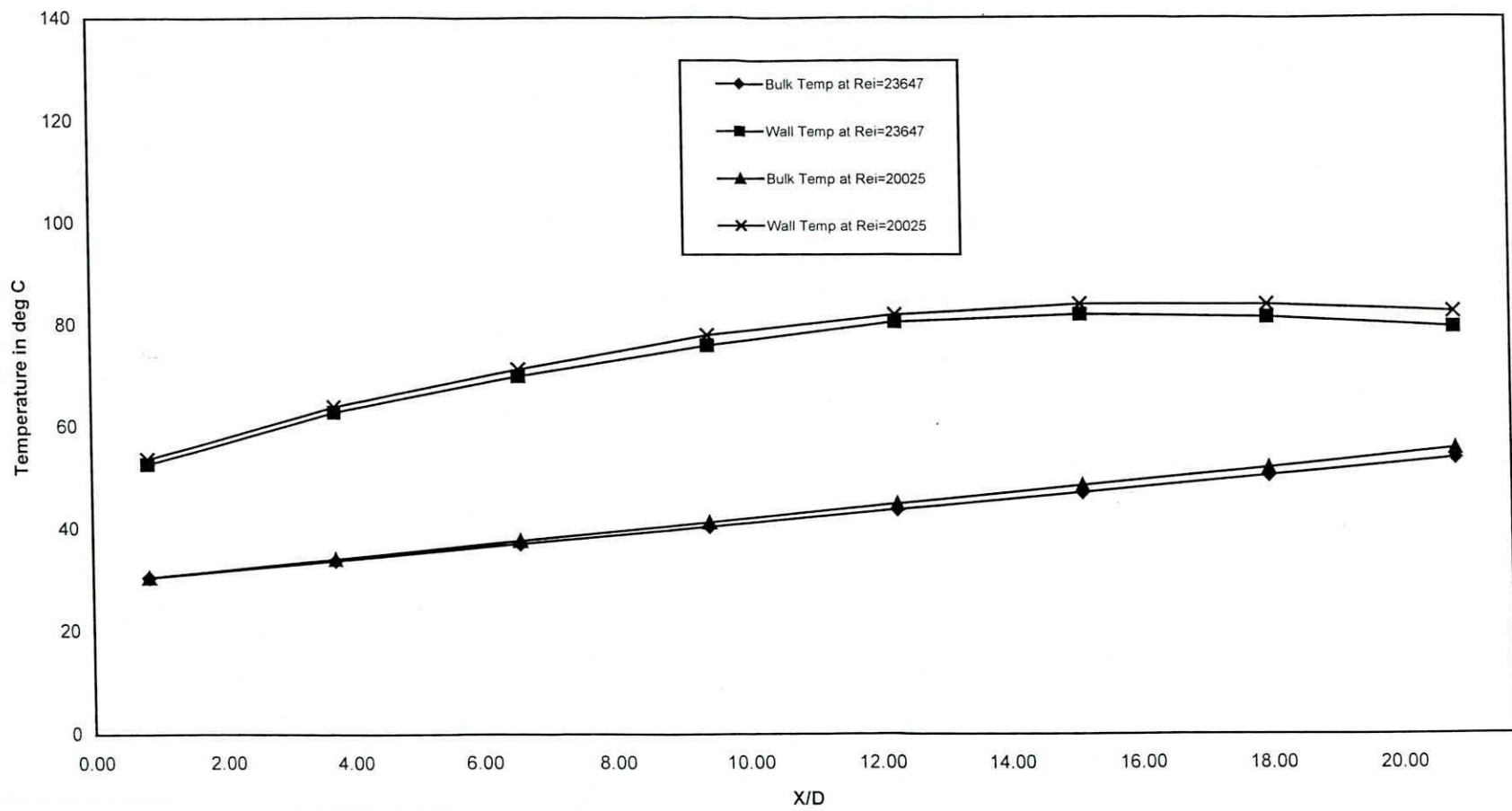


Fig. B24 Wall and Bulk Temperature Distribution Along The Length of In Line Finned Tube

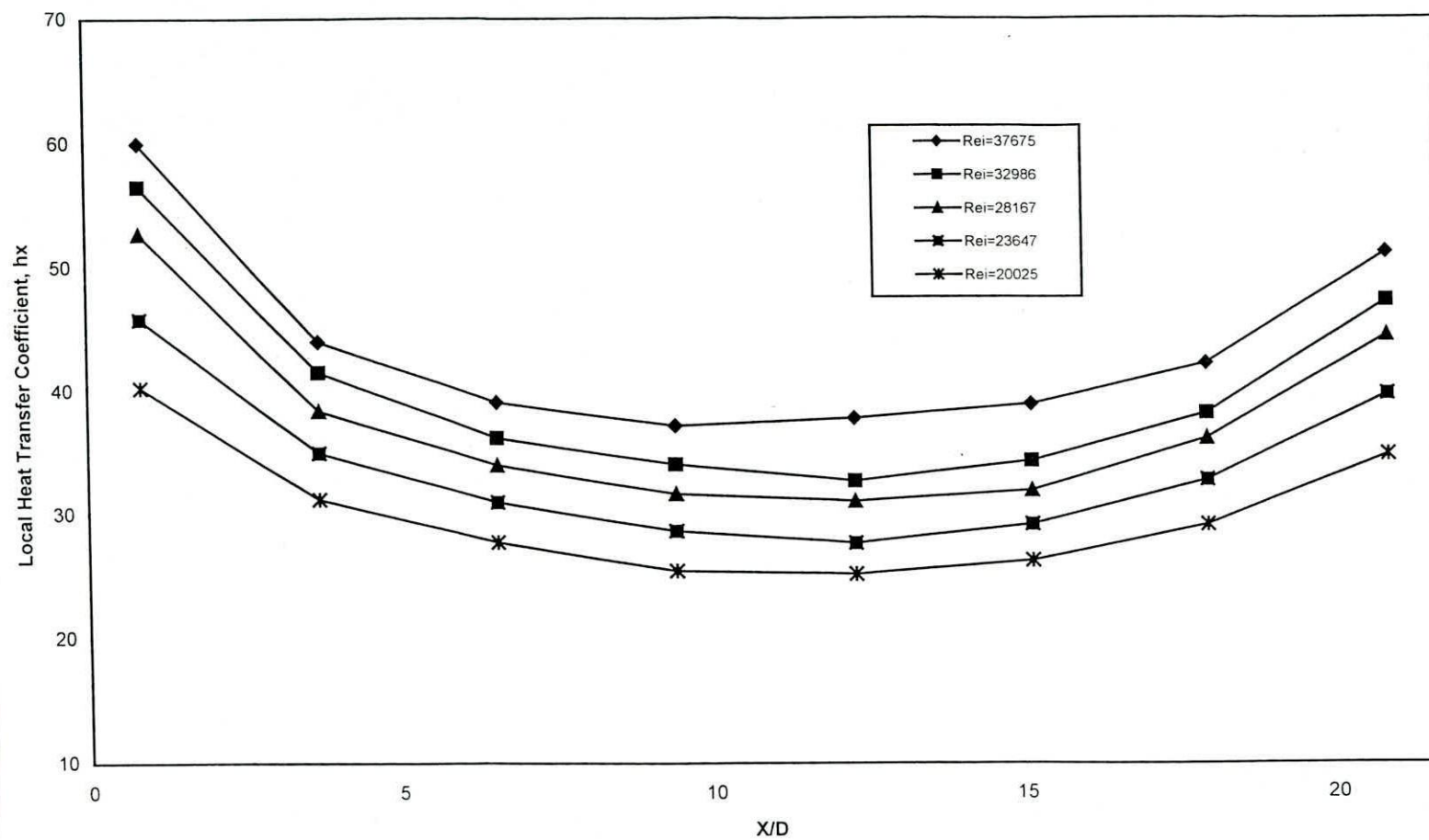


Fig. B25 Local Heat Transfer Coefficient Along the Length of In Line Finned Tube at Different Reynolds number

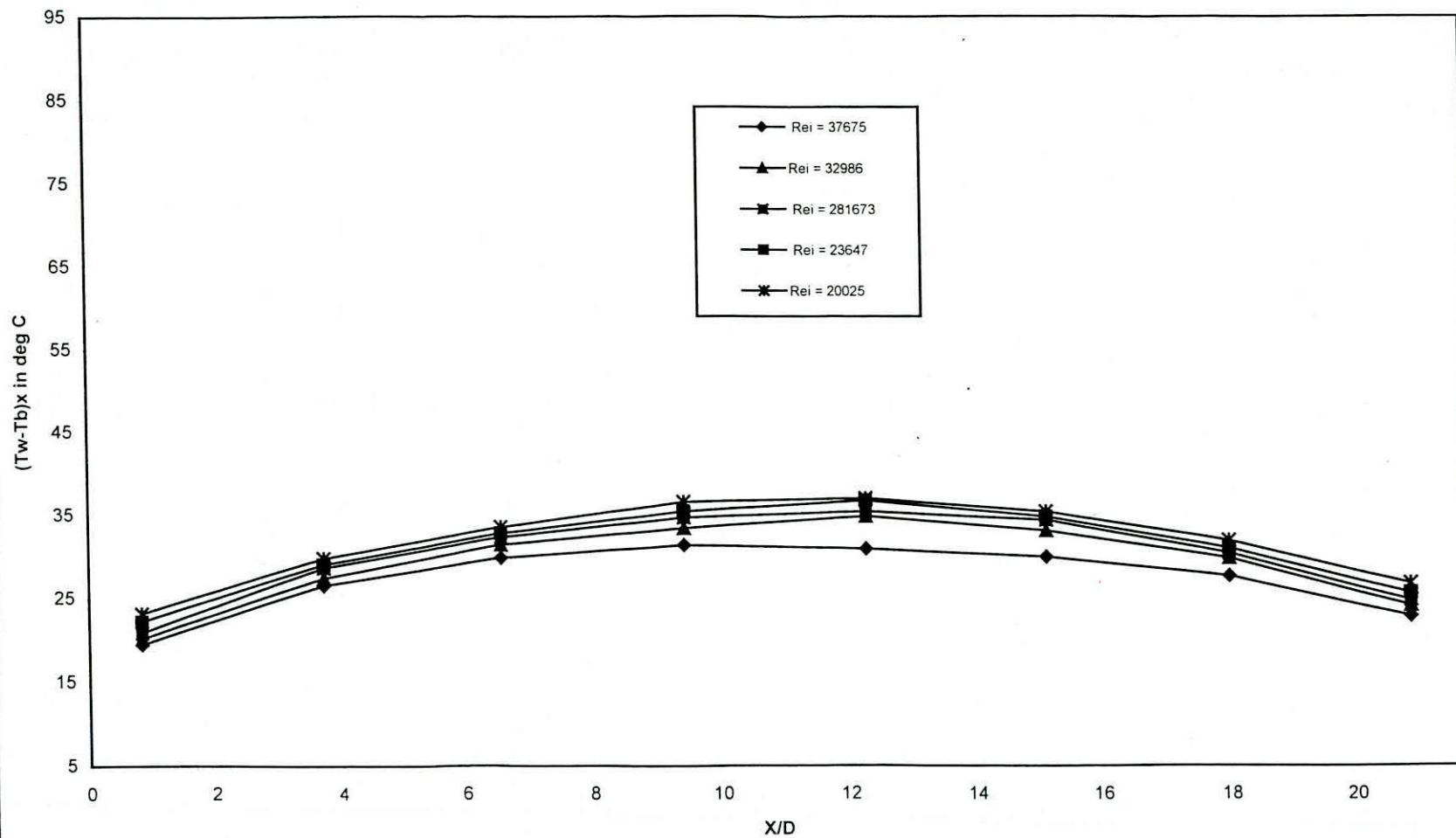


Fig. B26 Difference Between Wall and Bulk Temperature Along The Length of In Line Finned Tube

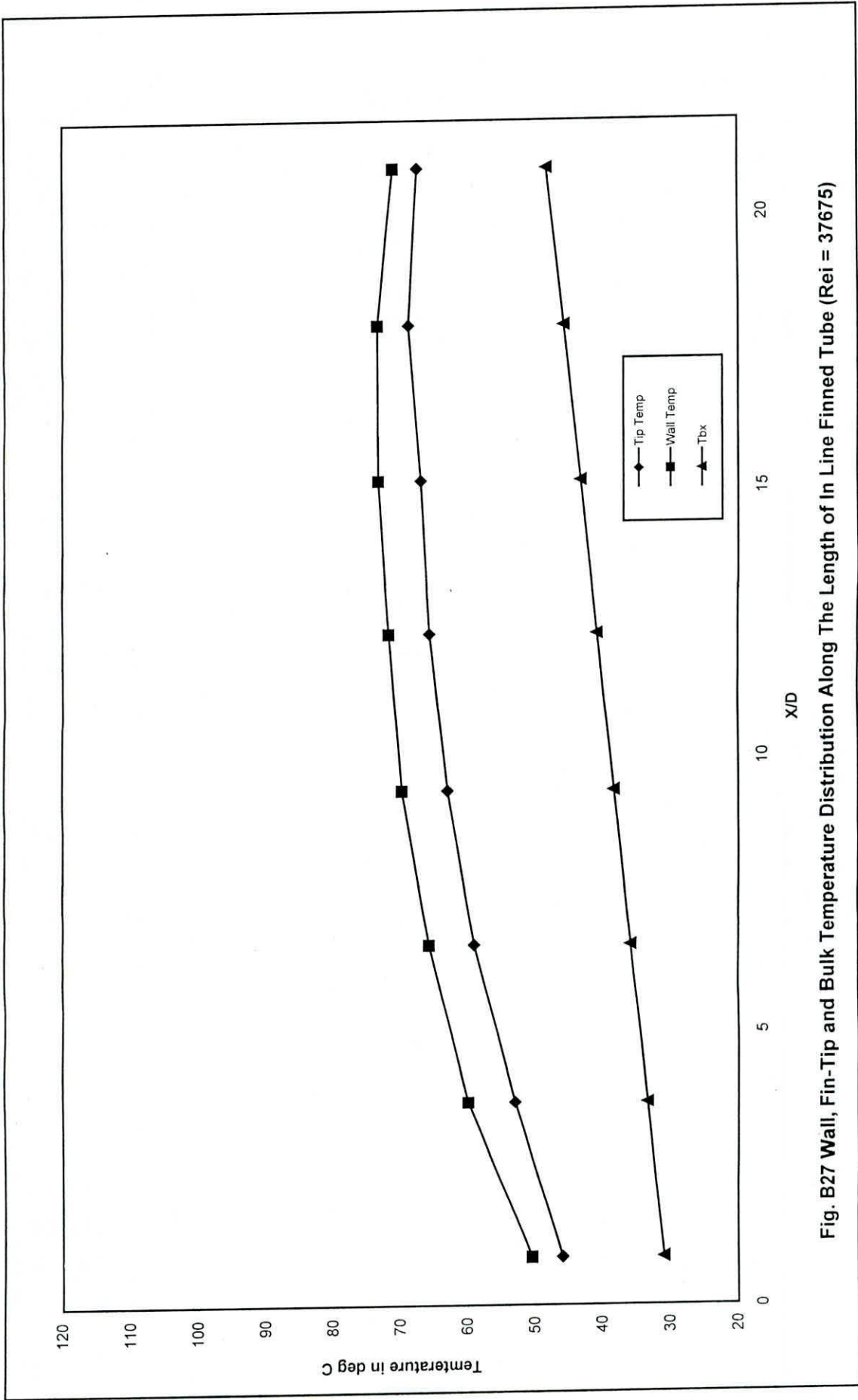


Fig. B27 Wall, Fin-Tip and Bulk Temperature Distribution Along The Length of In Line Finned Tube (Rei = 37675)

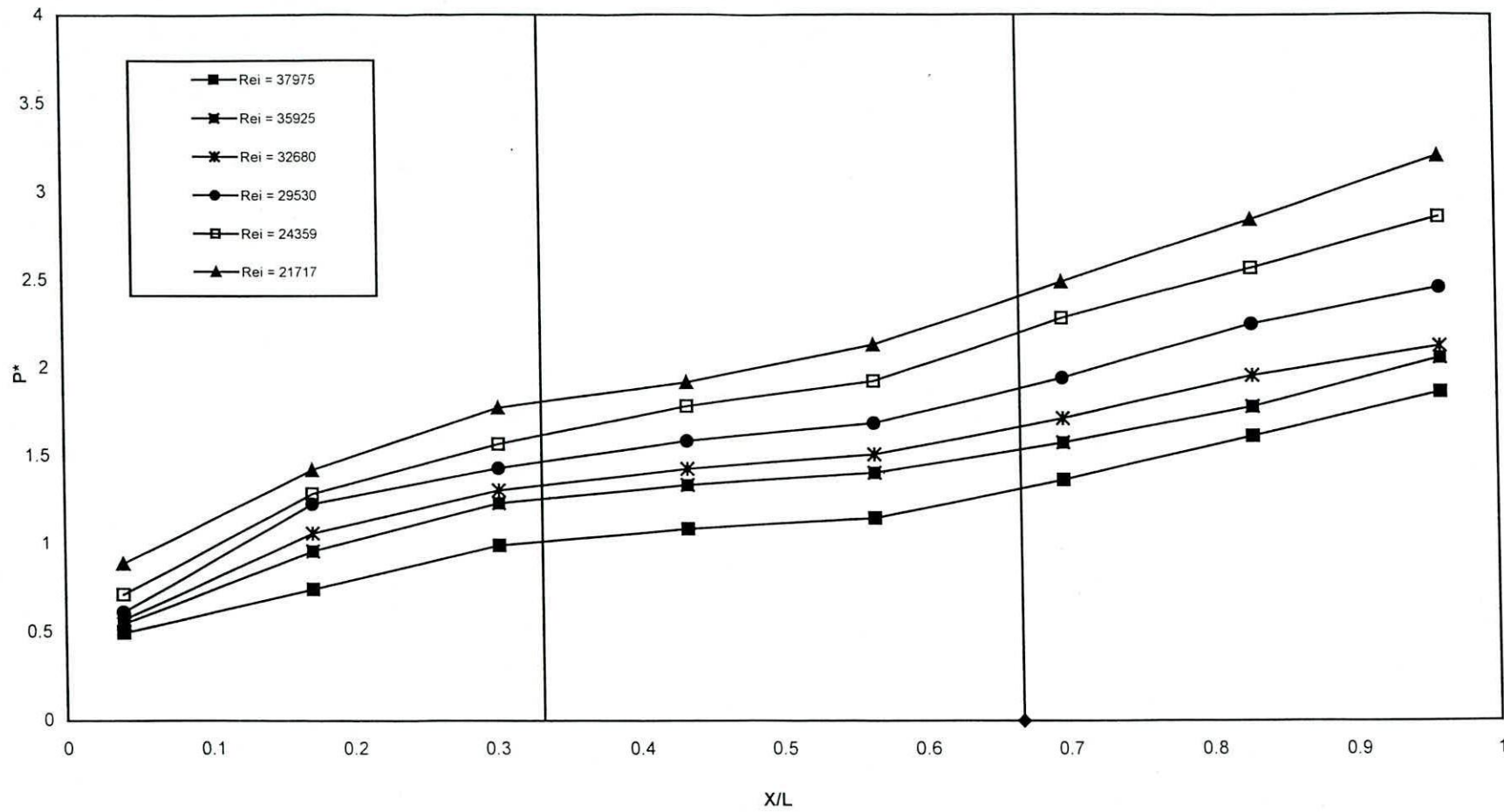


Fig.B28 Pressure Drop Along Axial Distance of the In Line Segmented Finned Tube.

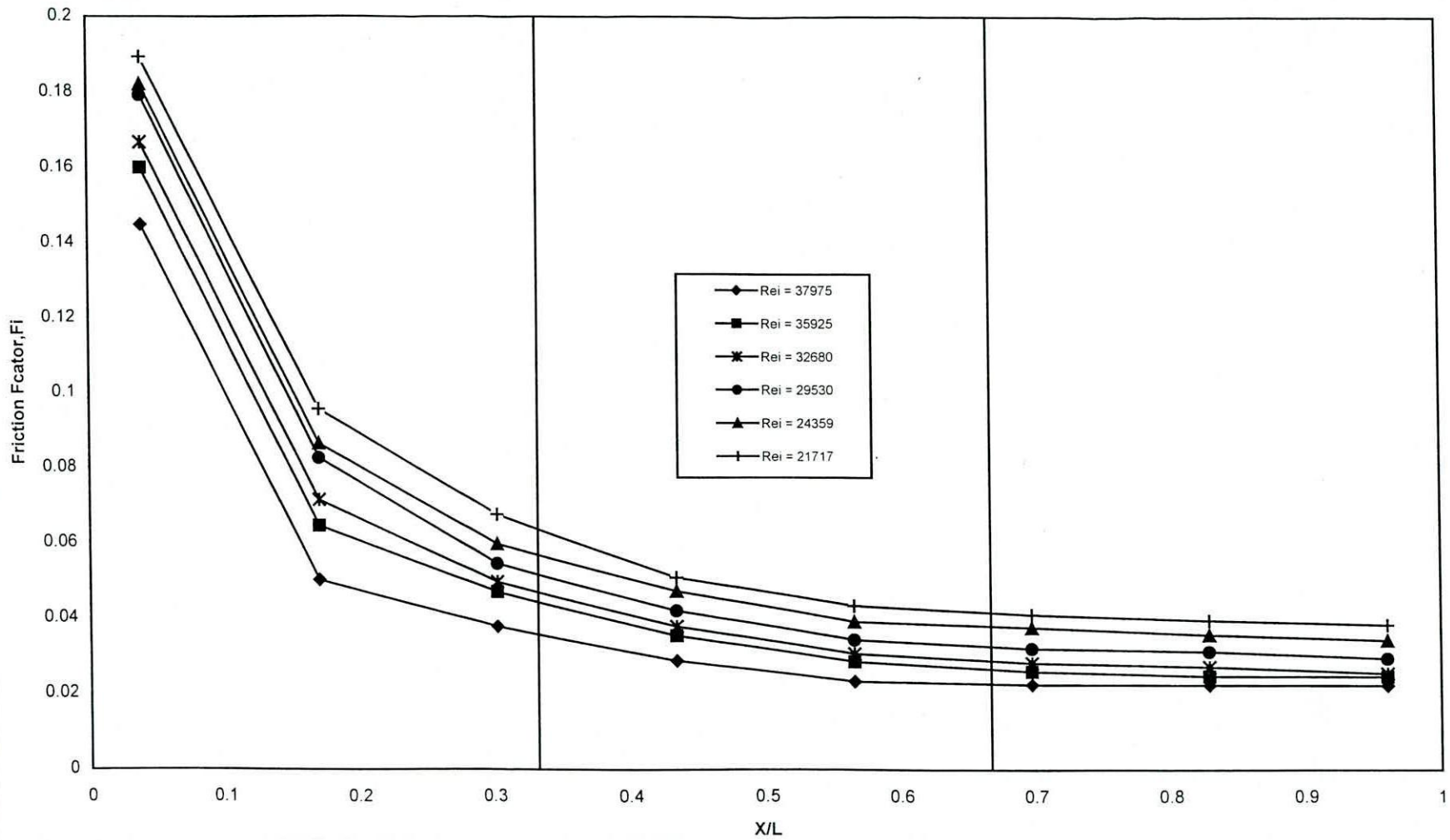


Fig.B29 Distribution of Friction Factor Along Axial Distance of the In Line Segmented Finned Tube

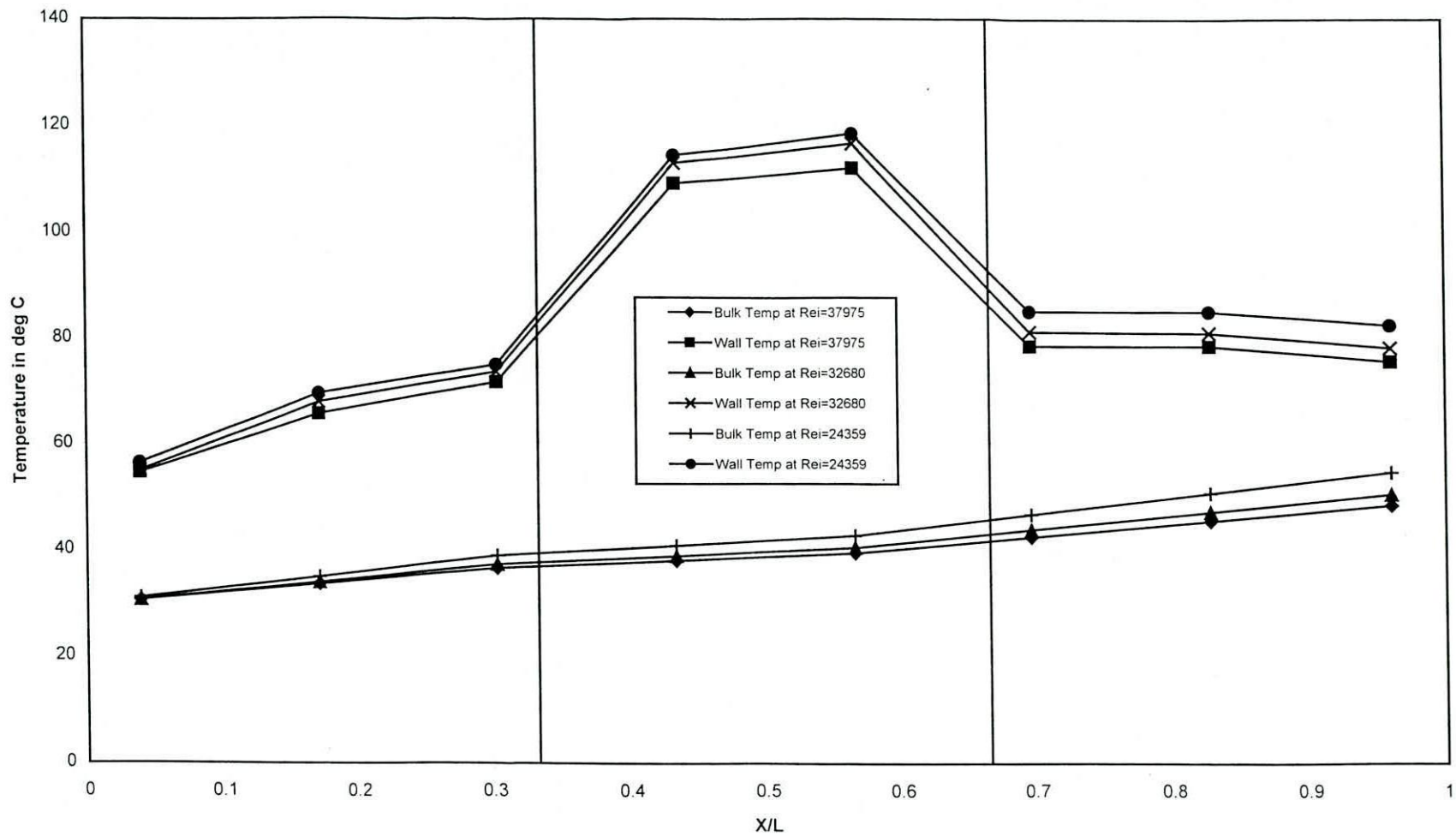


Fig. B30 Wall and Bulk Temperature Distribution Along Axial Distance of In Line Segmented Finned Tube

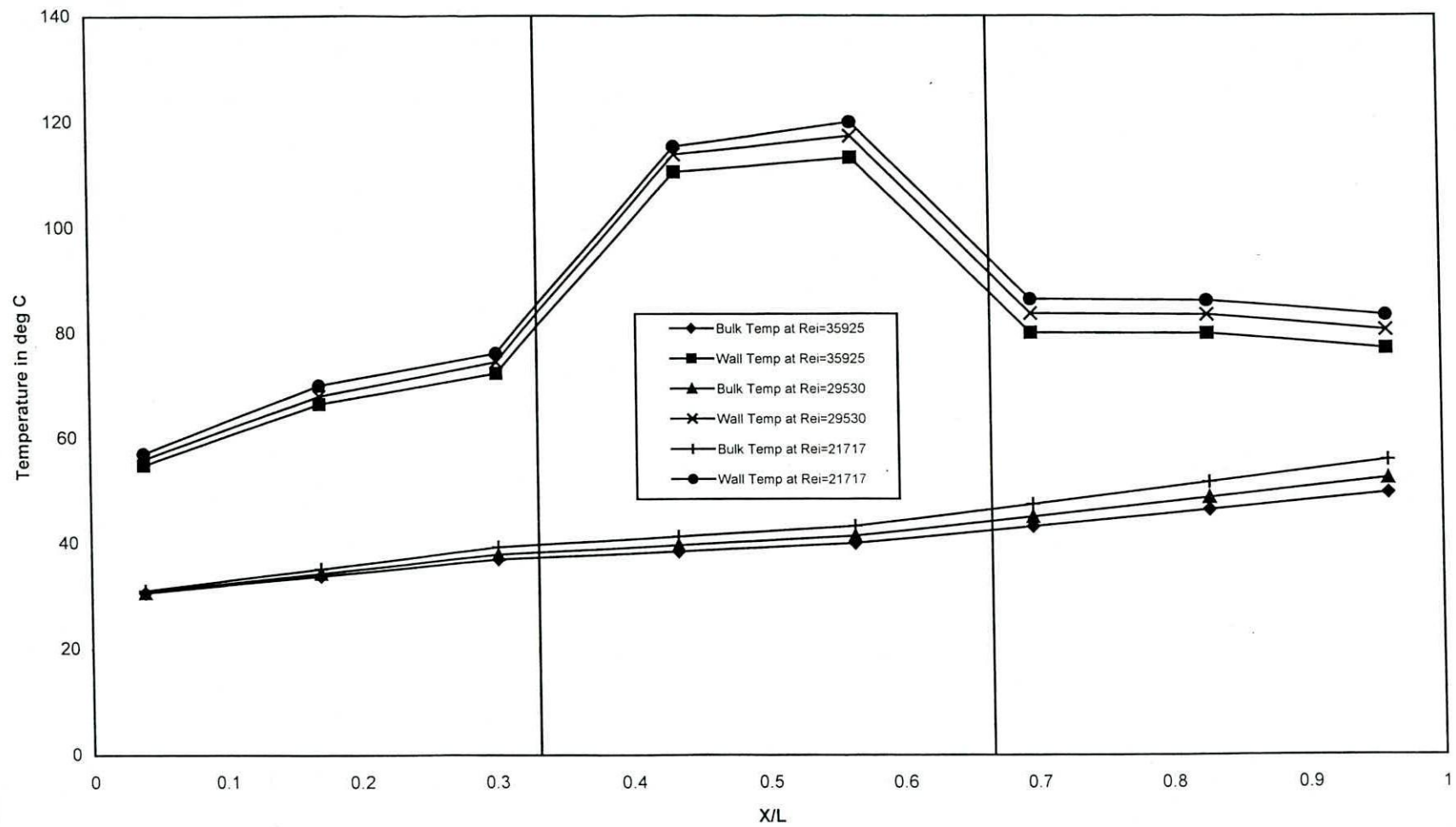


Fig. B31 Wall and Bulk Temperature Distribution Along Axial Distance of In Line Segmented Finned Tube

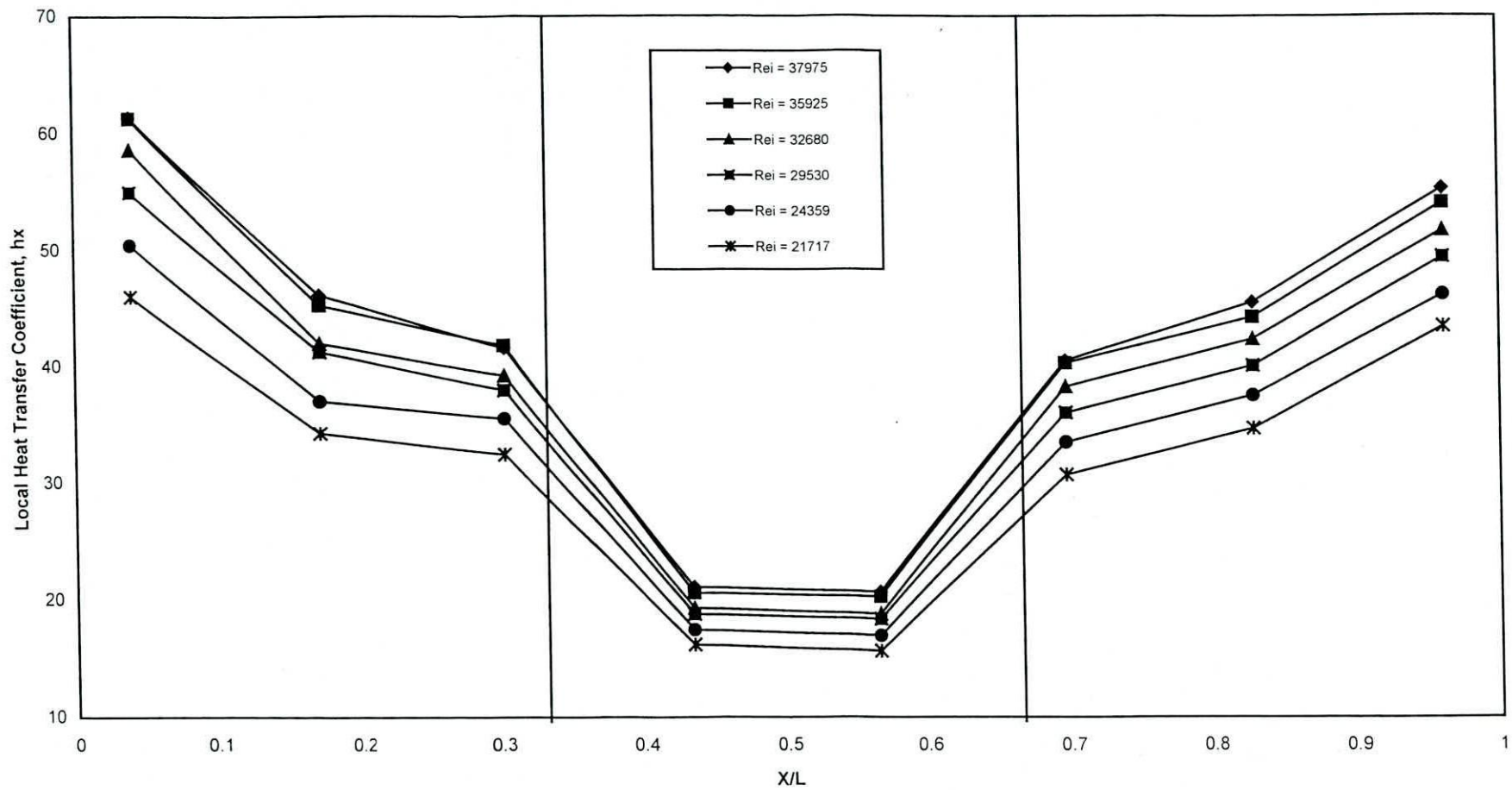
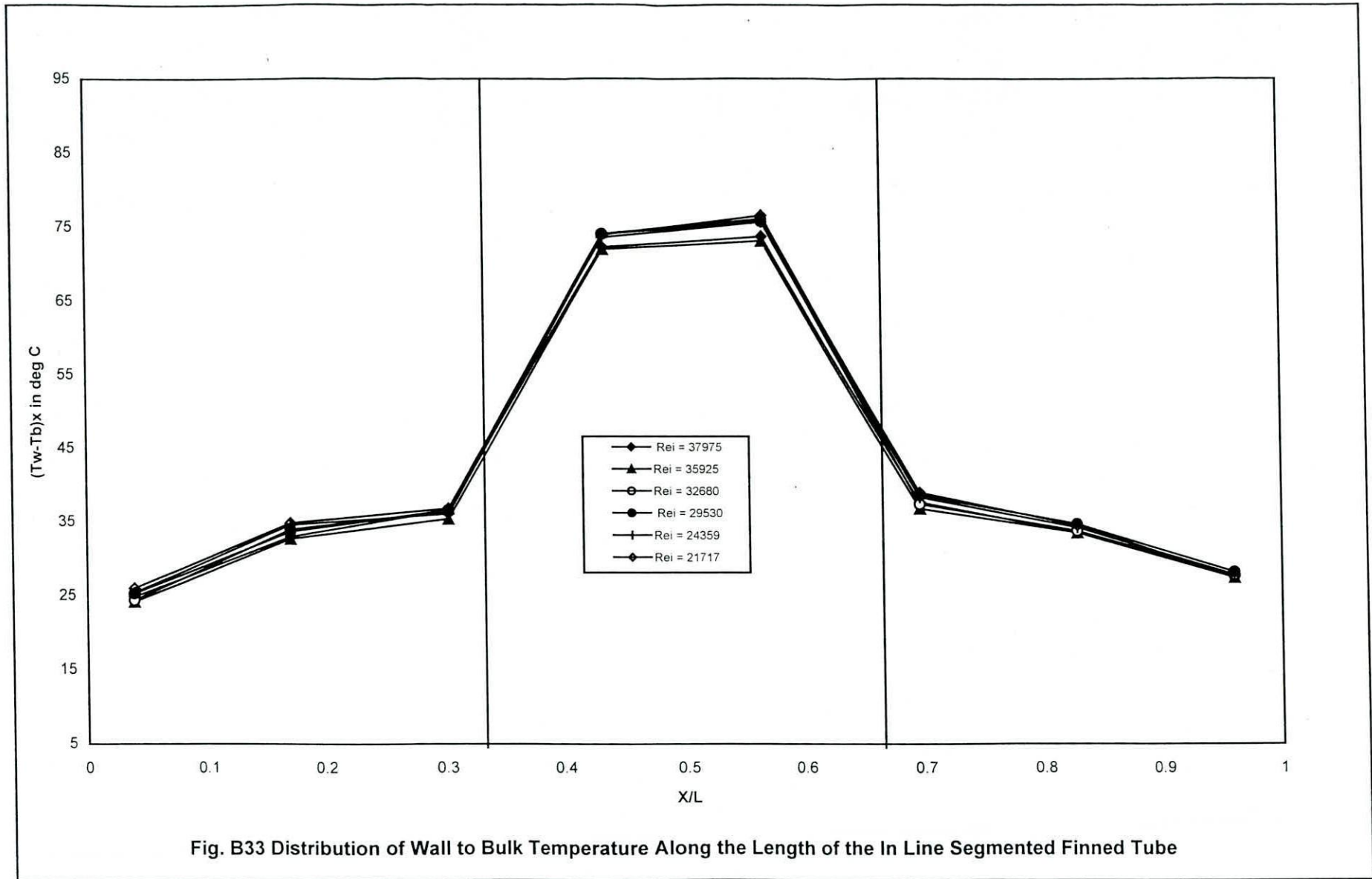


Fig. B32 Local Heat Transfer Coefficient Along Axial Distance of In Line Segmented Finned Tube at Different Reynolds Number



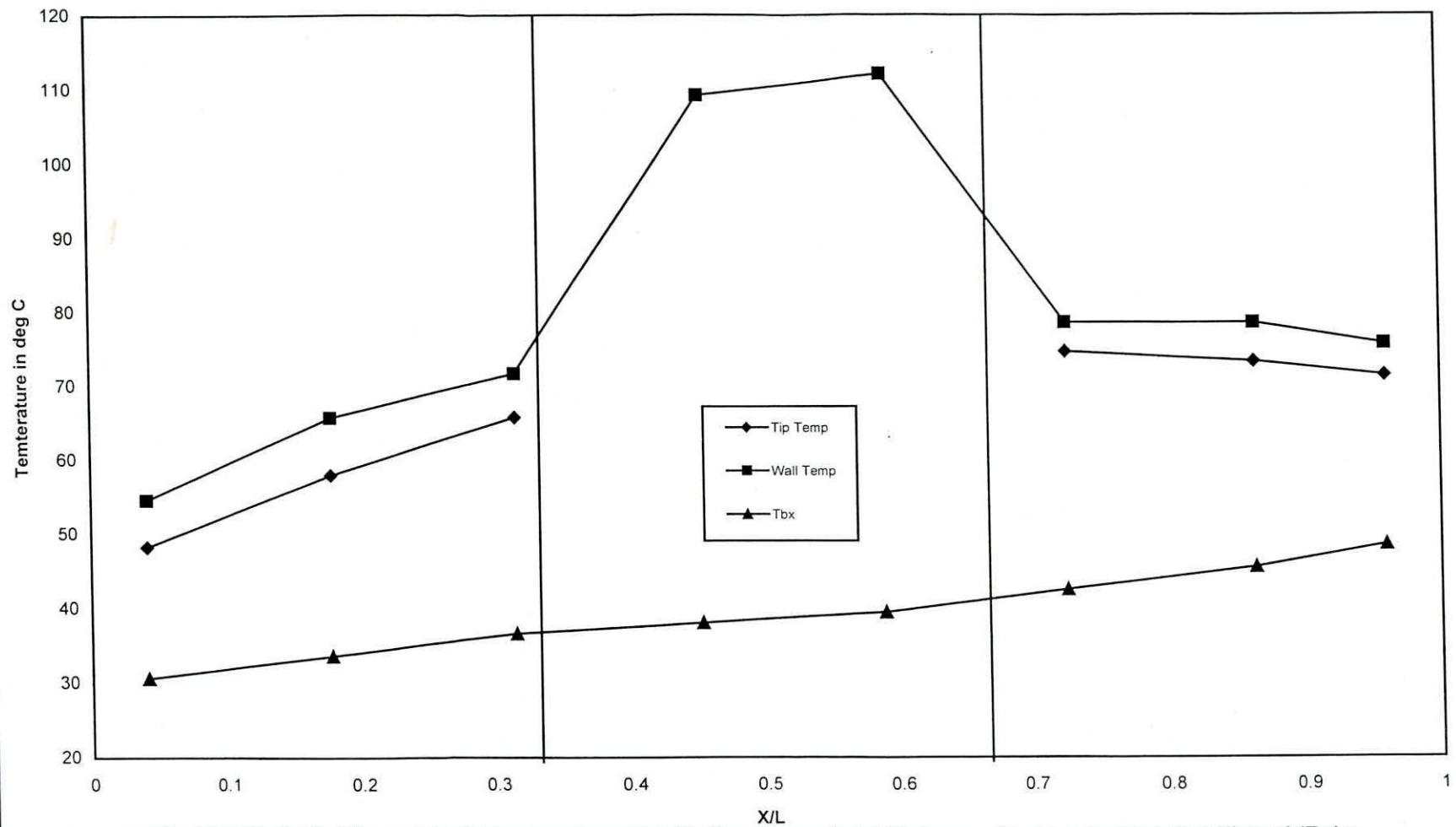


Fig. B34 Wall, Fin-Tip and Bulk Temperature Distribution Along Axial Distance of In Line Segmented Finned (Rei = 37975)

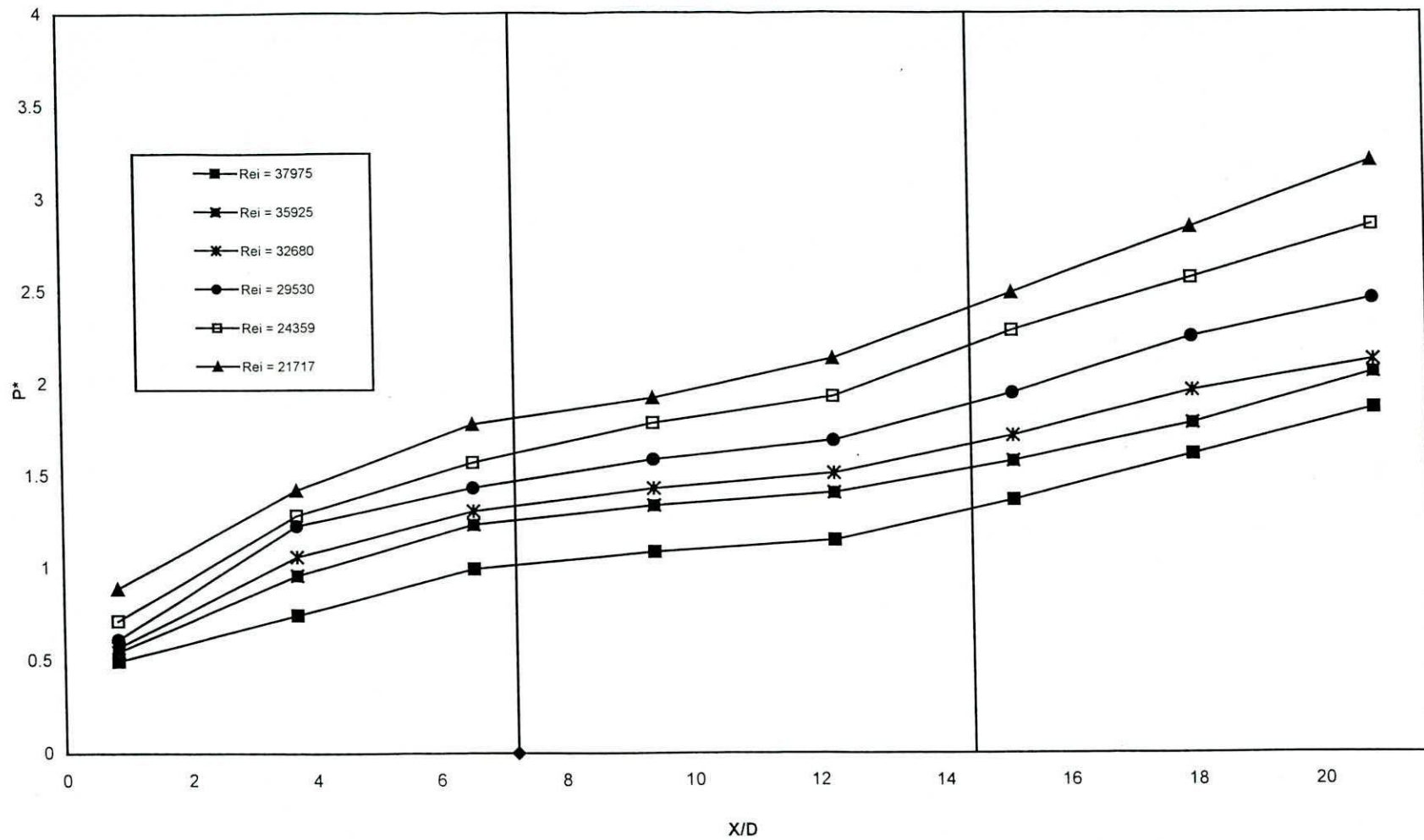


Fig.B35 Pressure Drop Along the Length of the In Line Segmented Finned Tube.

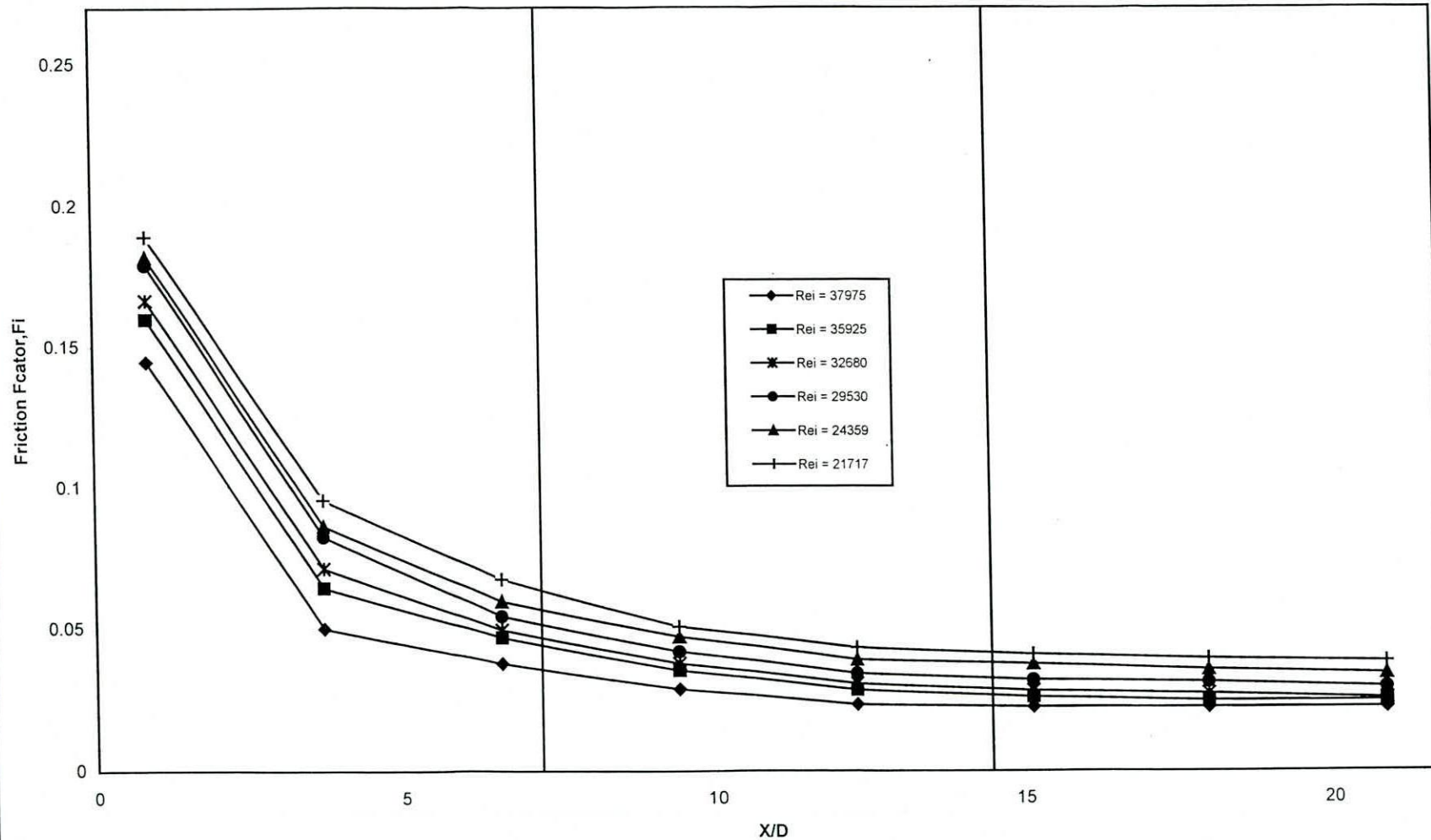


Fig.B36 Distribution of Friction Factor Along the Length of the In Line Segmented Finned Tube

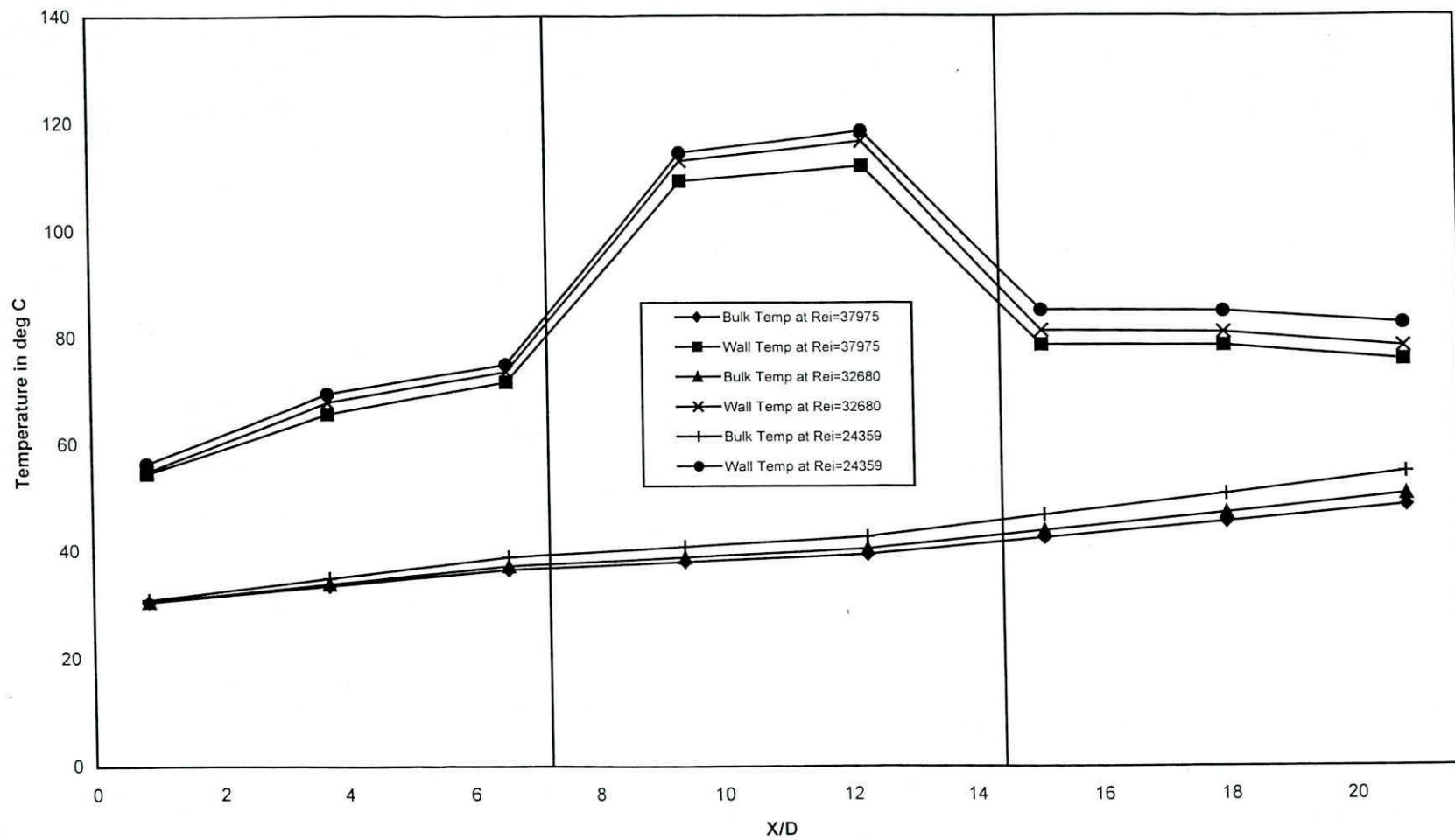


Fig. B37 Wall and Bulk Temperature Distribution Along The Length of In Line Segmented Finned Tube

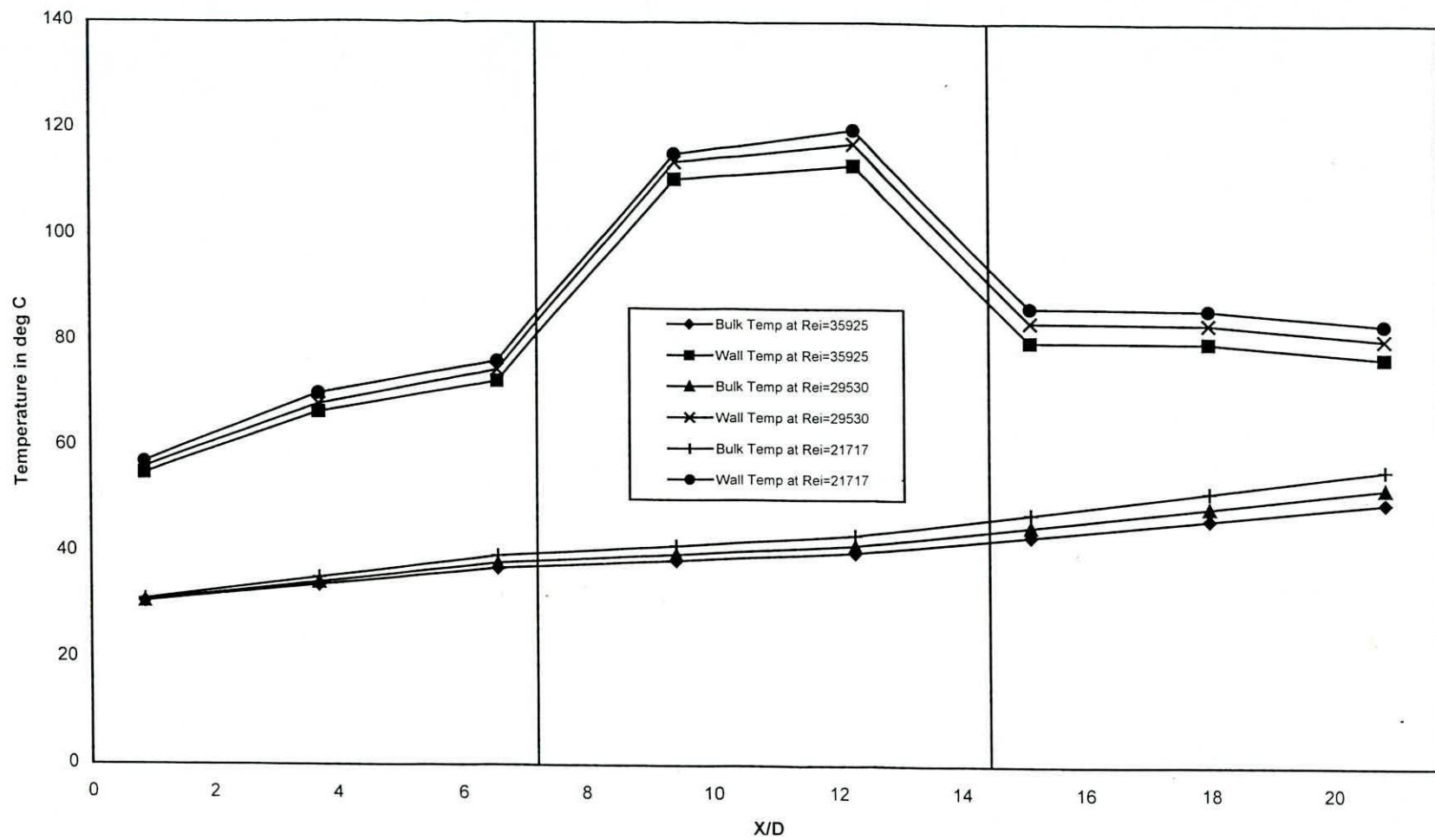


Fig. B38 Wall and Bulk Temperature Distribution Along The Length of In Line Segmented Finned Tube

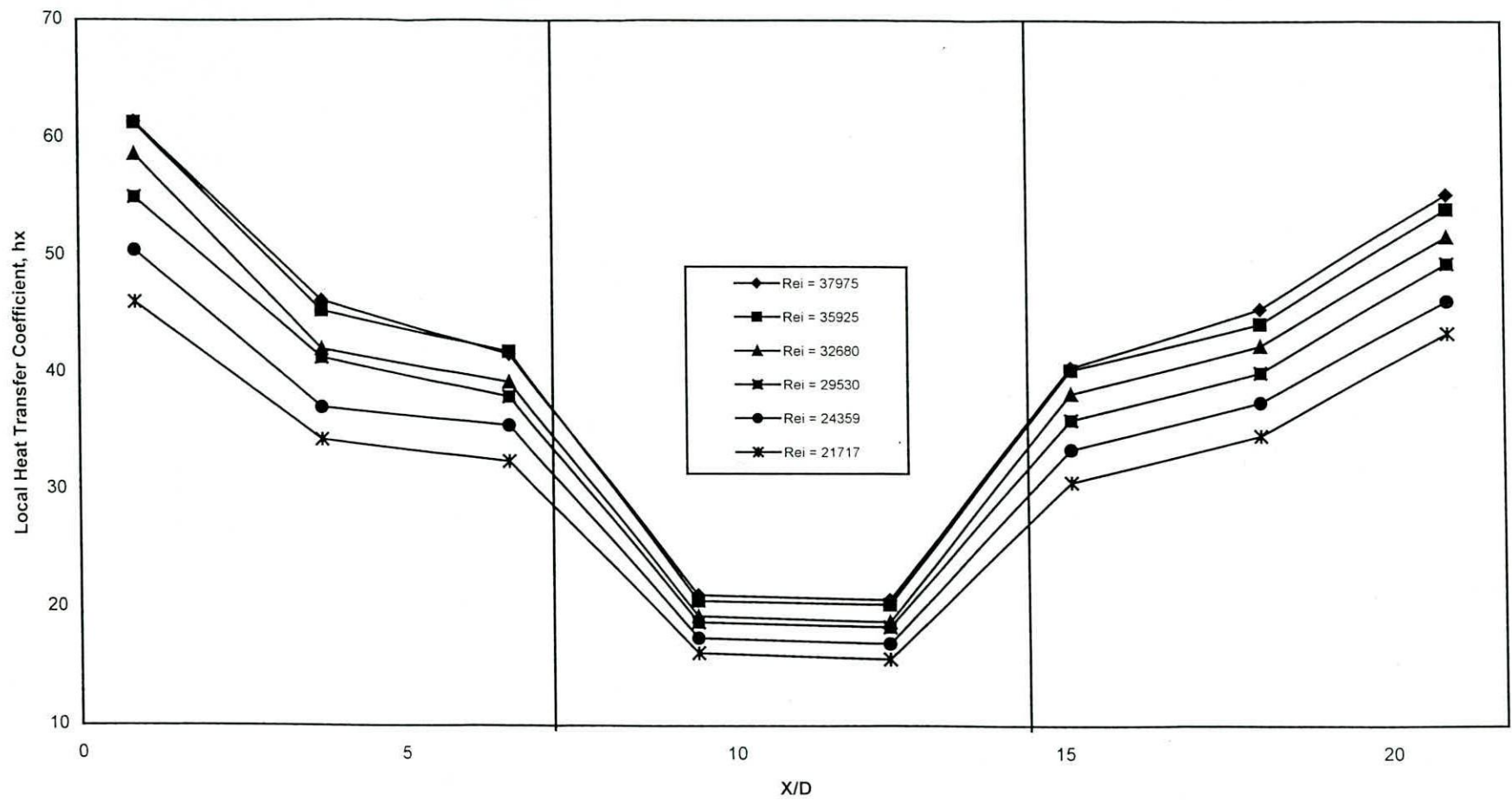


Fig. B39 Local Heat Transfer Coefficient as a function of X/D Along the Length of In Line Segmented Finned Tube at Different Reynolds Number

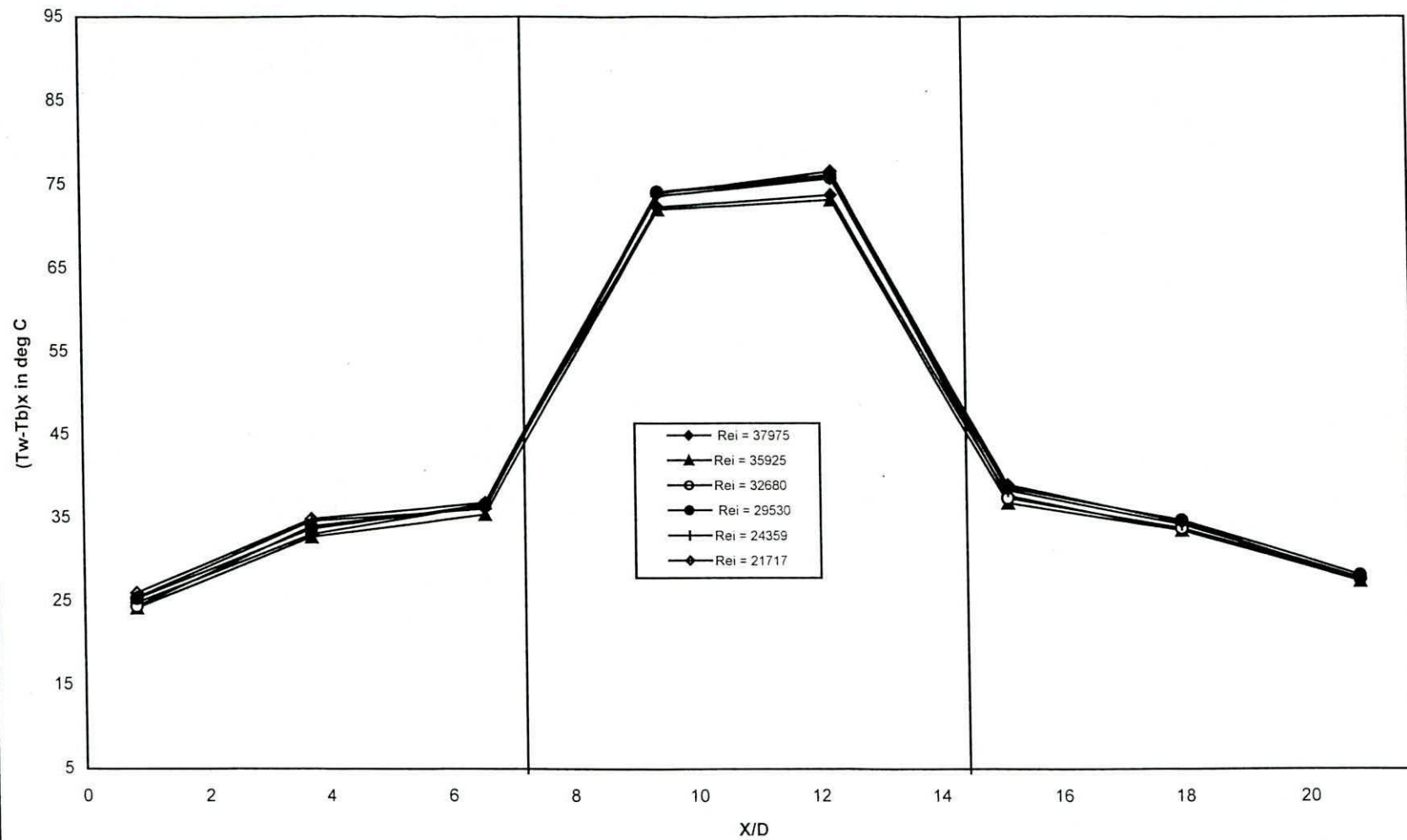


Fig. B40 Distribution of Wall to Bulk Temperature Along Axial Distance of the In Line Segmented Finned Tube

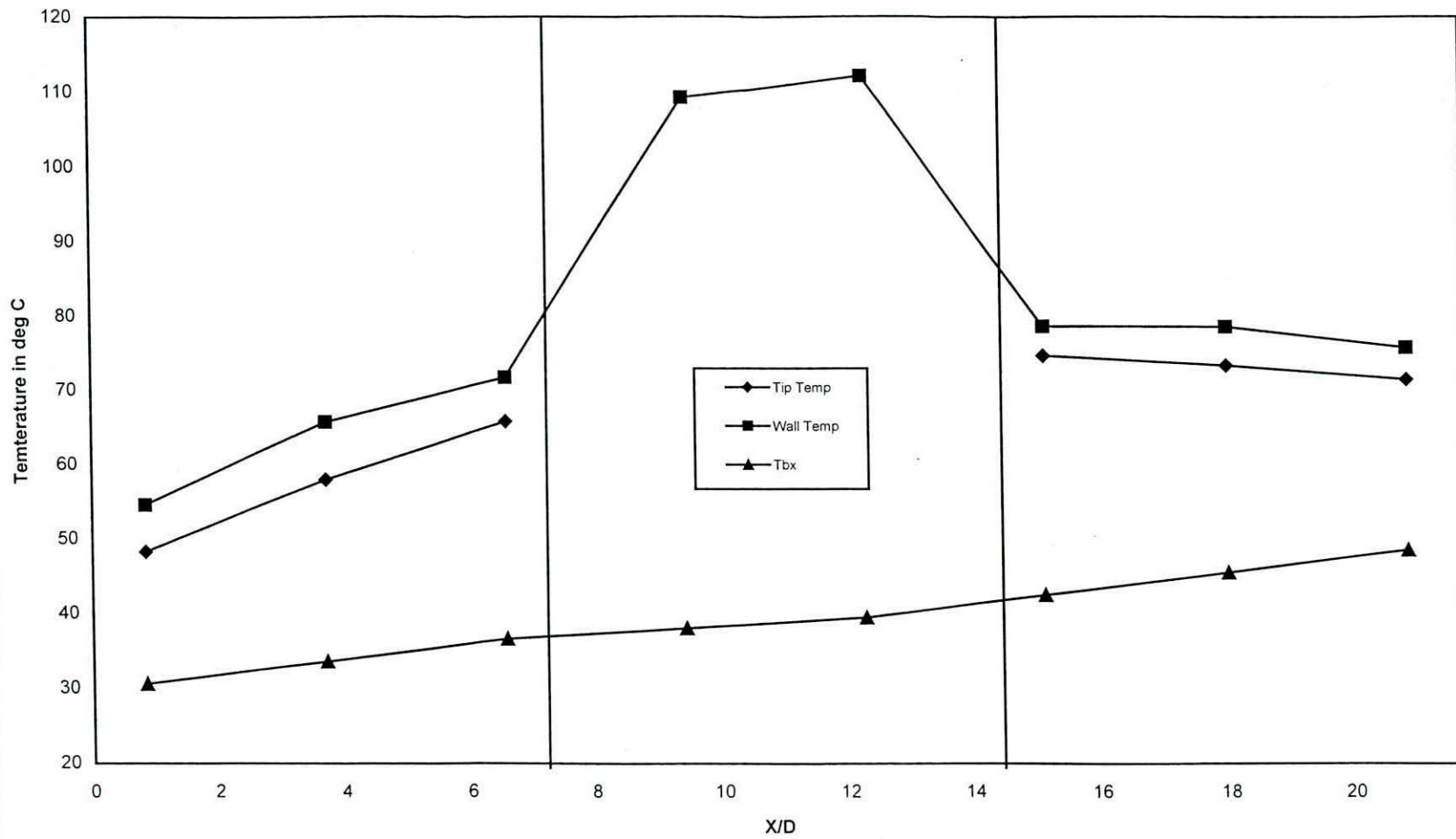


Fig. B41 Wall, Fin-Tip and Bulk Temperature Distribution Along The Length of In Line Segmented Finned (Rei = 37975)

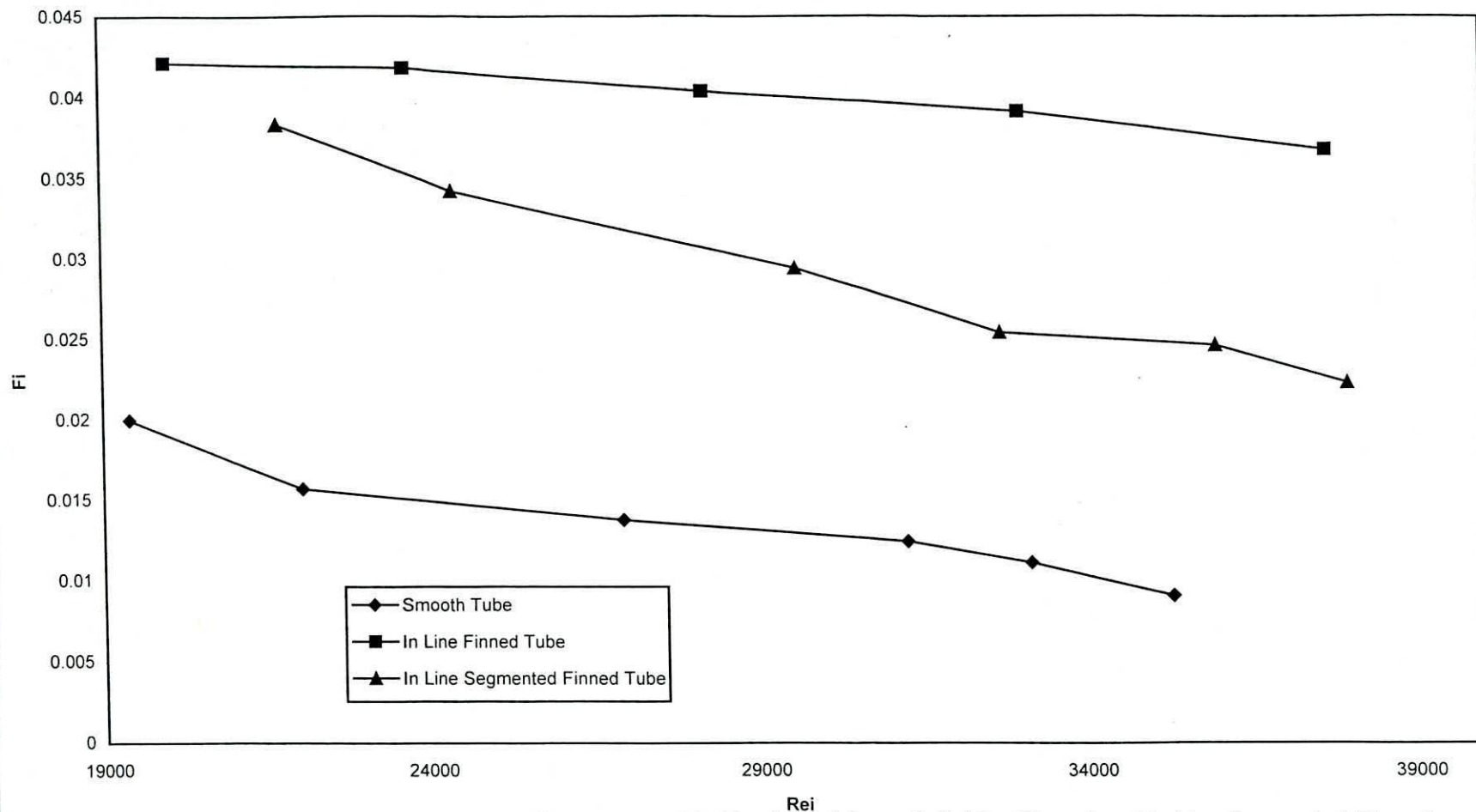


Fig. B42 Friction Factor at Different Reynolds Number of Smooth, In Line Finned and In Line Segmented Finned Tube

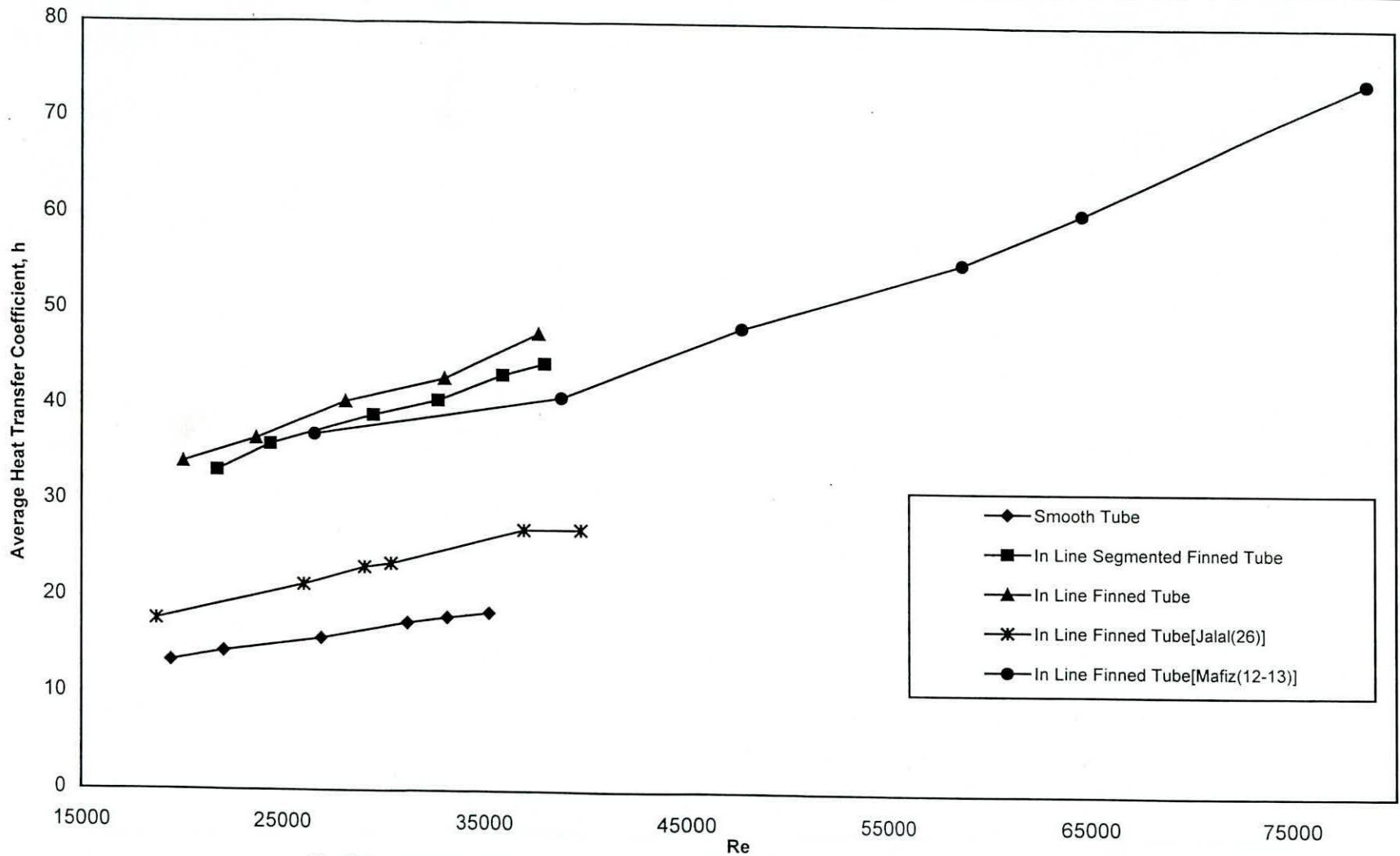
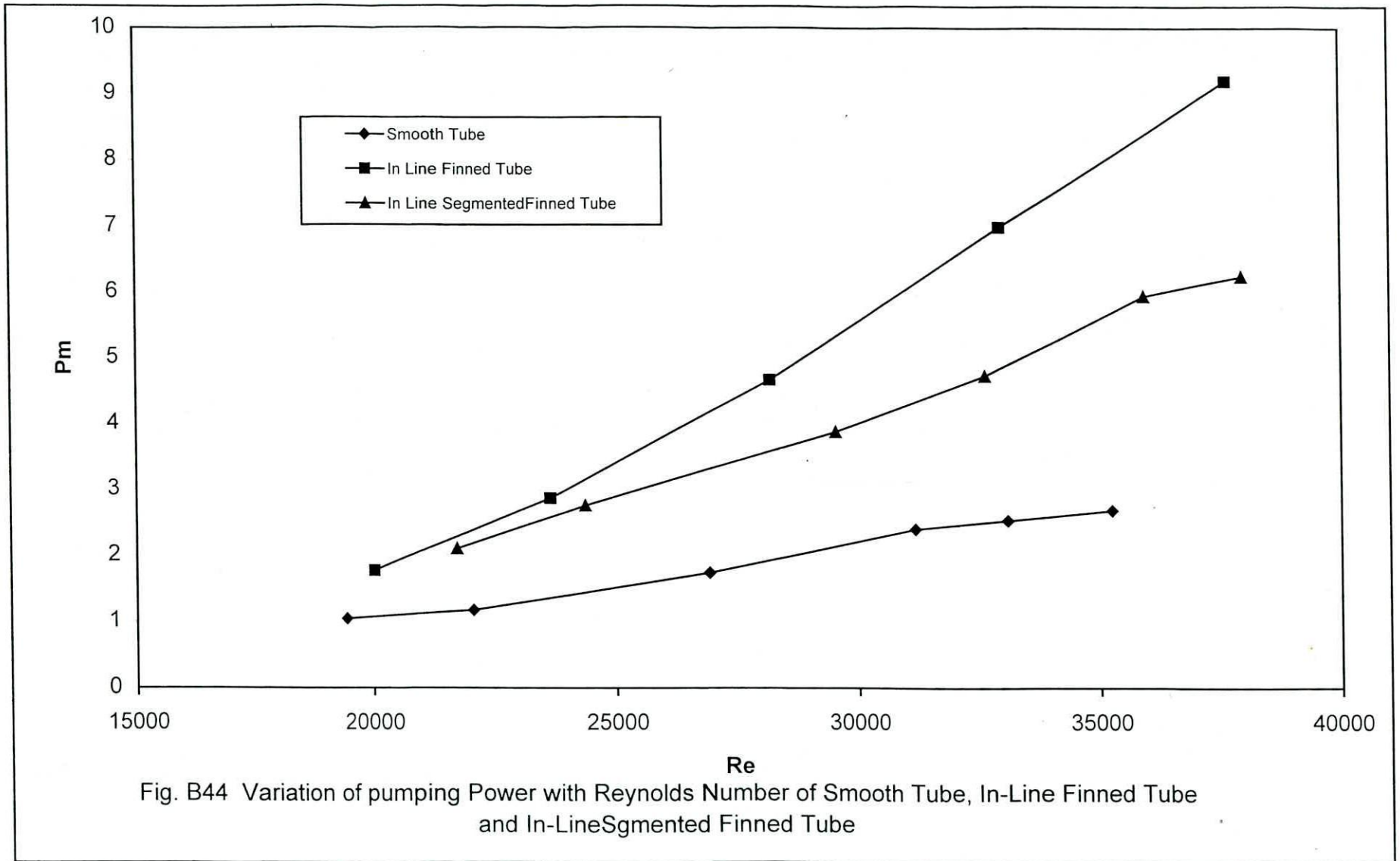
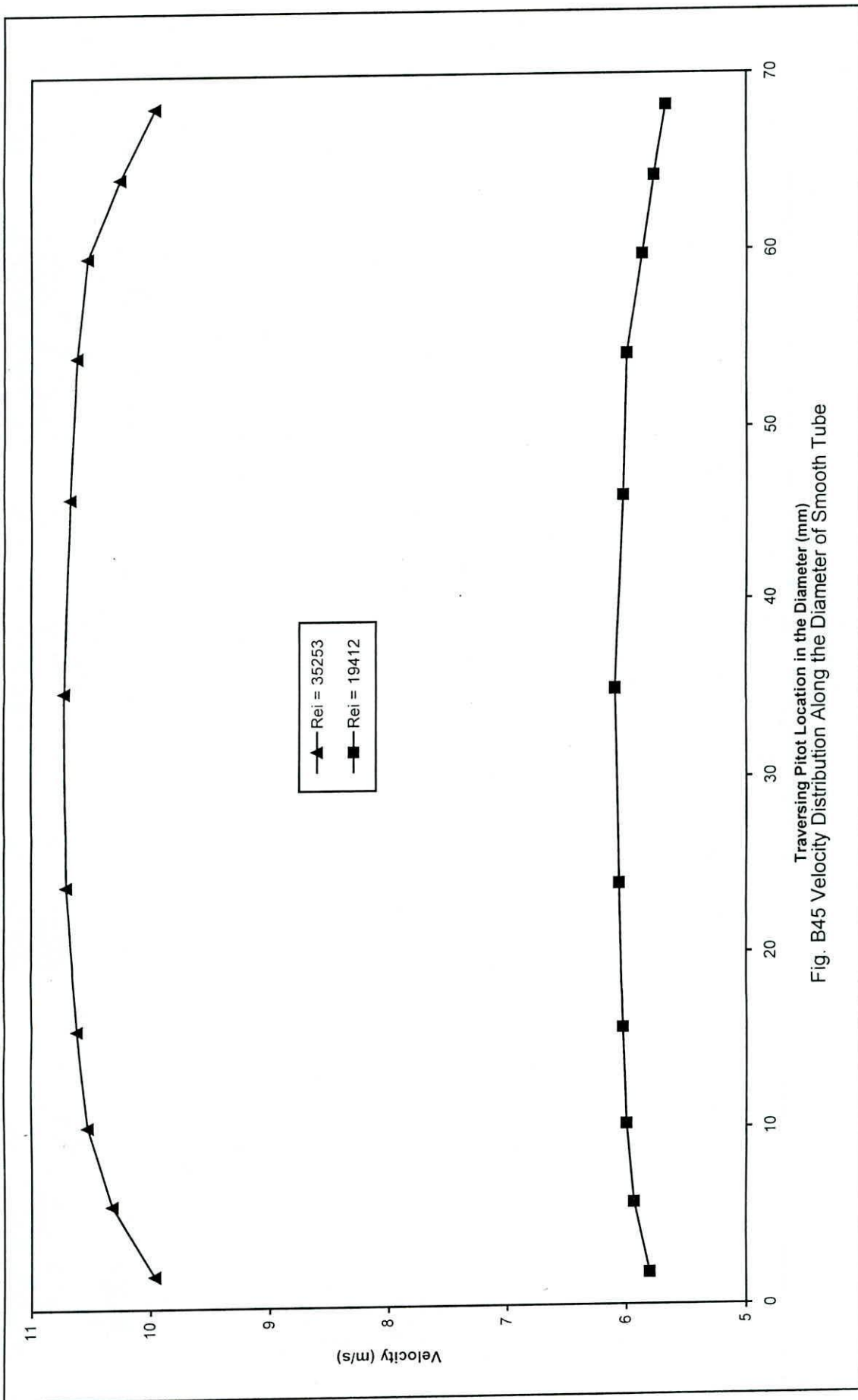


Fig. B43 Variation of Average Heat Transfer Coefficient with Reynolds number of Different Tubes
 (The wall Temperature of Present Work is Different Than That Of Previous work[(26),(12-13)]).





Traversing Pitot Location in the Diameter (mm)
 Fig. B45 Velocity Distribution Along the Diameter of Smooth Tube

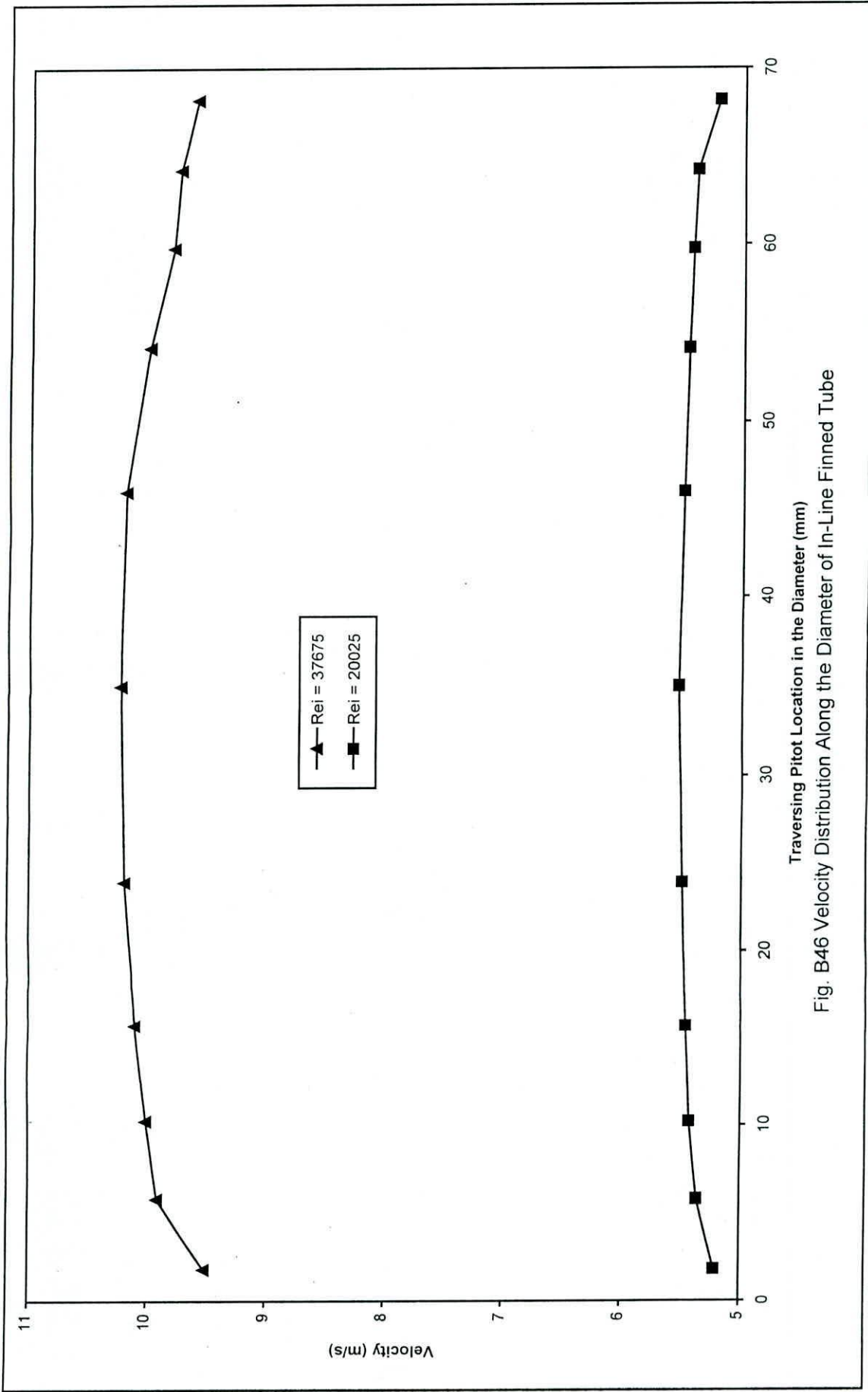


Fig. B46 Velocity Distribution Along the Diameter of In-Line Finned Tube

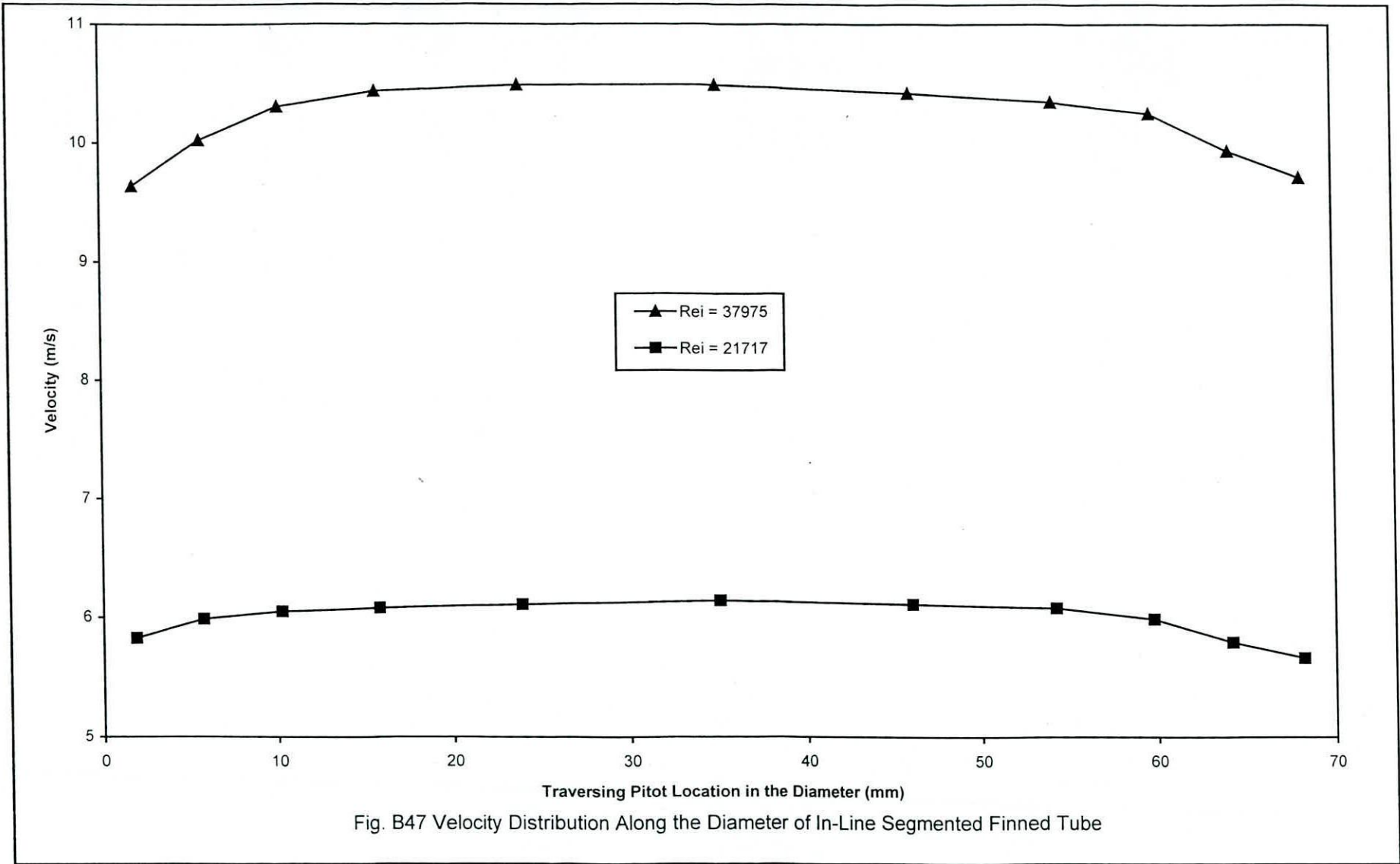


Fig. B47 Velocity Distribution Along the Diameter of In-Line Segmented Finned Tube

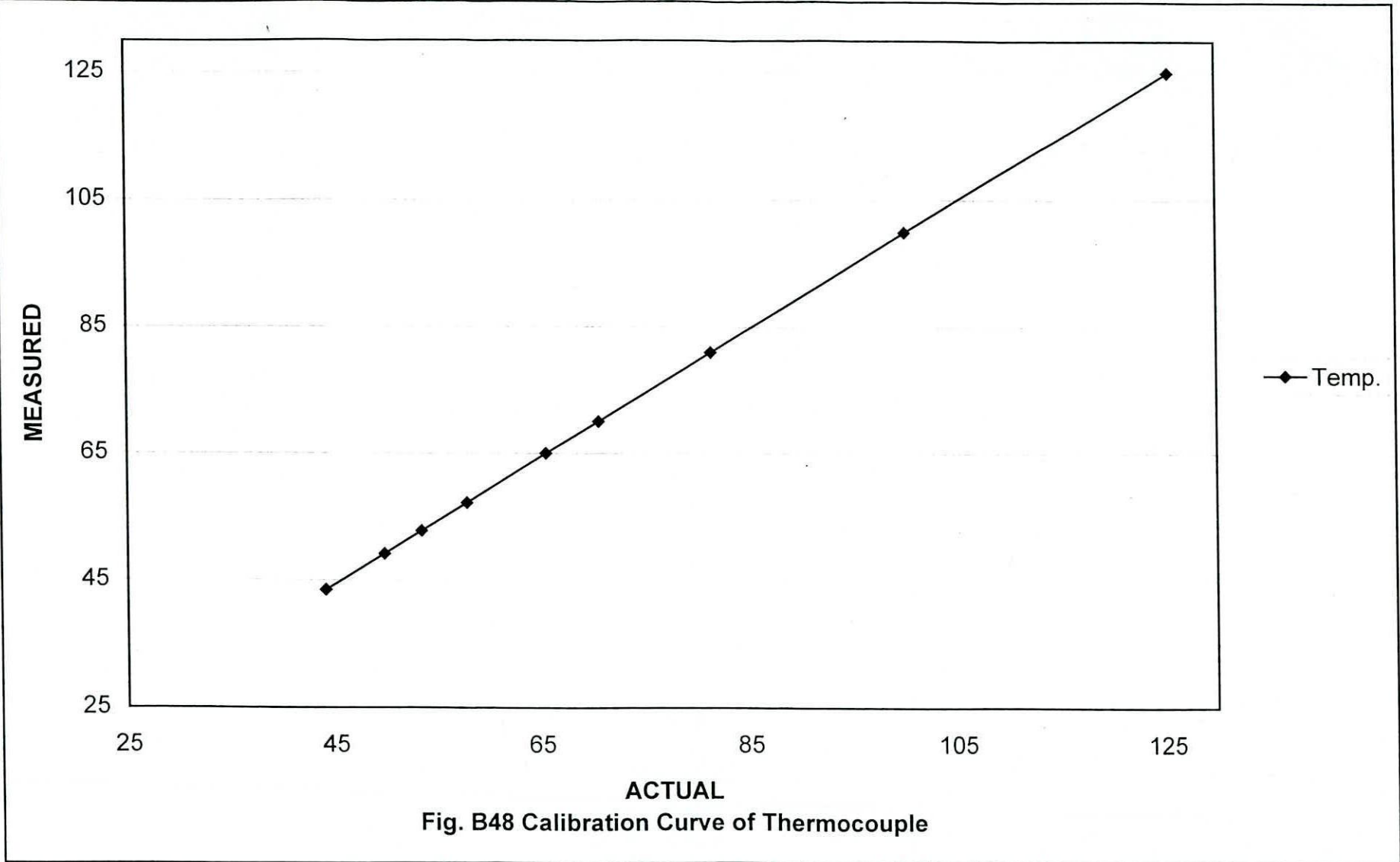
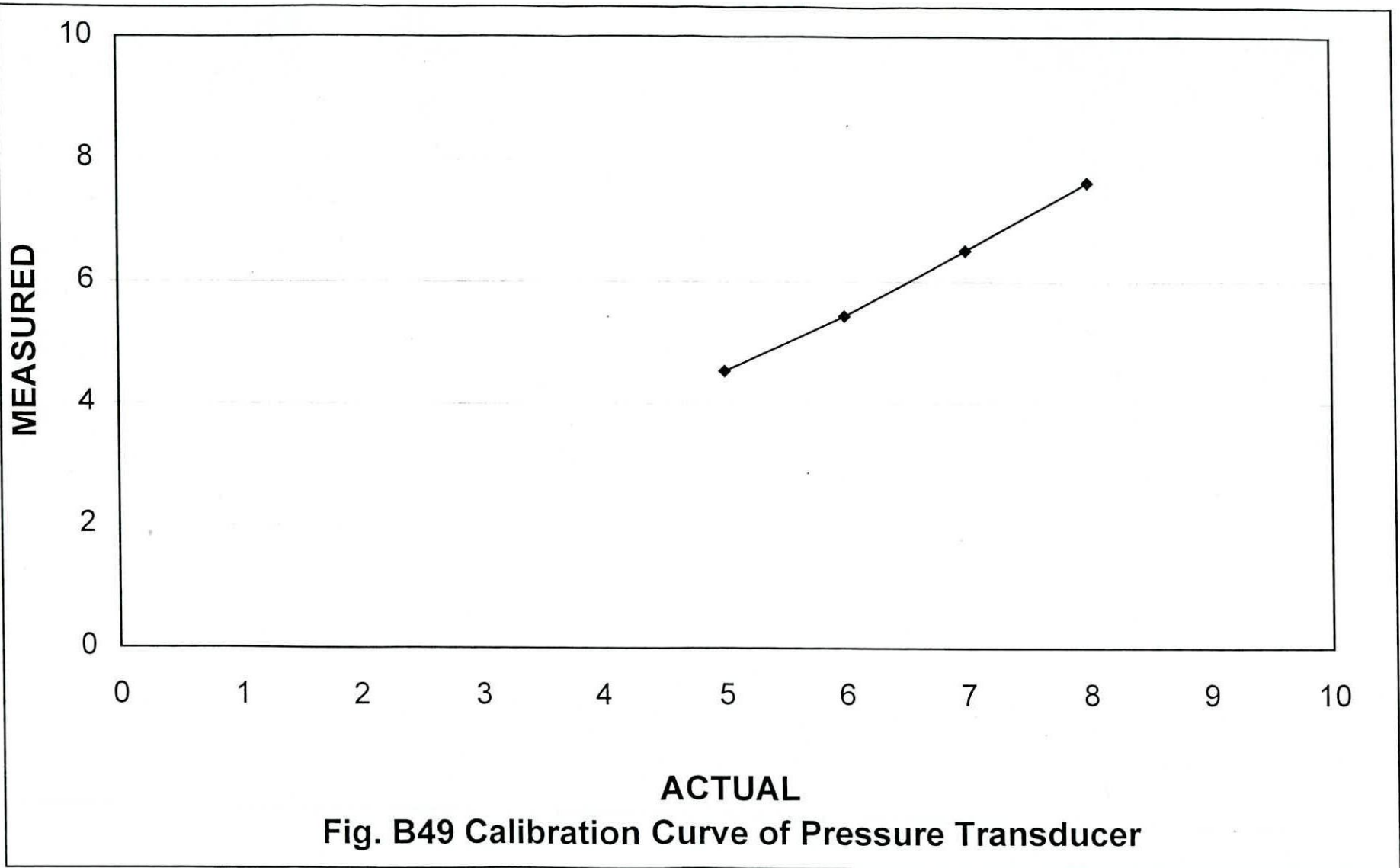


Fig. B48 Calibration Curve of Thermocouple



APPENDIX - C

SPECIFICATION

Table C1

1. Fan:

Capacity	:	30 m ³ /min.
Pressure	:	125 mm of water
H.P	:	3
Phase	:	3
Current	:	4.1 A
Voltage	:	380 V

2. Temperature Controller:

Range	:	0 - 200°C
Input voltage	:	220 V

3. Electric Heating System:

Heat Resistance	:	8.75 Ohm
Maximum Voltage	:	220 Volts
Maximum Current	:	25 A
Power	:	5.5 Kw

4. Data Acquisition System:

Cole – Parmer (USA origin)

Number of inputs	:	14 Model PCA – 14
Resolution	:	16 Bits
Accuracy	:	$\pm 0.02\%$ of range
Linearity	:	$\pm 0.015\%$
Input Impedence	:	10000 Megaohms/0.1 UF
Binary Inputs	:	11 ON – OFF TTL or Contact
Closure		or 10 – Bit pulse counter
Power	:	120 V 50/60 Hz 0.5 A

5. PRESSURE TRANSDUCERS:

OMEGA

PX202, PX203, PX205, PX212, PX213, PX215

M2165/0395

COMMON SPECIFICATIONS FOR ALL UNITS

ACCURACY (Linearity, Hysteresis and Repeatability)	0.25%	PROOF PRESSURE:	150%
		RESPONSE TIME:	1 msec
ZERO BALANCE:	1%FS	GAGE TYPE:	Chemical vapor

			deposited
COMPENSATED TEMP:	4° TO 176°F (-20° TO 80°C)	ELECTRICAL:	Polysilicon strain gages reverse polarity protected
THERMAL EFFECTS:	1.5%FS over	CONNECTION:	Miniature DIN conn.
VIBRATION:	Withstands 35g peak, 5 to 2000Hz	WETTED PARTS: CASE:	17-4 SS Stainless steel
PRESSURE PORT:	¼-18NPT	FATIGUE:	100 MILLION CYCLES FS
BURST PRESSURE:	400%, 17000 PSI max.	WEIGHT:	3.5 oz (100gm)
PX202, PX212 SERIES MILLIVOLT OUTPUT		PX203, PX213 SERIES VOLTAGE INPUT	
EXCITATION:	10Vds, 15Vdc max	EXCITATION:	24Vdc @ 15mA (7- 35 Vdc)
OUTPUT:	100mV +1mV	OUTPUT:	0.5 – 5.5Vdc

OPERATING:	-40° to 257°F	OPERATING:	-40° to 257°F
TEMPERATURE:	(40° to 125°C)	TEMPERATURE:	(40° to 125°C)
INPUT RESISTANCE:	2.5k to 6k Ω	OUTPUT RESISTANCE:	100 Ω
WIRING:	+EXC Red/Pin 1; +SIG White/Pin 2 -SIG Green/Pin 3; -EXC Black/Pin 4	WIRING:	+EXC Red/Pin 1; COMMON Black/Pin 2 +OUT White/Pin 3; EARTH Drain/Pin 4

PX205, PX215 SERIES
CURRENT OUTPUT

EXCITATION	:	24Vdc (7-35 Vdc) Reverse polarity protected
OUTPUT	:	4-20mA (2-wire)
OPERATING TEMPERATURE	:	-40° to 257°F (40° to 125°C)
SPAN TOLERANCE	:	1%FS
MAX. LOOP RESISTANCE	:	50 X (supply voltage – 7)
WIRING	:	+Red/Pin 1; -Black/Pin 2, EARTH Drain/Pin4 4

Rotary Selector Switches:

OMEGA

Insulation Resistance:	:	20 M Ω at 300 volts dc
Contact Resistance	:	0.004 Ω or less
Case material	:	Noryl SPN-420
Weight	:	
2-pole switch	:	$\frac{3}{4}$ lbs.
3-pole switch	:	1 lb.
4-pole switch	:	1-1 / 4 lb.
Hardware and box	:	$\frac{3}{4}$ lbs.
Continuos Use Temperature	:	110°C

DP24E Process Meter:

OMEGA

Analog Input Ranges	:	4-20 mA, 0-5 Vdc, 1-5 Vdc, 0-10 Vdc
Input Impedance	:	Voltage: 1.0 Meg Current: 20 Ω
Isolation 3mm	:	Dielectric strength to 2500V transient per spacing base on EN61010 for 260Vrms or dc working voltage
Accuracy	:	0.05%R +/-LSB
Tempco	:	+/-50 PPM/°C
Excitation Voltage	:	24 Vdc @ 25mA 10 Vdc @ 25 mA
Display	:	LED 7-segment, 14.2 mm (0.56") Range; +9999 to - 1999 Decimal Point: 4 positions

Power Supply
OMEGA Model U24Y101

Input Power	:	120VAC (Std) or 220VAC (Opt) +/-10%
Output Voltage	:	24 VDC +/-5%
Output Current	:	1 Amp (max)
Load/Line Regulation	:	+/- 2%
Output Protection	:	Current Limited and Thermal Limited
Input Protection	:	0.5 Amp Fuse
Operating Temp	:	20 to 60 Deg C
Storage Temp	:	30 to 70 Deg C

Table C2 Shaped Inlet.

Co-ordinates for Shaped Inlet

x/d	0	0.094	0.109	0.1225	0.141	0.156	0.172	0.188	0.203
y/d	0	0	0.001	0.001	0.002	0.003	0.004	0.006	0.008

x/d	0.218	0.234	0.250	0.266	0.281	0.297	0.312	0.328	0.344
y/d	0.057	0.067	0.078	0.091	0.107	0.127	0.154	0.219	0.284

x/d	0.438	0.422	0.406	0.391	0.375	0.359	0.344	0.328
y/d	0.308	0.325	0.338	0.347	0.353	0.358	0.361	0.362

APPENDIX-D

SAMPLE CALCULATIONS

Internal diameter of the tube, $D_i = 70$ mm

F_{in} height, $H = 15$ mm

F_{in} width, $W = 3$ mm

Number of fin, $N = 8$ mm

$$A_x = \frac{\pi D_i^2}{4} = 3.8485 \times 10^{-3} \text{ sq.}$$

$$A_{xf} = \left(\frac{\pi D_i^2}{4} \right) - WHN = 3.4885 \times 10^{-3} \text{ sq. m}$$

$$A_h = D_i + 2HN = 0.45991 \text{ m}$$

$$A_s = D_i = 0.2199$$

Hydraulic Diameter:

For Smooth tube

$$D_h = D_i$$

For Finned tube

$$D_h = \frac{4 A_{xf}}{\pi D_i + 2HN} = \frac{4 A_{xf}}{A_h} = 0.030340 \text{ m}$$

Determination of Mean Velocity:

$$\Delta P = \frac{1}{2} \rho V^2 \quad (D-1)$$

If V is to be m/s, ρ must be expressed in kg/m^3 and ΔP in Pascals (N/m^2). If h is the velocity head expressed in cm of water

$$\Delta P = \gamma h = 9.81 \times 10^3 \times \frac{h}{10^2} = 98.1 \times h \text{ Pa} \quad (D-2)$$

Standard atmospheric properties at the sea level are

Pressure = 760 mm of Hg

Temperature = 15°C

Density = 1.225 kg/m³

For any other temperature, t°C and pressure, b mm of Hg, the value of the density in kg/m³ is

$$\rho_2 = \frac{P_2}{P_1} \cdot \frac{T_1}{T_2} \cdot \rho_1 = \frac{b}{760} \times \frac{288}{t + 273} \times 1.225$$
$$\Rightarrow \rho_2 = 0.4642 \left(\frac{b}{273 + t} \right) \quad (D-3)$$

From equations (C-1), (C-2) and (C-3)

$$V = 20.56 \left(\frac{273 + t}{b} \right)^{1/2} (h)^{1/2}$$
$$\Rightarrow V = C (h)^{1/2}$$

$$\text{Where, } C = 20.56 \left(\frac{273 + t}{b} \right)^{1/2} \quad (D-4)$$

h = velocity head, in cm of water.

For Smooth Tube

For, room temperature, t = 30.8 °C

atm. pressure, b = 743.5 mm Hg

$$C = 13.124$$

The experiment was done using a manometric fluid of sp. gr. = 0.855 but it was recommended to perform with a fluid of sp. gr. = 0.834. This is why a correction is needed, which was as follows:

$$\omega_1 H_{\omega 1} = \omega_2 H_{\omega 2}$$

$$\Rightarrow 0.834 \times H_{\omega 1} = 0.855 \times 0.855 H_D$$

$$\begin{aligned} \therefore H_{\omega 1} = h_1 &= \frac{(0.855)^2 \times H_D}{0.834} \\ &= 0.877 \times 2.54 H_D \text{ cm} \end{aligned}$$

[H_D in inch of water]

Measurement of mean velocity by ten points Log Linear method is given by,

$$\begin{aligned} \text{Mean velocity, } V_i &= \frac{C}{10} (h_1^{1/2} + h_2^{1/2} + h_3^{1/2} + \dots + h_{10}^{1/2}) \\ \Rightarrow V_i &= 10.4455 \text{ m/s} \end{aligned}$$

$$\begin{aligned} \text{Mass Flow rate, } M &= A_x V_i \\ &= 1.1361 \times 0.00385 \times 10.4455 \\ &= 0.045687 \text{ kg/s} \\ [\rho &= 0.9947 \text{ kg/m}^3 \text{ of air at } 347.3958 \text{ K}] \end{aligned}$$

$$V = \frac{M}{\rho A_x} = 11.92987 \text{ m/s}$$

Reynolds Number:

$$R_{ei} = \frac{\rho V D_i}{\mu} = 35253$$

Friction Factor:

Local friction factor based on inside diameter is given by

$$\begin{aligned} F_i &= \frac{(-\Delta P/x) D_i}{2 \rho V^2} \\ &= \frac{(-\Delta P/x) \times 0.07 \times 9.81}{2 \times 0.9947 \times (11.92987)^2} \\ &= 2.4253 \times 10^{-3} (-\Delta P/x) \end{aligned} \quad (\text{D -5})$$

Local friction factor based on hydraulic diameter is given by

$$F_h = \frac{(-\Delta P / X) Dh}{2\rho V^2} \quad (D-6)$$

dell h (mm)	delP (mm)	density (w)	dl P (kg/m**2)	Dimless P	del X	delP/del X	Fi
6							
7	1	994.56	0.995	0.13784	0.06	16.576	0.0402
8	2	994.56	1.989	0.27567	0.26	7.650	0.0186
9	3	994.56	2.984	0.41351	0.46	6.486	0.0157
10	4	994.56	3.978	0.55135	0.66	6.028	0.0146
10.25	4.25	994.56	4.227	0.58581	0.86	4.915	0.0119
10.5	4.5	994.56	4.476	0.62027	1.06	4.222	0.0102
10.75	4.75	994.56	4.724	0.65473	1.26	3.749	0.0091
11.5	5.5	994.56	5.470	0.75811	1.46	3.747	0.0091

Pumping power can be defined as

$$\begin{aligned}
 P_m &= (-\Delta P/\rho) M \\
 &= \frac{4 F_f L}{D_i} \frac{V^2}{2} A_x V \rho \quad W \\
 &= 2.68873 \text{ W}
 \end{aligned}$$

Heat Transfer Calculation:

$$T_i = 30.8 \text{ }^\circ\text{C}$$

$$T_o = 41.12952 \text{ }^\circ\text{C}$$

Properties of air are calculated at $T_f = 347.3958 \text{ K}$

$$C_p = 1.006 \text{ KJ/kg-}^\circ\text{C}$$

$$K = 0.0298 \text{ w/m-}^\circ\text{C}$$

$$\mu = 20.6308 \text{ microkg/sec-m}$$

$$\rho = 0.9947 \text{ kg/m}^3$$

Total heat input to the air

$$Q = MC_p (T_o - T_i) = 474.7517 \text{ Watt.}$$

Q' = heat input per unit area

$$\begin{aligned} &= \frac{Q}{A_s L} \\ &= 1420.358 \quad W / m^2 \end{aligned}$$

The local bulk temperature of this fluid is,

$$\begin{aligned} T_{hx} &= T_i + \frac{Q' A_s x}{MC_p} \\ &= 30.8 + \frac{1420.358 \times (0.2199) \times x}{0.045687 \times 1.006 \times 10^3} \end{aligned}$$

$$T_{hx} = 31.2 + 6.796x \text{ } ^\circ\text{C}$$

(D-7)

X	Tbx	hx
0.06	31.20774	27.272
0.26	32.56689	19.610
0.46	33.92604	18.194
0.66	35.28519	17.396
0.86	36.64433	17.254
1.06	38.00348	17.268
1.26	39.36263	16.982
1.46	40.72178	17.225

Local convective heat transfer coefficient is given by,

$$\begin{aligned}h_x &= \frac{Q'}{(T_w - T_b)_x} \\&= \frac{1420.358}{(T_w - T_b)_x} \\&= \frac{1420.38}{(T_w - T_b)_x} W / m^2 \text{ } ^\circ C\end{aligned}\tag{D-8}$$

Average Heat Transfer Coefficient

$$\begin{aligned}\bar{h} &= \frac{Q}{A(T_{w_{av}} - T_{b_{av}})} \\&= \frac{474.75}{0.33425 \times (112.83 - 35.96)} \\&= 18.48 W / m^2 \text{ } ^\circ C\end{aligned}\tag{D-9}$$

For In line Finned Tube

For, room temperature, $t = 30.2 \text{ } ^\circ C$
atm. pressure, $b = 741.5 \text{ mm Hg}$
 $C = 13.128$

The experiment was done using a manometric fluid of sp. gr. = 0.855 but it was recommended to perform with a fluid of sp. gr. = 0.834. This is why a correction is needed, which was as follows:

$$\begin{aligned}\omega_1 H_{\omega 1} &= \omega_2 H_{\omega 2} \\ \Rightarrow 0.834 \times H_{\omega 1} &= 0.855 \times 0.855 H_D\end{aligned}$$

$$\begin{aligned} \therefore H_{o1} = h_1 &= \frac{(0.855)^2 \times H_D}{0.834} \\ &= 0.877 \times 2.54 H_D \text{ cm} \end{aligned}$$

[H_D in inch of water]

Measurement of mean velocity by ten points Log Linear method is given by,

$$\begin{aligned} \text{Mean velocity, } V_i &= \frac{C}{10} (h_1^{1/2} + h_2^{1/2} + h_3^{1/2} + \dots + h_{10}^{1/2}) \\ \Rightarrow V_i &= 9.942 \text{ m/s} \end{aligned}$$

$$\begin{aligned} \text{Mass Flow rate, } M &= A_x V_i \\ &= 1.135 \times 0.00385 \times 9.9425 \\ &= 0.04345 \text{ kg/s} \\ [\rho &= 1.0609 \text{ kg/m}^3 \text{ of air at } 324.2148 \text{ K}] \end{aligned}$$

$$V = \frac{M}{\rho A_x} = 11.74 \text{ m/s}$$

Reynolds Number:

$$R_{ei} = \frac{\rho V D_i}{\mu} = 37675$$

Friction Factor:

Local friction factor based on inside diameter is given by

$$\begin{aligned} F_i &= \frac{(-\Delta P / x) D_i}{2 \rho V^2} \\ &= \frac{(-\Delta P / x) \times 0.07 \times 9.81}{2 \times 1.0609 \times (11.74)^2} \\ &= 2.35 \times 10^{-3} (-\Delta P / x) \end{aligned} \tag{D-10}$$

Local friction factor based on hydraulic diameter is given by

$$F_h = \frac{(-\Delta P / X) D_h}{2\rho V^2} \quad (D-11)$$

del h (mm)	delP (mm)	density (w)	dl P (kg/m**2)	Dimless P	del X	delP/del X	Fi
4							
6	2	994.56	1.989	0.267	0.06	33.152	0.078
11	7	994.56	6.962	0.934	0.26	26.777	0.063
13	9	994.56	8.951	1.201	0.46	19.459	0.046
16.75	12.75	994.56	12.681	1.702	0.66	19.213	0.045
18.75	14.75	994.56	14.670	1.969	0.86	17.058	0.040
21	17	994.56	16.908	2.269	1.06	15.950	0.037
23	19	994.56	18.897	2.536	1.26	14.997	0.035
27	23	994.56	22.875	3.070	1.46	15.668	0.037

Pumping power can be defined as

$$\begin{aligned}
 P_m &= (-\Delta P / \rho) M \\
 &= \frac{4 F_i L}{D_i} \frac{V^2}{2} A_x V \rho \quad W \\
 &= 9.19128 \text{ W}
 \end{aligned}$$

Heat Transfer Calculation:

$$T_i = 30.2 \text{ }^\circ\text{C}$$

$$T_o = 48.92 \text{ }^\circ\text{C}$$

Properties of air are calculated at $T_f = 324.83 \text{ K}$

$$C_p = 1.0059 \text{ KJ/kg-}^\circ\text{C}$$

$$K = 0.0281 \text{ w/m-}^\circ\text{C}$$

$$\mu = 19.5701 \text{ microkg/sec-m}$$

$$\rho = 1.0609 \text{ kg/m}^3$$

Total heat input to the air

$$Q = MC_p (T_o - T_i) = 818.101 \text{ Watt.}$$

Q' = heat input per unit length

$$\begin{aligned} &= \frac{Q}{A_h L} \\ &= 1170.29 \quad \text{W/m}^2 \end{aligned}$$

The local bulk temperature of this fluid is,

$$\begin{aligned} T_{bx} &= T_i + \frac{Q' A_h x}{MC_p} \\ &= 30.2 + \frac{1170.29 \times (0.4599) \times x}{0.04345x \times 1.0059 \times 10^3} \end{aligned}$$

$$T_{bx} = 30.2 + 12.32x$$

(D-12)

X	Tbx	hx
0.06	30.939	59.984
0.26	33.402	44.037
0.46	35.864	39.110
0.66	38.327	37.199
0.86	40.790	37.790
1.06	43.252	38.942
1.26	45.715	42.216
1.46	48.178	51.159

Local convective heat transfer coefficient is given by,

$$\begin{aligned}
 h_x &= \frac{Q'}{(T_w - T_b)_x} \\
 &= \frac{1170.29}{(T_w - T_b)_x} \\
 &= \frac{1170.29}{(T_w - T_b)_x} W / m^2 C
 \end{aligned}
 \tag{D-13}$$

Average Heat Transfer Coefficient

$$\begin{aligned}
 \bar{h} &= \frac{Q}{A(T_{wav} - T_{hav})} \\
 &= \frac{1818.101}{0.699 \times (64.89 - 40.06)} \\
 &= 47.12 W / m^2 C
 \end{aligned}
 \tag{D-14}$$

For In line Segmented Finned Tube

For, room temperature, $t = 29.7 \text{ }^\circ\text{C}$
 atm. pressure, $b = 746.2 \text{ mm Hg}$
 $C = 13.076$

The experiment was done using a manometric fluid of sp. gr. = 0.855 but it was recommended to perform with a fluid of sp. gr. = 0.834. This is why a correction is needed, which was as follows:

$$\begin{aligned}
 \omega_1 H_{\omega 1} &= \omega_2 H_{\omega 2} \\
 \Rightarrow 0.834 \times H_{\omega 1} &= 0.855 \times 0.855 H_D \\
 \therefore H_{\omega 1} = h_1 &= \frac{(0.855)^2 \times H_D}{0.834} \\
 &= 0.877 \times 2.54 H_D \text{ cm}
 \end{aligned}$$

[H_D in inch of water]

Measurement of mean velocity by ten points Log Linear method is given by,

$$\text{Mean velocity, } V_i = \frac{C}{10} (h_1^{1/2} + h_2^{1/2} + h_3^{1/2} + \dots + h_{10}^{1/2})$$
$$\Rightarrow V_i = 10.1850852 \text{ m/s}$$

$$\begin{aligned} \text{Mass Flow rate, } M &= A_x V_i \\ &= 1.1443 \times 0.00385 \times 10.1850852 \\ &= 0.04487 \text{ kg/s} \\ [\rho &= 1.0541 \text{ kg/m}^3 \text{ of air at } 329.0157 \text{ K}] \end{aligned}$$

$$V = \frac{M}{\rho A_{sf}} = 12.2008 \text{ m/s}$$

Reynolds Number:

$$R_{ei} = \frac{\rho V D_i}{\mu} = 37975$$

Friction Factor:

Local friction factor based on inside diameter is given by

$$\begin{aligned} F_i &= \frac{(-\Delta P / x) D_i}{2 \rho V^2} \\ &= \frac{(-\Delta P / x) \times 0.07 \times 9.81}{2 \times 1.0541 \times (12.2008)^2} \\ &= 2.188 \times 10^{-3} (-\Delta P / x) \end{aligned} \tag{D-15}$$

Local friction factor based on hydraulic diameter is given by

$$F_h = \frac{(-\Delta P / X) Dh}{2 \rho V^2} \tag{D-16}$$

delh (mm)	delP (mm)	density (w)	dIP (kg/m**2)	Dimles s P	del X	delP/del X	Fi
6							
10	4	994.56	3.978	0.497	0.06	66.304	0.145
14	6	994.56	5.967	0.745	0.26	22.951	0.050
16	8	994.56	7.956	0.993	0.46	17.297	0.038
16.8	8.75	994.56	8.702	1.086	0.66	13.185	0.029
17.3	9.25	994.56	9.200	1.148	0.86	10.697	0.023
18.5	11	994.56	10.940	1.366	1.06	10.321	0.023
20	13	994.56	12.929	1.614	1.26	10.261	0.022
22	15	994.56	14.918	1.862	1.46	10.218	0.022

Pumping power can be defined as

$$P_m = (-\Delta P/\rho) M$$

$$= \frac{4 F_i L}{D_i} \frac{V^2}{2} A_x V \rho \quad W$$

$$= 6.24058 W$$

Heat Transfer Calculation:

$$T_i = 29.7 \text{ }^\circ\text{C}$$

$$T_o = 49.22 \text{ }^\circ\text{C}$$

Properties of air are calculated at $T_f = 329.0157 \text{ K}$

$$C_p = 1.0059 \text{ KJ/kg-}^\circ\text{C}$$

$$K = 0.0284 \text{ w/m-}^\circ\text{C}$$

$$\mu = 19.7898 \text{ microkg/sec-m}$$

$$\rho = 1.0541 \text{ kg/m}^3$$

Total heat input to the air

$$Q = MC_p (T_o - T_i) = 881.113 \text{ Watt.}$$

Heat input to the air per unit area

$$Q' = \frac{MC_p(T_o - T_i)}{(A_h + A_s + A_h)L}$$
$$= 1525.74 \text{ W/m}^2 \quad (\text{D-17})$$

The local bulk temperature of the fluid $T_b(x)$ can be defined as by the following heat balance equation

$$T_b(x) = T_i + \frac{Q' A_h x}{MC_p} \quad \text{When } x < L_1 \quad (\text{D-18})$$

$$= T_i + \frac{Q' A_h x}{MC_p}$$
$$= 29.7 + \frac{1525.74 \times (0.4599) \times x}{0.04487 \times 1.0059 \times 10^3}$$
$$= 29.7 + 15.55x$$

$$T_b(x)_I = (T_i)_{I-1} + \frac{Q' A_s (0.2)}{MC_p} \quad \text{When } L_1 < x < 2L_1 \quad (\text{D-19})$$

$$T_{b4} = T_{b3} + \frac{Q' A_s (0.2)}{MC_p}$$
$$= 36.85 + \frac{1525.74 \times (0.2199) \times 0.2}{0.04487 \times 1.0059 \times 10^3}$$

$$= 36.628 + 1.49$$

$$= 38.34$$

Similarly

$$T_h(x)_l = (T_h)_{l-1} + \frac{Q' A_h(0.2)}{MC_p} \quad \text{When } 2L_1 < x < 3L_1 \quad (\text{D-20})$$

$$\begin{aligned} T_{h6} &= T_{h5} + \frac{Q' A_h(0.2)}{MC_p} \\ &= 39.82 + \frac{1525.74 \times (0.4599) \times 0.2}{0.04487 \times 1.0059 \times 10^3} \end{aligned}$$

$$= 39.82 + 3.109$$

$$= 42.93^\circ \text{C}$$

X	Tbx	hx
0.06	30.633	61.410
0.26	33.742	46.187
0.46	36.851	41.654
0.66	38.338	21.097
0.86	39.824	20.682
1.06	42.934	40.484
1.26	46.043	45.511
1.46	49.152	55.298

Local convective heat transfer coefficient is given by,

$$\begin{aligned} h_x &= \frac{Q'}{(T_w - T_h)_x} \\ &= \frac{1525.74}{(T_w - T_h)_x} \\ &= \frac{1525.74}{(T_w - T_h)_x} \text{W/m}^2\text{C} \end{aligned} \quad (\text{D-21})$$

Average Heat Transfer Coefficient

$$\begin{aligned}\bar{h} &= \frac{Q}{A(T_{wav} - T_{hav})} \\ &= \frac{881.13}{0.5774 \times (73.7 - 39.46)} \\ &= 44.59W / m^2C\end{aligned}$$

(D-22)

